Casimir effect in Randall-Sundrum models

Casimir effekt i Randall-Sundrum modeller

Marianne Rypestøl

June 28, 2009

NTNU
Norwegian University of
Science and Technology

Preface

This master thesis was written in the spring 2009 in connection with the subject TFY4900 - Physics, Master Thesis. It concludes the fifth and final year of the Advanced Engineering/Master's Degree Programme in Applied Physics and Mathematics at The Norwegian University of Science and Technology.

The work includes a study of the Casimir effect from a bulk scalar in the Randall-Sundrum model, both at zero and finite temperature. Zeta regularization is employed throughout the paper. The thesis is a continuation of my project thesis - 'The Casimir effect in the presence of compactified universal extra dimensions'. In my work I have used Maple 12 for some analytic computations and MATLAB for all the plots.

This paper is written for people with knowledge to quantum mechanics, some general relativity and preferably quantum field theory or quantum optics. There is no need for understanding the details of zeta regularization if one accepts that the formulas given are correct.

I would like to thank my supervisor Iver Brevik for always having time to answer my questions. I am grateful for his advice on key roblems and his guidance to the right sources of information.

Marianne Rypestøl
June 28, 2009, Trondheim

Summary

We work with the two Randall-Sundrum models from 1999. The models are five-dimensional, that is they have one additional spatial dimension. We study the Casimir effect on two parallel physical plates in our ordinary spacetime, from a scalar field living in the extra dimension. The calculations cover different boundary conditions on the plates and are carried out both at zero and finite temperatures. We show that the correction to the ordinary Casimir force is small, and discuss in detail some of the key problems yet to be resolved in higher dimensional Casimir theory.

Sammendrag (Norsk)

Vi arbeider med de to Randall-Sundrum modellene fra 1999. Modellene er femdimensjonale, de har altså en ekstra romlig dimensjon. Vi ser på Casimir effekt på to parallelle plater i vårt fysiske rom fra et skalart felt som lever i den ekstra dimensjonen. Utregningene dekker forskjellige grensebetingelser på platene og er gjort både for null og endelig temperatur. Vi viser at forskjellen fra vanlig Casimir kraft er liten. I tillegg diskuteres noen av de uløste problemene i forbindelse med Casimir effekt i teorier med flere romlige dimensjoner.

Contents

Chapter 1

Introduction

For many years physicists have tried to unify the four fundamental forces of nature, electromagnetic, strong and weak nuclear forces and gravity, into one theory. Today three of four forces are incorporated in the standard model (SM) of physics, only gravity is left out. One of the fundamental problems when trying to unite gravity with the other forces is the hierarchy problem. It can be formulated as why gravity is so much weaker than the other forces. Gravitational interactions are suppressed by a very high energy scale, the Planck scale of size $M_{\rm Pl} = 2 \times 10^{18}$GeV, while the other three interactions are governed by the TeV scale. As early as in the 1920s, Kaluza and Klein attempted to unify electromagnetism and gravity by introducing an extra spatial dimension. In a flat 4+n dimensional theory, our four-dimensional Planck scale will be generated from a more fundamental 4+n-dimensional scale of gravity M by

$$M_{\rm Pl} = M^{n+1} V_n,$$

where V_n is the volume of the compactified dimensions. The n extra dimensions need to be large in order to produce the observed Planck scale. Unfortunately this model introduces a new hierarchy between the compactification scale $V_N^{-1/n}$ and the weak scale.

In 1999 Lisa Randall and Raman Sundrum published an article [1] where they proposed a model (RS) in which we live on a (3+1)-dimensional subspace, called a 3-brane, in a (4+1)-dimensional spacetime, referred to as the bulk. In addition to our visible 3-brane there exists an additional hidden 3-brane. All SM fields are confined to the branes, only gravity can propagate in the bulk. The extra dimension is a circle S^1, with radius r_c, represented by a coordinate ϕ with range $-\pi \leq \phi \leq \pi$. They also imposed Z_2 symmetry which means that (x^μ, ϕ) and $(x^\mu, -\phi)$ refers to the same point in spacetime. The hidden and visible branes are located at $\phi = 0$ and $\phi = \pi$ respectively. Henceforth this model will be referred to as RSI. Shortly after their first article they proposed a new model (RSII) where the hidden brane is sent to infinity, effectively removing it from the setup [28].

The major difference between the RS and other higher dimensional models is a warp-factor $e^{-2kr_c|\phi|}$ in the metric

$$\mathrm{d}s^2 = e^{-2kr_c|\phi|}\eta_{\mu\nu}\mathrm{d}x^\mu \mathrm{d}x^\nu - r_c^2 \mathrm{d}\phi^2.$$

Here, $\eta_{\mu\nu} = \mathrm{diag}(1, -1, -1, -1)$ is the Minkowski metric of flat spacetime, and k is a constant of order M_{Pl}. As we will see the warp-factor helps solving the hierarchy problem without introducing additional hierarchies.

While in the original setup the SM fields were confined to the visible brane, the possibilities of having other fields in bulk were soon explored. Starting with a scalar field [2, 3, 4, 5], introduced to stabilize the inter-brane distance. The following years various people studied the properties of fermion [6, 7] and gauge fields [8, 9, 7] in the bulk. Even models with the entire SM in bulk have proven interesting as long as the Higgs field stays on the visible brane [10]. The search for experiments that can verify or disprove the RS models or other higher dimensional theories has started. Observable effects from SM matter and gauge fields living in the bulk may be discovered at the LHC [11, 12][1]. Tests of Newton's gravitational law at short distances (sub-millimeter) may reveal aberrations [13, 14, 15]. Here we will explore the corrections to the Casimir effect in RSI and RSII.

The Casimir effect was predicted by H. B. Casimir in 1948 and even a book has been written on the subject [16]. Casimir predicted an attractive force between two perfectly conducting plates. The force is only observable at small distances, and has been experimentally verified with an accuracy of 1%, at distances down to 100nm [17]. Casimir effect in higher dimensional theories has gained a lot of interest recently (see e.g. [18] and the references therein), and also in RS [19, 20, 21, 22, 23, 24, 25]. While in the Casimir effect experiments there is the electromagnetic field that is measured, we will concentrate on a scalar field. The reason being that there are disagreements on how to address the polarizations of the photon in higher dimensional theories. An example is Ref.[26] and Ref.[27], where the extra dimension is a torus ($M^4 \times S^1$) and the spacetime is flat, a far simpler model than RS.

The thesis is organized as follows: First we give a general introduction to the RS models with focus on scalar fields in the bulk. We follow up with some basic Casimir theory. A thorough study of the free energy of a bulk scalar field is in order before starting with the main purpose of this work; the Casimir effect from a bulk scalar on two parallel plates on the visible brane. Before proceeding to finite temperature we study zero temperature. At the end we compare our results with previous work and discuss the controversies yet to be solved.

Throughout this thesis we will use zeta regularization as [19, 20, 23, 24, 25]. The authors of these articles have made some approximations to be

[1] The Large Hadron Collider (LHC) will hopefully be up and about in September 2009, only a few months from today. http://lhc.web.cern.ch/lhc/

able to use Epstein-Hurwitz zeta functions. Since we will use the Abel-Plana formula we do not need to make these approximations and our results are more precise. We will consider different boundary conditions (BC) on the physical plates in contrast to earlier work, which have only studied Dirichlet BC. To the authors knowledge all the finite temperature results presented herein are new.

Chapter 2

The Randall-Sundrum models

The original articles on the Randall-Sundrum models RSI and RSII was published in 1999 [1, 28]. Since then, a lot of articles have been written on the subject. We will present the results from some of these articles and try to give a general introduction to the models.

2.1 The setup, the metric and the action

We stick to the RSI model for most of the time. Results for RSII can be obtained from RSI by letting $r_c \to \infty$. In Figure 2.1 we have illustrated the setup with the visible and the hidden brane. The metric for RSI is

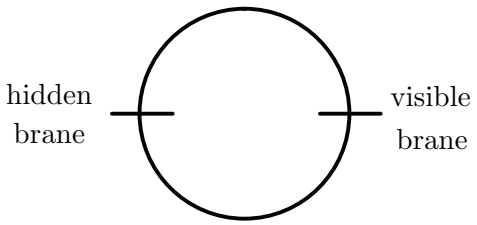

Figure 2.1: Illustration of the RSI branes.

$$\mathrm{d}s^2 = e^{-2kr_c|\phi|}\eta_{\mu\nu}\mathrm{d}x^\mu \mathrm{d}x^\nu - r_c^2 \mathrm{d}\phi^2, \tag{2.1.1}$$

where $\eta_{\mu\nu} = \mathrm{diag}(1,-1,-1,-1)$ is the Minkowski metric. The parameter k is of the Planck scale order. The most important difference from other higher dimensional models is the warp-factor in the metric $e^{-2kr_c\phi}$ which exponentially depends on ϕ. Arabic letters (N,M) are used to denote five-dimensional coordinates (e.g. G_{NM} is the five-dimensional metric) and

Greek letters (μ,ν) refers to a four-dimensional subspace. The metric on the hidden and visible brane are

$$\begin{aligned} g_{\mu\nu}^{\text{vis}} &\equiv G_{\mu\nu}(x^\mu, \phi = \pi) \\ g_{\mu\nu}^{\text{hid}} &\equiv G_{\mu\nu}(x^\mu, \phi = 0). \end{aligned} \tag{2.1.2}$$

The action of this model is

$$\begin{aligned} S &= S_{\text{gravity}} + S_{\text{vis}} + S_{\text{hid}} \\ S_{\text{gravity}} &= \int \mathrm{d}^4x \int_{-\pi}^{\pi} \mathrm{d}\phi \sqrt{-G} \left(-\Lambda + 2M^3 R\right) \\ S_{\text{vis}} &= \int \mathrm{d}^4x \sqrt{-g_{\text{vis}}} \left(\mathcal{L}_{\text{vis}} - V_{\text{vis}}\right) \\ S_{\text{hid}} &= \int \mathrm{d}^4x \sqrt{-g_{\text{hid}}} \left(\mathcal{L}_{\text{hid}} - V_{\text{hid}}\right). \end{aligned} \tag{2.1.3}$$

Here, Λ and R are the five-dimensional cosmological constant and Ricci scalar. In the Lagrangian density of the 3-branes a constant 'vacuum energy' (V_{vis} and V_{hid}) is separated from the rest of the Lagrangian ($\mathcal{L}_{\text{vis}}$ and $\mathcal{L}_{\text{hid}}$). According to Randall and Sundrum the 'vacuum energy' acts as a gravitational source even in the absence of particle excitations and the rest of the Lagrangian is unimportant. We need

$$V_{\text{vis}} = -V_{\text{vis}} = 24M^3k \tag{2.1.4}$$

and

$$\Lambda = -24M^3k^2 \tag{2.1.5}$$

in order to solve Einstein's equations for the action.

2.2 Solving the hierarchy problem

In this section we show that the relation between the fundamental scale M and the Planck scale for flat 4+n dimensional theory

$$M_{\text{Pl}} = M^{n+1}V_n \tag{2.2.1}$$

does not hold in the RS and we find the new relation between M_{Pl} and M. We start with the curvature term of the four-dimensional effective action S_{eff} from Eq.(2.1.3),

$$S_{\text{eff}} \supset \int \mathrm{d}^4x \int_{-\pi}^{\pi} \mathrm{d}\phi 2M^3 r_c e^{-2kr_c|\phi|} \sqrt{-\bar{g}}\bar{R}. \tag{2.2.2}$$

Here, $\bar{g}$ and $\bar{R}$ are the determinant and action of $\bar{g}_{\mu\nu}$. For the branes $g_{\mu\nu}^{\text{hid}} = \bar{g}_{\mu\nu}$ and $g_{\mu\nu}^{\text{vis}} = e^{-2kr_c\pi}\bar{g}_{\mu\nu}$. From this we see that the Planck scale is given by

$$M_{\text{Pl}}^2 = M^3 r_c \int_{-\pi}^{\pi} \mathrm{d}\phi e^{-2kr_x|\phi|} = \frac{M^3}{k}\left(1 - e^{-2kr_c\pi}\right). \tag{2.2.3}$$

In the limit of large kr_c the Planck mass depends only weakly on r_c, but it has a great impact on physical masses as we will see next. In RSII we let $r_c \to \infty$ leaving $M_{\rm Pl}^2 = \frac{M^3}{k}$. To see how RS solve the hierarchy problem we inspect the properties of the Higgs field. The action of the fundamental Higgs field H on the visible brane with one mass parameter v_0 is given by

$$\int \mathrm{d}^4x\sqrt{-g_{\rm vis}}\left(g^{\mu\nu}_{\rm vis}D_\mu H^\dagger D_\nu H - \lambda\left(|H|^2 - v_0^2\right)^2\right). \tag{2.2.4}$$

$D_\mu H$ is the covariant derivative of the Higgs field [1]. Substituting $g^{\rm vis}_{\mu\nu} = e^{-2kr_c\pi}\bar{g}_{\mu\nu}$ into the action yields

$$\int \mathrm{d}^4x\sqrt{-\bar{g}}e^{-4kr_c\pi}\left(\bar{g}^{\mu\nu}e^{2kr_c\pi}D_\mu H^\dagger D_\nu H - \lambda\left(|H|^2 - v_0^2\right)^2\right). \tag{2.2.5}$$

Performing renormalization by the substitution $H \to e^{kr_c\pi}H$ the action is

$$\int \mathrm{d}^4x\sqrt{-\bar{g}}\left(\bar{g}^{\mu\nu}D_\mu H^\dagger D_\nu H - \lambda\left(|H|^2 - v_0^2e^{-2kr_c\pi}\right)^2\right). \tag{2.2.6}$$

Compared with the physical action we see that $v \equiv v_0e^{-kr_c\pi}$. In other words, a mass parameter m_0 on the visible brane will correspond to a physical mass $m = m_0e^{-kr_c\pi}$. If m_0 is of the order of the Planck scale $m_0 \sim 10^{19}$GeV and $kr_c \sim 12$ we find $m \sim 1$TeV and the hierarchy problem is solved.

2.3 The Newtonian gravitational potential

In this section we quote some results concerning the Newtonian gravitational potential in RSI and RSII, to show how this differs from the traditional gravitational potential. The derivation is a transcript from [14] and is based on reduction of the five-dimensional Lagrangian of the graviton to four dimensions. This section not essential to the main part of this thesis but is included to demonstrate how we extract the four-dimensional physics form a higher dimensional theory. We start by rewriting the metric Eq.(2.1.1),

$$\mathrm{d}s^2 = e^{-2k|y|}\eta_{\mu\nu}\mathrm{d}x^\mu\mathrm{d}x^\nu - \mathrm{d}y^2 = \left(\frac{1}{1+k|z|}\right)^2\left(\eta_{\mu\nu}\mathrm{d}x^\mu\mathrm{d}x^\nu - \mathrm{d}z^2\right), \tag{2.3.1}$$

where we have changed coordinate from ϕ to

$$|z| = \frac{e^{kr_c|\phi|} - 1}{k}, \tag{2.3.2}$$

[1] Explicit expressions for the covariant derivative of the Higgs field can be found in e.g. [29]

which is easier to work with and frequently occur in the literature. In connection with RSII it is common to use $y = r_c\phi$ instead of ϕ. By introducing $A(z) = \frac{1}{1+k|z|}$ we can write the perturbed metric as

$$g_{MN} = A^2(z)(\eta_{MN} + h_{MN}) \tag{2.3.3}$$

with $\eta_{MN} = \text{diag}(1, -1, -1, -1, -1)$. Our starting point is the five-dimensional action Eq.(2.1.3), ignoring $\mathcal{L}_{\text{vis}}$ and $\mathcal{L}_{\text{hid}}$,

$$\begin{aligned} S = &\int \mathrm{d}^4x\mathrm{d}y\sqrt{-G}\left(-\Lambda + 2M^3R\right) \\ &+ 24M^3k\int \mathrm{d}^4x\mathrm{d}y(\sqrt{-g_{\text{vis}}}\delta(z - z_r) - \sqrt{-g_{\text{hid}}}\delta(z)), \end{aligned} \tag{2.3.4}$$

where z_r is the z-coordinate on the visible brane. Instead of making a copy of the entire calculation in [14] we list some of the main steps in finding the four-dimensional gravitons.

1. Decomposition of the five-dimensional graviton h_{MN} into

$$h_{MN} = \begin{pmatrix} h_{\mu\nu} & V_\mu \\ V_\nu & T \end{pmatrix}. \tag{2.3.5}$$

2. Choosing a convenient gauge: $V_\mu = 0$ and T independent of z.

3. Redefining the five-dimensional graviton $h_{\mu\nu}$ as

$$h_{\mu\nu} \to h_{\mu\nu} + f(y)\eta_{\mu\nu}T + g(y)\partial_\mu\partial_\nu T, \tag{2.3.6}$$

where

$$\begin{aligned} f(y) &= k|y| + f_0, \quad f_0 = \frac{ky_r}{e^{2ky_r} - 1} \\ g(y) &= \frac{1}{4k^2}\left[f_0\left(e^{2k|y|} - 1\right)^2 + e^{2k|y|}\left(1 - 2k|y|\right) - 1\right] + g_0 \end{aligned} \tag{2.3.7}$$

and $g_0 = g(0)$ can be chosen freely.

4. Since we find the term

$$\int \mathrm{d}^4x\frac{1}{2}\left(\frac{\frac{3}{2}M^3ky_r^2}{e^{2ky_r} - 1}\right)T_{,\alpha}T^{,\alpha} \tag{2.3.8}$$

in the action we can identify the physical radion φ as

$$\varphi = \sqrt{\frac{\frac{3}{2}M^3ky_r^2}{e^{2ky_r} - 1}}T. \tag{2.3.9}$$

We will return to the radion later in this chapter.

5. Expanding $h_{\mu\nu}$ in the eigenstates $\Phi_m(y)$,

$$h_{\mu\nu}(x,y) = 2M^{-\frac{3}{2}} \sum_m h^m_{\mu\nu} \Phi_m(y). \tag{2.3.10}$$

The eigenstates $\Phi_m(y)$ must satisfy the equation of motion, i.e.

$$\Phi''_m(y) + \frac{4A'}{A}\Phi'_m(y) + \frac{m^2}{A^2}\Phi(y) = 0 \tag{2.3.11}$$

and normalization

$$\begin{aligned} \int_{-y_r}^{y_r} A^2(y)\Psi_m(y)\Psi_{m'}(y)\mathrm{d}y &= \delta_{mm'} \\ \int_{-y_r}^{y_r} A^2(y)\Psi'_m(y)\Psi'_{m'}(y)\mathrm{d}y &= m^2\delta_{mm'}. \end{aligned} \tag{2.3.12}$$

After these steps the four-dimensional action is given by

$$\begin{aligned} S = \int \mathrm{d}^4x \Bigg[\sum_m \Bigg(& -\frac{1}{2} h^m{}_{,\alpha} h_m^{,\alpha} + \frac{1}{2} h^m_{\alpha\beta,\nu} h_m^{\alpha\beta,\nu} + h_m^{\alpha\nu}{}_{,\alpha} h^m{}_{,\nu} \\ & - h_m^{\alpha\nu}{}_{,\alpha} h^\beta_{m\ \nu,\beta} - \frac{1}{2} m^2 (h^m_{\alpha\beta} h_m^{\alpha\beta} - h_m^2) \Bigg) + \frac{1}{2} \varphi_{,\mu} \varphi^{,\mu} \Bigg]. \end{aligned} \tag{2.3.13}$$

The notation $\sum_m$ means that we sum over all relevant modes with mass m. This action consists of a massless graviton, a tower of massive gravitons with mass m and a massless scalar field (the radion). The energy-momentum tensor for a source at $y = y'$ is given by

$$T^{MN}(x,y) = \delta^M_\mu \delta^N_\nu T^{\mu\nu}(x)\delta(y - y') \tag{2.3.14}$$

and thus the action for the interaction with matter can be written as

$$S_{int} = -\int \mathrm{d}^4x \mathrm{d}y M^{-\frac{3}{2}} h_{MN} T^{MN} = -\int \mathrm{d}^4x \frac{1}{2} A^2(y') T^{\mu\nu}(x) h_{\mu\nu}(x,y') \tag{2.3.15}$$

with

$$\begin{aligned} h_{\mu\mu}(x,y') = & M^{-\frac{3}{2}} \sum_m h^m_{\mu\nu}(x)\Phi_m(y') \\ & + \sqrt{\frac{e^{2ky_r} - 1}{\frac{3}{2}M^3 k y_r^2}} \left(f(y')\eta_{\mu\nu} + g(y')\partial_\mu\partial_\nu \right) \phi(x). \end{aligned} \tag{2.3.16}$$

The four-dimensional energy-momentum tensor is conserved ($\partial_\mu T^{\mu\nu} = 0$), hence the term with $g(y')$ disappears after partial integration. The Lagrangian density for the interaction with matter is then

$$\begin{aligned} \mathcal{L}_{int} = & -M^{-\frac{3}{2}} A(y') \Big[\sum_m h^m_{\mu\nu}(x)\Phi_m(y') T^{\mu\nu} \\ & + \sqrt{\frac{e^{2ky_r} - 1}{\frac{3}{2}M^3 k y_r^2}} f(y')\eta_{\mu\nu}\varphi(x) T \Big]. \end{aligned} \tag{2.3.17}$$

We can now find the Fourier-transform of the gravitational potential between one mass m_1 on the brane, and another mass m_2 at the point (x, y),

$V(\boldsymbol{k}, p) =$ 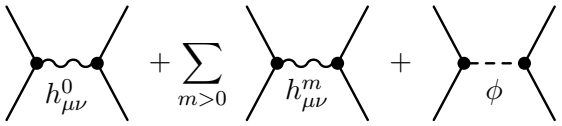

$$
\begin{aligned}
=&\frac{m_1 m_2}{M^3 e^{2ky}}\left[\frac{\Phi_0(0)\Phi_0(p)}{2\boldsymbol{k}^2}+\frac{2}{3}\sum_{m>0}\frac{\Phi_m(0)\Phi_m(p)}{\boldsymbol{k}^2+m^2}\right. \\
&\left.+\frac{e^{2ky_r}-1}{6ky_r^2}\frac{f(0)f(p)}{\boldsymbol{k}^2}\right].
\end{aligned}
\tag{2.3.18}
$$

Afterwards we find the gravitational potential from the Fourier-transform

$$
\begin{aligned}
V(r,y) =& \int \frac{\mathrm{d}^3k}{(2\pi)^3}\frac{1}{y_r}\sum_p V(\boldsymbol{k},p)e^{i\boldsymbol{k}\cdot\boldsymbol{r}}e^{ipy} \\
=&-\frac{m_1 m_2}{8\pi M^3 r e^{2ky}}\left[\Phi_0(0)\Phi_0(y)+\frac{4}{3}\sum_{m>0}\Phi_m(0)\Phi_m(y)e^{-mr}\right. \\
&\left.+\frac{1}{3}\left(\frac{ky}{y_r}+\frac{ke^{-2ky_r}}{1-e^{-2ky_r}}\right)\right].
\end{aligned}
\tag{2.3.19}
$$

Again, the notation $\sum_p$ mean that we sum over all relevant values of p. While k is continuous, p is not since y is periodic, not infinite. Now, in order to find Φ_0 and Φ_m we need to solve Eq.(2.3.11). After inserting $A(y)$ the equation reads

$$
\Psi_m''(y) - 4k\Psi_m'(y) + m^2 e^{-2ky}\Psi_m(y) = 0. \tag{2.3.20}
$$

An equation of the form

$$
y''(x) + ay'(x) + be^{2kx}y(x) + cy(x) = 0 \tag{2.3.21}
$$

has the solution

$$
y(x) = e^{-\frac{1}{2}ax}\left(C_1 J_\nu\left(\frac{\sqrt{b}}{k}e^{kx}\right) + C_2 Y_\nu\left(\frac{\sqrt{b}}{k}e^{kx}\right)\right), \tag{2.3.22}
$$

with $\nu = \sqrt{a^2-4c}/(2k)$. J_ν and Y_ν are the Bessel functions of first and second kind. This solution can be found by either rewriting the equation to the Bessel equation or by using a program like Maple. From Eq.(2.3.22) and Eq.(2.3.20) we find

$$
\Psi_m(y) = \frac{e^{2ky}}{N_m}\left(A_m J_2\left(\frac{m}{k}e^{ky}\right) + B_m Y_2\left(\frac{m}{k}e^{ky}\right)\right) \tag{2.3.23}
$$

and

$$\Psi_0(y) = \sqrt{\frac{k}{1 - e^{-2ky_r}}} \tag{2.3.24}$$

(solving Eq.(2.3.20) when $m = 0$ is rather trivial). We are interested in the potential between two points on the brane at $y = 0$

$$V(r) = -\frac{m_1 m_2}{8\pi M^3 r}\left[\frac{k\left(1 + \frac{1}{3}e^{-2ky_r}\right)}{1 - e^{-2ky_r}} + \frac{4}{3}\sum_{m>0}\Phi_m(0)^2 e^{-mr}\right]. \tag{2.3.25}$$

We can include the effect of the radion in the Planck mass and change Eq.(2.2.3) to

$$M_{\rm Pl}^2 = \frac{M^3}{k}\frac{1 - e^{-2kr_c\pi}}{1 + \frac{1}{3}e^{-2kr_c\pi}}. \tag{2.3.26}$$

This leaves the potential

$$V(r) = -\frac{Gm_1 m_2}{r}\left[1 + \frac{4}{3k}\frac{1 - e^{-2kr_c\pi}}{1 + \frac{1}{3}e^{-2kr_c\pi}}\sum_{m>0}\Phi_m(0)^2 e^{-mr}\right], \tag{2.3.27}$$

where $G = (8\pi M_{Pl}^2)^{-1}$ is the gravitational constant. In the RSII model ($r_c \to \infty$) we have [14, 5, 15]

$$\Psi_m^2(0) = \frac{2k}{\pi m z_r}\frac{1}{J_1^2(m/k) + Y_1^2(m/k)} \tag{2.3.28}$$

and the leading terms in the potential are [15]

$$\begin{aligned} V_{\rm RSII}(r) =& \frac{Gm_1 m_2}{r}\left[1 + \frac{8}{3\pi^2}\int_0^\infty \frac{{\rm d}m\ e^{-mr}}{J_1^2(m/k) + Y_1^2(m/k)}\right] \\ & - \frac{Gm_1 m_2}{r} - \frac{Gm_1 m_2}{r}\begin{cases} \frac{4}{3\pi kr} & kr \ll 1 \\ \frac{2}{3k^2r^2} & kr \gg 1. \end{cases} \end{aligned} \tag{2.3.29}$$

At small distances it should be possible to detect aberrations from the gravitational law. Recent experiments have tested the gravitational force down to 0.218mm [13]. More accurate measurements in the future will be interesting for testing the RS models.

2.4 Scalar fields in bulk

Shortly after the publication of [1] and [28] people started to investigate the possibility of having other fields than the gravitational field in bulk. Goldberger and Wise studied a non-gravitational bulk scalar [2]. They performed a Kaluza-Klein reduction of a (five-dimensional) bulk scalar field with mass of order $M_{\rm Pl}$ to find how such a field would appear to a four-dimensional

(3+1 dimensions) observer. A first guess would be that the field would appear as a tower of scalar fields with masses of the same size as the field itself $\sim M_{\rm Pl}$. As we go through the arguments of Goldberger and Wise we see that contrary to the initial guess, the masses of the modes are suppressed with the factor $e^{-kr_c\pi}$ and are in fact of order TeV. Below we only go through the basic formalism, skipping all the calculations which are the same as in Section 4.2.2. The mathematics involved is not the focus of this section and want to study the behavior of scalar bulk fields without being distracted by mathematical formalism.

As always we start with action of the bulk scalar field in question

$$S_\Phi = \frac{1}{2}\int \mathrm{d}^4x \int_{-\pi}^{\pi} \mathrm{d}\phi \, \sqrt{G}\left(G^{AB}\partial_A\Phi\partial_B\Phi - m^2\Phi^2\right). \tag{2.4.1}$$

A Kaluza-Klein reduction from a higher to a lower dimensional space starts by decomposition of the scalar field. Here we choose

$$\Psi(x,\phi) = \sum_N X_N(x)\psi_N(\phi) \tag{2.4.2}$$

with normalization

$$\frac{1}{r_c}\int_{-\pi}^{\pi} \mathrm{d}\phi e^{-2kr_c|\phi|}\psi_N(\phi)\psi_{N'} = \delta_{NN'}. \tag{2.4.3}$$

This decomposition is the same as in Section 4.2.2 and as we will see there the essential equation in this problem is

$$-\frac{1}{r_c^2}e^{2kr_c|\phi|}\left(-\frac{\mathrm{d}}{\mathrm{d}\phi}e^{-4kr_c|\phi|}\frac{\mathrm{d}\psi_N(\phi)}{\mathrm{d}\phi}\right) + e^{-2kr_c|\phi|}m^2 = M_N^2\psi_N(\phi). \tag{2.4.4}$$

By solving this equation we find ψ_N, and using boundary conditions for the bulk field on the brane we can find all allowed values of M_N, the masses of the Kaluza-Klein modes ψ_N. After integrating out the ϕ dependence using the normalization condition for ψ_N the action is

$$S = \sum_N \frac{1}{2}\int \mathrm{d}^4x \left(\eta^{\mu\nu}\partial_\mu X_N(x)\partial_\nu X_N(x) - M_N^2 X_N(x)^2\right). \tag{2.4.5}$$

From this we conclude that for a four-dimensional observer the bulk scalar field with mass m appears as an infinite 'tower' of scalars $X_N(x)$ with mass M_N, not m. To find the values of M_N^2 we need to solve the equation for ψ_N and impose the correct boundary conditions to the bulk field. This will be done in Section 4.2.2, but here we give the result in advance

$$\psi_N(\phi) = \frac{e^{2kr_c|\phi|}}{C_N}\left(J_\nu\left(\frac{M_N}{k}e^{kr_c|\phi|}\right) + b_\nu(M_N)Y_\nu\left(\frac{M_N}{k}e^{kr_c|\phi|}\right)\right), \tag{2.4.6}$$

with $\nu = \sqrt{4+m^2}$. The Kaluza-Klein masses are

$$M_N = k\pi e^{-k\pi r_c}\left(N + \frac{1}{2}\nu - \frac{3}{4}\right),\ N = 1, 2, \ldots \tag{2.4.7}$$

when we assume $e^{-k\pi r_c} \ll 1$. In the Randall-Sundrum scenario k is assumed to be of the same order as the Planck mass. Thus the lightest masses ($N = 1, 2, \ldots$) are characterized by the TeV scale, not the Planck scale. According to Goldberger and Wise this can be explained by looking at how modes (ψ_N) behave. Close to the TeV brane (at $\phi = \pi$) the ψ_N's are large. Hence it is more likely to find the Kaluza-Klein excitations near that brane and it is reasonable that the modes behave similarly as scalar fields confined to it. Since the masses on the TeV brane are characterized by the TeV scale it is not surprising that the Kaluza-Klein modes of a bulk scalar field are characterized by that same scale.

In Ref.[2] the self-interactions of the bulk scalar are also treated. To a four-dimensional observer this will appear as the coupling between the Kaluza-Klein modes. By concentrating on the light modes, Goldberger and Wise were able to show that the couplings are suppressed by the TeV scale instead of the Planck scale. All in all an exited Kaluza-Klein mode of the bulk scalar field behaves much in the same way as a scalar field confined to the TeV brane with mass M_N. By performing a similar calculation for vector fields in the bulk one can show that the same thing happens. They mimic vector fields confined to the visible brane. Hence, bulk fields can be standard model matter fields with excitations corresponding to standard model particles.

2.5 Stabilization of the radion

One of the first problems of the Randall-Sundrum scenario was how to stabilize the interbrane distance r_c. Naturally there must be some sort of dynamics that govern the behavior of r_c. In this section we will go through the articles by Goldberger and Wise and their attempt to stabilize the model.

2.5.1 The radion field

In the original article by Randall and Sundrum [1] the fluctuations around the background geometry are given by

$$\mathrm{d}s^2 = e^{-2kT(x)}\left(\eta_{\mu\nu} + h_{\mu\nu}\right)\mathrm{d}x^\mu \mathrm{d}x^\nu - T(x)^2 \mathrm{d}\phi^2, \tag{2.5.1}$$

where h is the fluctuations about Minkowski space and represents the four-dimensional physical graviton as in Section 2.3. The reduction of the five-dimensional theory to four-dimensions in order to find the corrections to Newton's gravitational potential was given in Section 2.3. Our current focus

is the modulus field, or radion $T(x)$, found there. This is a massless scalar field and the vacuum expectation value of the radion is the compactification radius of the RSI model r_c. For now we ignore $h_{\mu\nu}$ and write the metric as

$$\mathrm{d}s2 = e^{-2kT(x)} g_{\mu\nu}(x)\mathrm{d}x^\mu \mathrm{d}x^\nu - T(x)^2 \mathrm{d}\phi^2. \tag{2.5.2}$$

We want to demonstrate how the radion occurs naturally in the reduction of the five-dimensional Einstein-Hilbert action,

$$S = \int \mathrm{d}^4x \int_{-\pi}^{\pi} \mathrm{d}\phi \sqrt{G}(-\Lambda + 2M^3 R), \tag{2.5.3}$$

to four dimensions as shown in [4]. In the action above, R is the five-dimensional Ricci scalar and $\Lambda = -24M^3k^2$. Inserting from Eq.(2.5.2) we can write this action as

$$\begin{aligned} S = 2M^3 \int \mathrm{d}^4x \int_{-\pi}^{\pi} \mathrm{d}\phi \sqrt{-g} e^{-2k|\phi|T(x)} \Big(& 6k|\phi| \partial_\mu T \partial^\mu T \\ & - 2k^2 |\phi|^2 T \partial_\mu \partial^\mu T + T R^{(4)} \Big). \end{aligned} \tag{2.5.4}$$

To get the effective four-dimensional theory we integrate out ϕ

$$\begin{aligned} S = & \frac{2M^3}{k} \int \mathrm{d}^4x \sqrt{-g} \left(1 - e^{-2k\pi T(x)}\right) R^{(4)} \\ & + \frac{12M^3}{k} \int \mathrm{d}^4 \sqrt{-g} \partial_\mu \left(e^{-k\pi T(x)}\right) \partial^\mu \left(e^{-k\pi T(x)}\right). \end{aligned} \tag{2.5.5}$$

We can identify the physical radion as $\varphi(x) = f e^{-k\pi T(x)}$ with $f = \sqrt{24M^3/k}$. The five-dimenisonal Einstein-Hilbert action reduces to

$$S = \frac{2M^3}{k} \int \mathrm{d}^4x \sqrt{-g} R^{(4)} + \frac{1}{2} \int \mathrm{d}^4x \sqrt{-g} \left(\partial_\mu \varphi \partial^\mu \varphi - \frac{2}{f^2} R^{(4)} \varphi^2 \right). \tag{2.5.6}$$

If we include the action on the respective branes as in Section 2.1 we conclude that this is the four-dimensional Einstein-Hilbert action plus a four-dimensional massless scalar field φ coupled to gravity with $\zeta = 2/f^2$. However, the action above gives no potential for the radion and thus no way of stabilizing it, and no way to get the right vacuum expectation value r_c. For this reason Goldberger and Wise tried to insert a massive scalar in the bulk with interaction terms on each brane.

2.5.2 Inserting a massive scalar in the bulk

To try to stabilize the interbrane distance in the Randall-Sundrum model Goldberger and Wise put a massive scalar in the bulk, with interaction terms

on the two branes [3, 4]. The action for the scalar field Φ in the bulk with mass m is

$$S_{\text{bulk}} = \frac{1}{2}\int \mathrm{d}^4x \int_{-\pi}^{\pi} \mathrm{d}\phi\sqrt{G}\left(G^{AB}\partial_A\Phi\partial_B\Phi - m^2\Phi\right) \tag{2.5.7}$$

and the interaction terms chosen was

$$S_{\text{hid}} = -\int \mathrm{d}^4x\sqrt{-g_{\text{hid}}}\lambda_{\text{hid}}(\Phi^2 - v_{\text{hid}}^2)^2 \tag{2.5.8}$$

and

$$S_{\text{vis}} = -\int \mathrm{d}^4x\sqrt{-g_{\text{vis}}}\lambda_{\text{vis}}(\Phi^2 - v_{\text{vis}}^2)^2. \tag{2.5.9}$$

The details on how they found the potential for r_c is not important in this setting. In brief they solved the equations of motion (Lagrangian equations) for Φ, put the solution back into the action and did the integration over ϕ. The result was a four-dimensional potential for r_c, capable of stabilizing the system

$$V(\varphi) = \frac{k^3}{144M^6}\varphi^4\left(v_{\text{vis}} - v_{\text{hid}}(\varphi/f)^{\epsilon}\right)^2. \tag{2.5.10}$$

Two assumptions were made to retrieve this potential

- $\epsilon = m^2/4k^2 \ll 1$ (terms of order ϵ have been neglected)
- The parameters λ_{vis} and λ_{hid} are large.

Ignoring terms proportional to ϵ we easily see that the potential has a minimum for

$$kr_c = k\langle T\rangle = \left(\frac{4k^2}{\pi m^2}\right)\ln\left(\frac{v_{\text{vis}}}{v_{\text{hid}}}\right). \tag{2.5.11}$$

To solve the hierarchy problem we need $kr_c \approx 12$. This can be obtained in a number of ways without fine-tuning the parameters. The example used in [3] is $v_{\text{vis}}/v_{\text{hid}} = 1.5$ and $m/k = 0.2$ which gives the wanted value of kr_c. The minimum in Eq.(2.5.11) also holds to the leading term in $1/\lambda_{\text{vis/hid}}$.

Chapter 3

The Casimir effect

In 1948 Casimir published his famous article where he predicted an attractive force between two perfectly conducting plates. This force is today known as the Casimir force. The subject has been studied widely since, and whole books have been devoted to the phenomenon [16].

3.1 Electromagnetic fields

Casimir's original article considered the electromagnetic field between two perfectly conducting plates separated by a distance a. The effect arises because the field has to be zero on the plates. Even though the plates are chargeless with nothing but vacuum between them, they still attract due to vacuum fluctuations in the electromagnetic field. The expectation values of the electric field $\mathbf{E}$ and magnetic field $\mathbf{B}$ might be zero, but the expectation values of the square of the two fields are not. This leads to a non-zero expectation value of the zero-point energy equal to

$$E = \frac{1}{2}\int \mathrm{d}^3 r \left(\epsilon_0 \mathbf{E}^2(\mathbf{r}) + \frac{1}{\mu_0}\mathbf{B}^2(\mathbf{r})\right). \tag{3.1.1}$$

The Casimir effect depends on the boundaries to which the field is confined. For parallel plates and an electromagnetic field the zero-point energy and the attractive forces depend on the distance between the plates. Casimir's result was that the energy per unit area between the plates is proportional to $1/a^3$

$$E/V_\perp = -\frac{\pi^2 \hbar c}{720 a^3}$$

and the force per unit area $P = -\frac{\partial E}{\partial a}$ is proportional to $1/a^4$

$$P/V_\perp = -\frac{\pi^2 \hbar c}{240 a^4}. \tag{3.1.2}$$

Above we have introduced the area of the plates or alternatively the volume of the transverse directions $V_\perp$. There are different ways of calculating the Casimir energy and force at zero temperature.

In quantum mechanics all physical observables have a corresponding operator. The energy operator is the Heisenberg operator $\hat{H}$. The eigenfunctions of this operator satisfying the boundary conditions are often referred to as the modes of the system. It is a common technique to sum over the energy eigenvalues of each mode to find the Casimir energy. After second quantization [30] one can show that the vector potential operator $\hat{\mathbf{A}}$ is

$$\hat{\mathbf{A}}(\mathbf{r}) = \sum_{\mathbf{k},\lambda} \sqrt{\frac{\hbar}{2\epsilon_0 V c k}} \mathbf{e}_{k,\lambda} \left(\hat{a}_{\mathbf{k},\lambda} e^{i\mathbf{k}\cdot\mathbf{r}} + \hat{a}^\dagger_{\mathbf{k},\lambda} e^{-i\mathbf{k}\cdot\mathbf{r}} \right). \tag{3.1.3}$$

Here $\mathbf{k}$ is the wave number of a photon, λ the polarizations and V a large quantization volume. $\hat{a}_{\mathbf{k},\lambda}$ and $\hat{a}^\dagger_{\mathbf{k},\lambda}$ are the annihilation and creation operators respectively. They satisfy the commutation relations $\left[\hat{a}_{\mathbf{k},\lambda}, \hat{a}^\dagger_{\mathbf{k}',\lambda'}\right] = \delta_{\mathbf{k},\mathbf{k}'}\delta_{\lambda,\lambda'}$ and $\left[\hat{a}_{\mathbf{k},\lambda}, \hat{a}_{\mathbf{k}',\lambda'}\right] = \left[\hat{a}_{\mathbf{k},\lambda}, \hat{a}^\dagger_{\mathbf{k}'^\dagger,\lambda'}\right] = 0$. Using $\hat{\mathbf{E}} = -\frac{\partial \hat{\mathbf{A}}}{\partial t}$ and $\hat{\mathbf{B}} = \nabla \times \hat{\mathbf{A}}$ in Eq.(3.1.1) one can show that the energy of the system is

$$E = \sum_{\mathbf{k},\lambda} (\frac{1}{2} + n_{\mathbf{k},\lambda}) \hbar \omega_{\mathbf{k},\lambda}. \tag{3.1.4}$$

Here, $\omega_{\mathbf{k},\lambda}$ is the frequency corresponding to the mode with wave number $\mathbf{k}$ and polarization λ and $n_{\mathbf{k},\lambda}$ is the eigenvalues of the number operator $\hat{n}_{\mathbf{k}\lambda} = \hat{a}^\dagger_{\mathbf{k},\lambda}\hat{a}_{\mathbf{k},\lambda}$, i.e. the number photons within the cavity with energy $\hbar\omega_{\mathbf{k},\lambda}$. Even without any photons in the cavity ($n_{\mathbf{k},\lambda} = 0$ for all $\mathbf{k}$ and λ) the system has a non-zero energy due to the constant $\frac{1}{2}$.

For the system of parallel plates the fields have to be zero on the plates. This leads to quantized wave numbers of the modes orthogonal to the plates say the x-direction. Hence, the energy eigenvalues

$$\hbar\omega_{\mathbf{k},\lambda} = \hbar c \sqrt{k^2 + \frac{n^2\pi^2}{a^2}}, \tag{3.1.5}$$

with $k_\perp^2 = k_y^2 + k_z^2$. The energy depends on a which leads to Casimir forces.

3.2 Massless scalar fields

Electromagnetic fields are not easy to work with because there are modes both parallel and orthogonal to the plates in addition to different polarizations. Imposing boundary conditions can be tricky. It is easier, and also instructive, to consider massless scalar fields instead of electromagnetic fields in complicated calculations. In many situations the results only differ by a

factor of 2 [16]. It can be shown that the zero-point energy density of a massless scalar field between parallel plates is

$$E = \int \frac{\mathrm{d}^2 k_\perp}{(2\pi)^2} \sum_{n=1}^{\infty} \sqrt{k_\perp^2 + \frac{n^2\pi^2}{a^2}}, \tag{3.2.1}$$

Here we have assumed homogenous Dirichlet boundary conditions. In other words; the field has to be zero on the plates. We have also used natural units $\hbar = c = k_B = 1$ which we continue to do throughout this paper. Casimir forces of scalar fields in rectangular cavities are studied in detail by S.C. Lim and L.P. Teo in [31]. The Casimir energy and force per unit area for a massless scalar field is

$$E/V_\perp = -\frac{\pi^2 \hbar c}{1440 a^3} \tag{3.2.2}$$

$$P/V_\perp = -\frac{\pi^2 \hbar c}{480 a^4}. \tag{3.2.3}$$

The above energies and forces are all at zero temperature but it is possible to generalize to finite temperatures.

3.3 Regularization

The sum and integral in Eq.(3.2.1) is highly divergent. To get a finite result we have to regularize the energy. The most intuitive way is to use cut-off-regularization. We introduce an exponential factor $\exp\left(-\alpha\sqrt{k_\perp^2 + \frac{n^2\pi^2}{a^2}}\right)$ to make the integral and sum converge and in the end we let $\alpha \to 0$. Hence, the final answer will not depend on α. There is also dimensional regularization and zeta regularization [32, 33]. The article by Reuter and Dittrich [34] gives an excellent introduction to all three regularization schemes. In this paper we will use zeta regularization because it is practical when dealing with an arbitrary number of succeeding sums. To but it briefly; zeta-regularization consists of using the analytic continuation of Eq.(3.2.1) to the complex plane

$$\zeta(s) = \int \frac{\mathrm{d}^2 k_\perp}{(2\pi)^2} \sum_{n=1}^{\infty} \left(k_\perp^2 + \frac{n^2\pi^2}{a^2}\right)^{-s}. \tag{3.3.1}$$

We need the real part of s to be greater than one ($\mathrm{Re}(s) > 1$) for the expression to converge. In the end we set $s = -\frac{1}{2}$ and obtain the finite answer. Understanding zeta regularization can be hard and we will not try to give the full picture on this elegant way to remove infinities. Curious readers may look up the books by E. Elizalde et al. [32, 33] for further information on the subject.

Chapter 4

The free energy of a bulk scalar field

In order to find the Casimir effect of a bulk scalar field in RS we need the free energy. In this chapter we find the free energy of such a field and other relevant information which we will need later. The bulk scalar field in this chapter is very general and we will choose use specific fields in later chapters.

The setup with the physical plates on the visible brane is illustrated in Figure 4.1 with a interplate distance a. We calculate the free energy of the

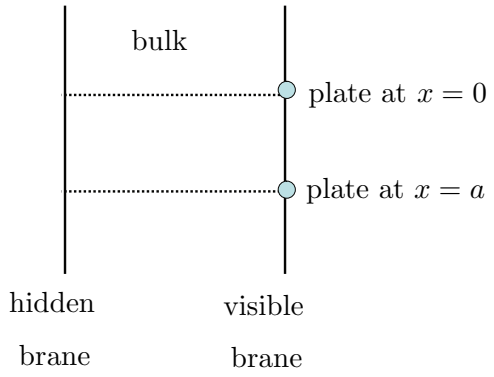

Figure 4.1: Illustration of how the physical plates are located at the visible brane.

area indicated by the dotted lines.

4.1 The partition function of a scalar field

To find the partition function of a non-minimally coupled scalar field Φ with mass m in the RSI we follow a Kaluza-Klein reduction approach like in [35].

We start with the Lagrangian density for such a field,

$$\mathcal{L} = \sqrt{-G}\left(\frac{1}{2}\partial_A\Phi\partial^A\Phi - \frac{1}{2}(m^2 + \zeta R + c_{\text{hid}}\delta(z) + c_{\text{vis}}\delta(z - z_r))\Phi^2\right). \tag{4.1.1}$$

Here, R is the Ricci scalar and $c_{\text{hid/vis}}$ are the boundary mass terms of the field. The partition function is generally given by

$$Z = \int \mathcal{D}\Phi e^{iS[\Phi]} = \int \mathcal{D}\Phi \exp\left(i\int \mathrm{d}^4x\mathrm{d}z\mathcal{L}\right). \tag{4.1.2}$$

Inserting Eq.(4.1.1) and performing a partial integration leaves the partition function

$$\begin{aligned} Z = \int \mathcal{D}\Phi \exp\Bigg[i\int \mathrm{d}^4x\mathrm{d}z\frac{1}{2}\Phi\Big(&- \partial_A A(z)^5\partial^A\Phi \\ &- A(z)^5(m^2 + \zeta R + c_{\text{hid}}\delta(z) + c_{\text{vis}}\delta(z - z_r))\Phi\Big)\Bigg]. \end{aligned} \tag{4.1.3}$$

Remember from Section 2.3 that $|z| = \frac{e^{k|r_c\phi|}-1}{k}$ and $A(z) = \frac{1}{1+k|z|}$. Now we analytically continue t to imaginary times $\tau = it$. Hence, we let $\tilde{x}^i = x^i$, $i = 1, 2, 3$, and $\tilde{x}^0 = ix^0$. After a partial integration the partition function reads

$$\begin{aligned} Z = \int \mathcal{D}\Phi \exp\Bigg[- \int \mathrm{d}^4\tilde{x}\mathrm{d}z\frac{1}{2}\Phi A(z)^3\Bigg(&\underbrace{\tilde{\eta}^{\mu\nu}\partial_\mu\partial_\nu}_{\hat{p}^2} \\ &\underbrace{A(z)^{-3}(-\partial_z A(z)^3\partial_z + A(z)^5(m^2 + \zeta R + c_{\text{hid}}\delta(z) + c_{\text{vis}}\delta(z - z_r)))}_{\hat{M}_z^2}\Phi\Bigg)\Bigg], \end{aligned} \tag{4.1.4}$$

where $\tilde{\eta}^{\mu\nu} = -1\delta^{\mu\nu}$ is the metric for the new coordinates $\tilde{x}$. To proceed we assume it is possible to expand the scalar field in the eigenfunctions $\psi_n(z)$ and $\chi(x^\mu)$ of $\hat{M}_z^2$ and $\hat{p}^2$ respectively,

$$\Phi(\tilde{x}, z) = \sum_{N,p} c_N(p)\chi_p(\tilde{x})\psi_N(z). \tag{4.1.5}$$

The eigenvalue equations for the operators are

$$\hat{M}_z^2\psi_N(z) = M_N^2\psi_N(z), \tag{4.1.6}$$

and

$$\hat{p}^2\chi_p(\tilde{x}) = p^2\chi_p(\tilde{x}) \tag{4.1.7}$$

with normalization

$$\int_{-z_r}^{z_r} \mathrm{d}z \psi_N(z) A(z)^3 \psi_{N'}(z) = \delta_{NN'}, \tag{4.1.8}$$

and

$$\int \mathrm{d}^4\tilde{x} \chi_p(\tilde{x}) \chi_{p'}(\tilde{x}) = \delta_{pp'}. \tag{4.1.9}$$

The fields also have to satisfy the boundary conditions. After inserting the expansions the partition function reads

$$\begin{aligned} Z &= \int \prod_{N,p} \mathrm{d}c_N(p) \exp\left[-\frac{1}{2} \sum_{N,N'} \sum_{p,p'} \delta_{NN'} \delta_{pp'} c_N(p) c_{N'}(p') (M_N^2 + p^2) \right] \\ &= \int \prod_{N,p} \mathrm{d}c_N(p) \exp\left[-\sum_{N,p} c_N(p)^2 \frac{1}{2} (M_N^2 + p^2) \right] \\ &= \left(\prod_{N,p} \sqrt{2\pi} \right) \exp\left[\sum_{M_N} \sum_{p} \ln(M_n^2 + p^2) \right]. \end{aligned} \tag{4.1.10}$$

Here we have made use of

$$\int_{-\infty}^{-\infty} \mathrm{d}x e^{-\lambda x} = \sqrt{\frac{\pi}{\lambda}} = e^{-\frac{1}{2}\ln(\lambda/\pi)} \tag{4.1.11}$$

with $\lambda = \frac{1}{2}(M_N^2 + p^2)$. The notation $\sum_N$ stands for the sum over all relevant eigenvalues M_N and similarly for $\sum_p$. In this case the relevant values are all eigenvalues M_N and p, with eigenfunctions that satisfies the boundary conditions. The next step is to identify the eigenvalues M_N and p that we need to sum over.

4.2 Eigenfunctions and eigenvalues of $\hat{M}_N^2$ and $\hat{p}^2$

In this section we find the eigenfunctions and eigenvalues of $\hat{M}_N^2$ and $\hat{p}^2$ occuring in the partition function of a scalar field.

4.2.1 Eigenfunctions and eigenvalues of $\hat{p}^2$

We start with Eq.(4.1.7)

$$-(\partial_\tau^2 + \partial_x^2 + \partial_y^2 + \partial_z^2)\chi_p(\tilde{x}) = p^2 \chi_p(\tilde{x}). \tag{4.2.1}$$

Remember $\tau = it$, imaginary time. In our three-dimensional physical space we assume Robin boundary conditions on the walls, i.e.

$$(1 + \beta_0 \partial_x)\chi_p(\tilde{x})|_{x=0} = 0 \tag{4.2.2}$$

and

$$(1 - \beta_a \partial_x)\chi_p(\tilde{x})|_{x=a} = 0. \tag{4.2.3}$$

Later we may specify Dirichlet ($\beta = 0$) or Neumann ($\beta = \infty$) BC if desired. We observe that the eigenfunctions are of the form

$$\chi_p(\tilde{x}) = N e^{i(\epsilon_l \tau + k_y y + k_z z)} \cos(k_x x + \alpha) \tag{4.2.4}$$

with eigenvalues

$$p^2 = \epsilon_l^2 + k_x^2 + k_y^2 + k_z^2. \tag{4.2.5}$$

There are constraints on both ϵ_l and k_x. For a boson field τ is periodic in β thus ϵ_l is equal to the Matsubara frequencies

$$\epsilon_l = \frac{2\pi}{\beta} l = 2\pi T, \quad l \in \mathbb{Z}. \tag{4.2.6}$$

Here, T is the temperature. Inserting $\chi_p(\tilde{x})$ into Eq.(4.2.2) we get the constraints on α,

$$\cos\alpha = \frac{\beta_0 k_x}{\sqrt{1 + \beta_0^2 k_x^2}} \quad \text{or} \quad \sin\alpha = \frac{1}{\sqrt{1 + \beta_0^2 k_x^2}}. \tag{4.2.7}$$

There is however one boundary condition left. To satisfy Eq.(4.2.3) we need

$$F_x(k_x a) = \sin(k_x R)(1 - k_x^2 \beta_1 \beta_2) - k_x(\beta_1 + \beta_2)\cos(k_x a) = 0. \tag{4.2.8}$$

At this point we do not need the function F_x, but we will return to it later in connection with the Abel-Plana formula.

4.2.2 Eigenfunctions and eigenvalues of $\hat{M}_N^2$

Now, we turn to the more complicated eigenvalue problem Eq.(4.1.6),

$$\begin{aligned} &A(z)^{-3}\Big[- \partial_z A(z)^3 \partial_z + A(z)^5 (m^2 + \zeta R \\ &+ c_{\text{hid}}\delta(z) + c_{\text{vis}}\delta(z - z_r))\Big]\psi_N(z) = M_N^2 \psi_N(z). \end{aligned} \tag{4.2.9}$$

The five-dimensional Ricci scalar for the Randall-Sundrum metric is

$$R = -20k^2 + 16k(\delta(z) - \delta(z - z_r)). \tag{4.2.10}$$

We choose to solve the eigenequation for the bulk first to avoid the delta functions on the branes. The Z_2 symmetry allows us to only simplify by solving only for positive values of y (or z), $0 < y < \pi r_c$ (or $0 < z < z_r$). Later we will take the branes into consideration. To solve the equation above we change the coordinates back to y using

$$\frac{\mathrm{d}}{\mathrm{d}z} = A(y)\frac{\mathrm{d}}{\mathrm{d}y} \tag{4.2.11}$$

and rewrite the eigenequation

$$\begin{aligned} -A(y)^{-2}\frac{\mathrm{d}}{\mathrm{d}y}\left(A(y)^4\frac{\mathrm{d}\psi_N(y)}{\mathrm{d}y}\right) + A(y)^2(m^2-20\zeta k^2)\psi_N(y) &= M_N^2\psi_N(y) \\ 4k\psi_N'(y) - \psi_N''(y) + (m^2-20\zeta k^2)\psi_N(y) &= e^{2ky}M_N^2\psi_N(y) \\ \psi_N''(y) - 4k\psi_N'(y) + \left(M_N^2e^{2ky} - (m^2-20\zeta k^2)\right)\psi_N(y) &= 0. \end{aligned} \tag{4.2.12}$$

We have already seen a similar expression in Section 2.3 and use Eq.(2.3.22) to find the solution

$$\psi_N(y) = \frac{e^{2ky}}{C_N}\left(J_\nu\left(\frac{M_N}{k}e^{ky}\right) + b_\nu(M_N)Y_\nu\left(\frac{M_N}{k}e^{ky}\right)\right), \tag{4.2.13}$$

with $\nu = \sqrt{4+(m/k)^2-20\zeta}$. This is the same result as in [7], except we include arbitrary coupling to curvature ($\zeta \neq 0$) in our model. To account for the delta functions induced by the Ricci scalar and mass boundary terms we integrate Eq.(4.1.6) over both branes. This will give us the boundary conditions for ψ_N. First we integrate over the hidden brane from $-\epsilon$ to ϵ

$$\begin{aligned} \int_{-\epsilon}^{\epsilon}\frac{\mathrm{d}}{\mathrm{d}y}\left(e^{4k|y|}\frac{\mathrm{d}\psi_N(y)}{\mathrm{d}y}\right)\mathrm{d}y - \int_{-\epsilon}^{\epsilon}e^{-4k|y|}\Big[m^2-20\zeta k^2 + (16\zeta k + c_{\mathrm{hid}})\delta(0) \\ + (-16\zeta k + c_{\mathrm{vis}})\delta(y-\pi r_c)\Big]\mathrm{d}y = \int_{-\epsilon}^{\epsilon}e^{-2k|y|}M_N^2\mathrm{d}y. \end{aligned} \tag{4.2.14}$$

In the limit $\epsilon \to 0$ only two terms remain

$$\begin{aligned} e^{4k|y|}\frac{\mathrm{d}\psi_N(y)}{\mathrm{d}y}\bigg|_{-\epsilon}^{\epsilon} - (16\zeta + c_{\mathrm{hid}})\psi_N(0) &= 0 \\ \Rightarrow \frac{\mathrm{d}\psi_N(y)}{\mathrm{d}y}\bigg|_{0^+} - \frac{\mathrm{d}\psi_N(y)}{\mathrm{d}y}\bigg|_{0^-} &= (16\zeta k + c_{\mathrm{hid}})\psi_N(0). \end{aligned} \tag{4.2.15}$$

Similarly the integration over the visible brane yields

$$\frac{\mathrm{d}\psi_N(y)}{\mathrm{d}y}\bigg|_{y_r^+} - \frac{\mathrm{d}\psi_N(y)}{\mathrm{d}y}\bigg|_{y_r^-} = (-16\zeta k + c_{\mathrm{vis}})\psi_N(y_r). \tag{4.2.16}$$

Apparently the derivative of $\psi_N(y)$ can have a jump across the branes, even though $\psi_N(y)$ is continuous across them. To proceed further we have to distinguish between even and odd scalar fields.

Even fields

Even fields have the symmetry

$$\psi_N(-y) = \psi_N(y) \quad \text{and consequently} \quad \frac{\mathrm{d}\psi_N(-y)}{\mathrm{d}y} = -\frac{\mathrm{d}\psi_N(y)}{\mathrm{d}y}. \tag{4.2.17}$$

Inserting the derivative into Eq.(4.2.15) and Eq.(4.2.16) results in

$$\left.\frac{\mathrm{d}\psi_N(y)}{\mathrm{d}y}\right|_{0^+} = (8k\zeta + c_{\mathrm{vis}})\psi_N(0) \tag{4.2.18}$$

and

$$\left.\frac{\mathrm{d}\psi_N(y)}{\mathrm{d}y}\right|_{y_r^-} = -(-8k\zeta + c_{\mathrm{hid}})\psi_N(y_r). \tag{4.2.19}$$

Odd fields

Odd fields have the symmetry

$$\psi_N(-y) = -\psi_N(y) \quad \text{and consequently} \quad \frac{\mathrm{d}\psi_N(-y)}{\mathrm{d}y} = \frac{\mathrm{d}\psi_N(y)}{\mathrm{d}y}. \tag{4.2.20}$$

Again, inserting this into Eq.(4.2.15) and Eq.(4.2.16) results in

$$(8k\zeta + c_{\mathrm{hid}})\psi_N(0) = (-8k\zeta + c_{\mathrm{vis}})\psi_N(y_r) = 0. \tag{4.2.21}$$

Odd fields have no restrictions on $\psi'_N(y)$ but have to be zero at the branes. If $(\pm 8k\zeta + c_{\mathrm{hid/vis}}) = 0$ Equation (4.2.21) is fulfilled without restrictions on $\psi_N(y)$, but the field still have to be zero due to Eq.(4.2.20) at $y = 0$ and $y = r_r = \pi r_c$.

To summarize:

- Even scalar fields must obey Robin boundary conditions on the brane ($\psi'_N(y)|_{\mathrm{brane}} + (\mathrm{const.})\ \psi_N(y)|_{\mathrm{brane}} = 0$). If the field is minimally coupled ($\zeta = 0$) and we have no mass boundary term ($c_{\mathrm{brane}} = 0$) the boundary conditions reduce to Neumann BC ($\psi'_N(y)|_{\mathrm{brane}} = 0$).

- Odd scalar fields must obey Dirichlet boundary conditions at the branes.

The odd and the even case can be treated simultaneously by writing the boundary conditions as Robin conditions

$$(1 - \beta_{\mathrm{hid}}\partial_y)\,\psi_N(y)|_{y=0^+} = 0 \quad \text{and} \quad (1 - \beta_{\mathrm{vis}}\partial_y)\,\psi_N(y)|_{y=y_r^-} = 0, \tag{4.2.22}$$

where $\beta_{\mathrm{hid}}^{-1} = (8k\zeta + c_{\mathrm{hid}}/2)$ and $\beta_{\mathrm{vis}}^{-1} = (8k\zeta - c_{\mathrm{vis}}/2)$. The limit $\beta_{\mathrm{brane}} \to \infty$ leaves Neumann BC and $\beta_{\mathrm{brane}} \to 0$ changes it to Dirichlet. The BC are the same as found in [7]. We want to find a function F_N who's zeros give the values of M_N. Inserting Eq.(4.2.13) into Eq.(4.2.22) yields

$$b_\nu(M_N/k) = -\frac{j_\nu^{\mathrm{hid}}(M_N/k)}{y_\nu^{\mathrm{hid}}(M_N/k)} = -\frac{j_\nu^{\mathrm{vis}}(e^{k\pi r_c}M_N/k)}{y_\nu^{\mathrm{vis}}(e^{k\pi r_c}M_N/k)}. \tag{4.2.23}$$

Here we have introduced

$$\begin{aligned} j_\nu^{\text{brane}}(z) &= (2-(k\beta_{\text{brane}})^{-1})J_\nu(z) + zJ'_\nu(z) \\ y_\nu^{\text{brane}}(z) &= (2-(k\beta_{\text{brane}})^{-1})Y_\nu(z) + zY'_\nu(z). \end{aligned} \tag{4.2.24}$$

For the special case $\beta_{\text{brane}} = 0$ we can replace $j_\nu^{\text{brane}}(z)$ with $J_\nu(z)$ and similarly $y_\nu^{\text{brane}}(z)$ with $Y_\nu(z)$. The constraint on M_N can be written as $F_N(z) = 0$, where $z = e^{k\pi r_c}M_N/k$, $d = e^{-k\pi r_c}$ and

$$F_N(z) = j_\nu^{\text{hid}}(zd)y_\nu^{\text{vis}}(z) - j_\nu^{\text{vis}}(z)y_\nu^{\text{hid}}(zd). \tag{4.2.25}$$

This is in accordance with [36] if we choose a minimally coupled field ($\zeta = 0$) and $c_{\text{hid}} = -c_{\text{vis}} = 2\alpha/k$.

Important remark on $M_N = 0$

For fields with $m^2 - 20\zeta k^2 \neq 0$ we have no solution to Eq.(4.2.12) with $M_N = 0$ that satisfy Robin BC on both branes. For an even field with $m^2 - 20\zeta k^2 \neq 0$ (e.g. a massless, minimally coupled field), with no boundary mass term the situation is different.

$\psi_0 =$ constant is a solution to both Eq.(4.2.12) and the boundary conditions which in that case are Neumann BC. We will later see that the $M_N = 0$ mode have profound consequences for the Casimir force from a bulk scalar. The massless mode is troublesome as we will discuss in Chapter 7 and the reason for this is the localization properties of it. As a consequence we will give a brief review of the localization properties of all the Kaluza-Klein modes.

Localization of the modes

In Section 2.4 we looked at the massive bulk scalar field introduced by Goldberger and Wise [2]. They argued that the modes (all massive) of the bulk scalar was localized near the TeV brane and therefore it is natural to expect mode masses of order TeV. Too see where a field is localized you have to look at the wave function of the field to see if you can find some sort of probability function.

Let us take a familiar example form quantum mechanics; the hydrogen atom [30]. If you have an electron in the state 1s its wave function[1] is $\psi_{1s} = 1/\sqrt{\pi a_0^3}e^{-r/a_0}$, with a_0 being the Bohr radius. The probability for finding the electron in the volume element $\mathrm{d}V$ is $\psi_{1s}^2\mathrm{d}V$, but the probability $p(r)$ of finding the electron between r and $r + \mathrm{d}r$ is $4\pi r^2\psi_{1s}^2\mathrm{d}r = p(r)\mathrm{d}r$. The normalization of the wave function tells us $\int_{allspace}\psi_{1s}^2(r)\mathrm{d}^3r = 1$ and after integrating out the angles we are left with $\int_0^\infty 4\pi r^2\psi_{1s}^2(r)\mathrm{d}r = 1$. You can read $p(r)$ out of the normalization.

[1] We are looking at the hydrogen atom in the Schrödinger picture.

If we now turn our attention to the modes of a bulk scalar we have the normalization

$$\int_{-\pi r_c}^{\pi r_c} e^{-2k|y|}\Psi_N(|y|)^2 \mathrm{d}y = 2\int_0^{\pi r_c} e^{-2ky}\Psi_N(y)^2 \mathrm{d}y = 1. \tag{4.2.26}$$

It is not only Ψ_N^2 that tells us something about where to look for the mode excitations, but $p_N(y) = 2e^{-2ky}\Psi_N^2(y)$. For the massive modes $p_N(y)$ is much larger near the visible (TeV) than the hidden (Plank) brane and thus the massive modes are localized near the visible brane. The massless mode ($M_N = 0$) has $p_0(r) \propto e^{-2ky}$ and is localized near the hidden brane at $y = 0$. This applies to RSI. In RSII the situation is reversed. The massless mode is localized near the visible brane at $y =$ and the massive modes are delocalized.

The questions addressed in recent papers [22, 37] are: Should the massless mode contribute to the Casimir force between two physical plates on the visible brane in the same manner as the massive modes? Or should the massless mode in RSI be given less weight due to the fact that it is localized on the hidden brane, far from the localization of the plates? We will comment on this question in Section 7.4.

4.2.3 Approximations of the mode masses

We assume $d \ll 1$, but keep $z \not\ll 1$ to find explicit expression for all the Kaluza-Klein masses. This implies that $M_N/k \ll 1$ and $e^{k\pi r_c}M_N/k \not\ll 1$. To find the zeros of $F_N(z)$ we investigate how $j_\nu^{\text{brane}}(z)$ and $y_\nu^{\text{brane}}(z)$ in Eq.(4.2.24) behave for small arguments. The properties of the Bessel functions J_ν and Y_ν can be found in [38]

$$\begin{aligned} J_\nu(z) &= \frac{\left(\frac{1}{2}z\right)^\nu}{\Gamma(\nu+1)}, z \ll 1 \\ Y_\nu(z) &= -\frac{\Gamma(\nu)}{\pi}\left(\frac{1}{2}z\right)^{-\nu}, z \ll 1. \end{aligned} \tag{4.2.27}$$

The derivatives of the Bessel functions are

$$\begin{aligned} J'_\nu(z) &= -J_{\nu+1}(z) + \frac{\nu}{z}J_\nu(z) \\ Y'_\nu(z) &= -Y_{\nu+1}(z) + \frac{\nu}{z}Y_\nu(z). \end{aligned} \tag{4.2.28}$$

From this we can conclude that $j_\nu^{\text{brane}}(z) \ll y_\nu^{\text{brane}}(z)$ when $z \ll 1$. In this limit Eq.(4.2.25) reduces to

$$j_\nu^{\text{vis}}(e^{k\pi r_c}M_N/k) = 0. \tag{4.2.29}$$

We need all the zeros of this functions and have to remember that $e^{k\pi r_c}M_N/k$ is not small. This situation can be split into two: Dirichlet and non-Dirichlet BC.

Dirichlet boundary conditions ($\beta_{\text{brane}} = 0$)

From Eq.(4.2.24) we see that when we to employ Dirichlet BC we need the zeros of $J_2(z)$. For large values of z

$$J_\nu(z) \sim \sqrt{\frac{2}{\pi z}} \cos(z - \frac{1}{2}\nu\pi - \frac{1}{4}\pi). \tag{4.2.30}$$

Hence, the Bessel function of first kind share zeros with $\cos\left(z - \frac{1}{2}\nu\pi - \frac{1}{4}\pi\right)$ when z is large. An example where $\nu = 2$ is plotted in Figure 4.2. The plot is of $\cos\left(z - \frac{5}{4}\pi\right)/\sqrt{z}$, $J_2(z)$ and $10^{-21}F_N(z)$ for $d = 10^{-12}$. It is the zeros that are important so the scaling factor in front of the functions are irrelevant. We see that the first couple of zeros are slightly off but the others

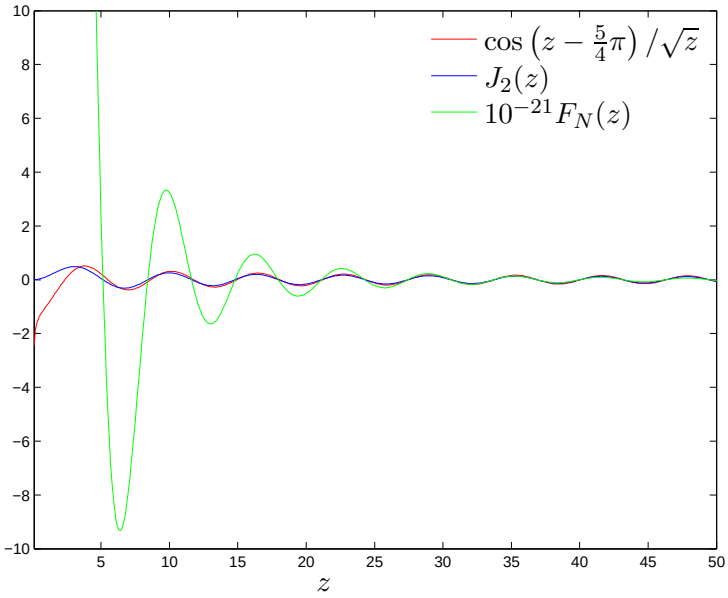

Figure 4.2: Plot of $\cos\left(z - \frac{5}{4}\pi\right)/\sqrt{z}$, $J_2(z)$ and $10^{-21}F_N(z)$ with $d = 10^{-12}$ to illustrate how the zeros of the functions coincide for large z.

match quite well. The zero of the cosine matching the Nth zero ($z_N^{k\beta_{\text{brane}}=0}$ in Figurefig:errjandcos) of $F_M(z)$ is $\left(N + \frac{3}{4}\right)\pi$. The error in the zeros can be seen in Figure 4.3 and it approaches zero as N increases. Thus, the approximation

$$M_N = k\pi e^{-k\pi r_c}\left(N + \frac{1}{2}\nu - \frac{1}{4}\right), \; N = 1, 2, \ldots \tag{4.2.31}$$

is fairly good for Dirichlet boundary conditions.

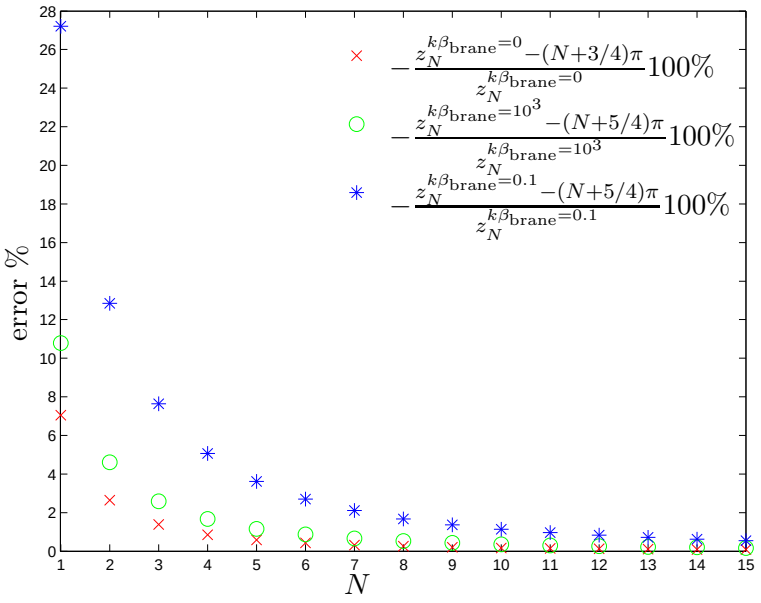

Figure 4.3: Plot of the error for the N'th zero of F_M with $d = 10^{-12}$ and $\nu = 2$ when we approximate the zeros with the zeros of $\cos\left(z - \frac{5}{4}\pi\right)$ for $k\beta_{\text{brane}} = 0$ and $\cos\left(z + \frac{1}{4}\pi\right)$ for $k\beta_{\text{brane}} = 10^3$ and $k\beta_{\text{brane}} = 0.1$.

Non-Dirichlet boundary conditions ($\beta_{\text{brane}} \neq 0$)

Secondly we treat non-Dirichlet BC and Eq.(4.2.29) can be written as

$$j_\nu(z) = (2 + \nu - (k\beta)^{-1})J_\nu(z) - zJ_{\nu+1}(z). \tag{4.2.32}$$

At large arguments $zJ_{\nu+1}$ dominates and the function shares zeros with $\cos\left(z - \frac{1}{2}\nu\pi - \frac{3}{4}\pi\right)$. Figure 4.4 shows $F(z)$, $J_{\nu+1}(z)$ and $10^{-23}F_M(z)$ for $\nu = 2$ and $d = 10^{-12}$. If $k\beta > 1$ the accordance between $-j_2(z)$ and $\cos\left(z + \frac{1\pi}{4}\right)$ is good, even for the first couple of zeros. For $k\beta = 0.1$ the first zeros are completely off and this is generally true for small values of $k\beta$. As pointed out in [7] the approximation

$$M_N = k\pi e^{-k\pi r_c}\left(N + \frac{1}{2}\nu - \frac{3}{4}\right), \; N = 1, 2, \ldots \tag{4.2.33}$$

is good for $k\beta > 1$ and gets better for higher N as long as $k\beta > 0$. We see an example of the errors made in Figure 4.3 where $\nu = 2$, $d = 10^{-12}$ and $k\beta_{\text{brane}} = 0.1$ or $k\beta_{\text{brane}} = 10^3$.

We are now finished with the eigenfunctions and eigenvalues of $\hat{M}_N^2$ and $\hat{p}^2$. It is time to find the free energy of the bulk scalar from the partition function.

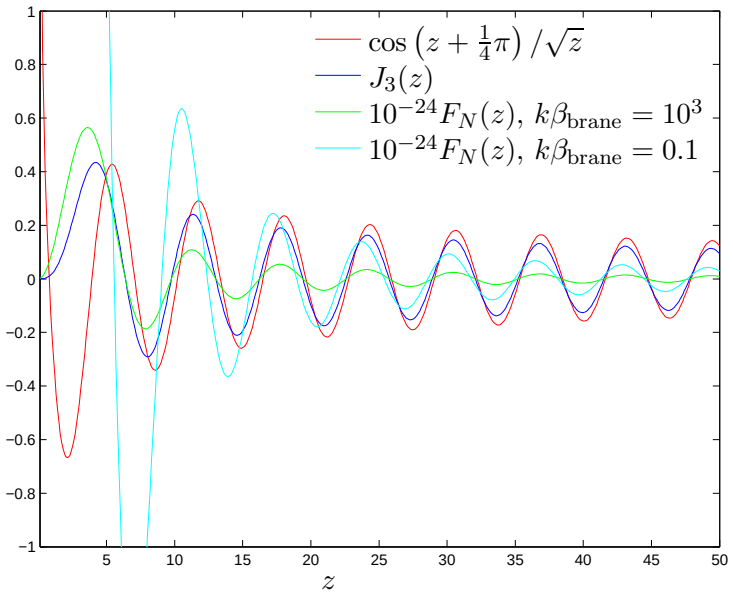

Figure 4.4: Plot of $\cos\left(z+\frac{1}{4}\pi\right)/\sqrt{z}$, $J_3(z)$ and $10^{-24}F_N(z)$ for both $k\beta_{\text{brane}}=10^3$ and $k\beta_{\text{brane}}=0.1$ and $d=10^{-12}$ to illustrate how the zeros of the functions coincide for large z.

4.3 Free Energy

Ignoring the unimportant prefactor of Eq.(4.1.10) the free energy reads

$$F=-\frac{1}{\beta}\ln Z=\frac{1}{2\beta}\sum_{M_N}\sum_{p}\ln\left(M_N^2+p^2\right), \tag{4.3.1}$$

with the sum running over the values of M_N and p we found in Section 4.2. Inserting the results give

$$F=-\frac{1}{\beta}\ln Z=\frac{1}{2\beta}V_\perp\int\frac{\mathrm{d}^2k}{(2\pi)^2}\sum_{l=-\infty}^{\infty}\sum_{M_N,k_x}\int\ln\left(M_N^2+\epsilon_l^2+k_x^2+k_\perp^2\right). \tag{4.3.2}$$

where $k_\perp=k_y^2+k_z^2$ and the sum over k_x and M_N are given by all the real zeros of the functions

$$F_x(k_x)=\sin(k_xR)(1-k_x^2\beta_1\beta_2)-k_x(\beta_1+\beta_2)\cos(k_xR) \tag{4.3.3}$$

and

$$F_N(M_N)=j_\nu^{\text{hid}}(M_N/k)y_\nu^{\text{vis}}(e^{k\pi r_c}M_N/k)-j_\nu^{\text{vis}}(e^{k\pi r_c}M_N/k)y_\nu^{\text{hid}}(M_N/k) \tag{4.3.4}$$

respectively. It is important not to mix up the free energy F with the functions F_x and F_N. The free energy density is highly divergent as it stands and needs regularization. For a positive definite operator Ω with eigenvalues λ_J the zeta function ζ is defined as

$$\zeta(\Omega \mid s) = \sum_J \lambda_J^{-s}. \tag{4.3.5}$$

This series will converge for large values of $\mathrm{Re}(s)$ and can be analytically continued to the entire complex plane. It is possible to define the regularized determinant of Ω as

$$\det \Omega = \exp\left\{ -\left.\frac{\mathrm{d}\zeta(\Omega \mid s)}{\mathrm{d}s}\right|_{s=0} \right\}. \tag{4.3.6}$$

The motivation for this is

$$\begin{aligned} \exp\left\{ -\left.\frac{\mathrm{d}\zeta(\Omega \mid s)}{\mathrm{d}s}\right|_{s=0} \right\} &= \exp\left\{ \left. \sum_J \ln \lambda_J e^{-s \ln \lambda_J} \right|_{s=0} \right\} \\ &= \exp\left\{ \sum \ln \lambda_J \right\}. = \prod_J \lambda_J \end{aligned} \tag{4.3.7}$$

In our case $\Omega = \hat{M}_N^2 + \hat{p}^2$ and $\lambda = M_N^2 + k_\perp^2 + k_x^2 + \epsilon_l^2$, and accordingly the correct zeta function is

$$\zeta(s) = \sum_{l=-\infty}^{\infty} V_\perp \int \frac{\mathrm{d}^2 k}{(2\pi)^2} \sum_{M_N, k_x} \left(M_N^2 + \epsilon_l^2 + k_x^2 + k_\perp^2 \right)^{-s}. \tag{4.3.8}$$

We follow the same steps as in [39] when regularizing. The free energy is expressed with the zeta function as

$$F = -\frac{1}{2\beta} \frac{\partial}{\partial s} \mu^{2s} \zeta(s), \tag{4.3.9}$$

where μ is an arbitrary parameter with the dimension of mass.

Note: We need an additional factor $-\frac{\mathcal{N}}{\beta}\log(\beta)$ in the free energy, with $\mathcal{N}$ being the number of modes with $k_\perp^2 + k_x^2 + M_n^2 = 0$ [31]. We only need to take this into consideration when $M_N = 0$.

We will calculate two different, but equivalent, expressions for the free energy density. One where we do the integration over the transverse mode and one where we leave all the integrations for later.

4.3.1 The classical expression for the free energy

We will find the classical expression for the free energy rewriting using that the Mellin transform of $b^{-z}\Gamma(z)$ is e^{-bt}, i.e.

$$b^{-z}\Gamma(z) = \int_0^\infty t^{z-1} e^{-bt} \mathrm{d}t \Rightarrow b^{-z} = \frac{1}{\Gamma(z)} \int_0^\infty t^{z-1} e^{-bt} \mathrm{d}t. \tag{4.3.10}$$

Inserting $\epsilon_l = 2\pi l/\beta$ we write

$$F = \frac{1}{2\beta}\frac{\partial}{\partial s}\frac{\mu^s}{\Gamma(s)}V_\perp \int \frac{\mathrm{d}^2k}{(2\pi)^2}\sum_{M_N,k_x}\sum_{l=-\infty}^{\infty}\int_0^\infty \mathrm{d}t\; t^{s-1}e^{-t\left(\epsilon_l^2+k_x^2+k_\perp^2+M_N^2\right)} \tag{4.3.11}$$

and apply the Poisson summation formula

$$\sum_{l=-\infty}^{\infty} b(l) = 2\pi \sum_{p=-\infty}^{\infty} c(2\pi p) \tag{4.3.12}$$

where $c(\alpha)$ is the Fourier-transform of $b(l)$. With

$$b(l) = e^{-t\frac{(2\pi)^2}{\beta^2}l^2}, \tag{4.3.13}$$

we find

$$c(\alpha) = \frac{1}{2\pi}\int_{-\infty}^{\infty} b(l)e^{-i\alpha l}\mathrm{d}l = \frac{\beta}{4\pi\sqrt{\pi t}}e^{-\frac{\beta^2\alpha^2}{4t(2\pi)^2}}. \tag{4.3.14}$$

After the transformations the free energy reads

$$F = \frac{1}{4\sqrt{\pi}}V_\perp \int \frac{\mathrm{d}^2k}{(2\pi)^2}\sum_{M_N,k_x}\sum_{p=-\infty}^{\infty}\int_0^\infty \mathrm{d}t\; t^{-\frac{1}{2}-1}e^{-\frac{p^2\beta^2}{4t}-t\left(k_x^2+k_\perp^2+M_N^2\right)}. \tag{4.3.15}$$

We have used that for any function $g(z)$

$$\frac{\mathrm{d}}{\mathrm{d}z}\left(\frac{g(z)}{\Gamma(z)}\right)\bigg|_{z=-n} = \frac{(-1)^n}{n!}g(-n), \tag{4.3.16}$$

for $n = 0 \pm 1, \pm 2\ldots$ Separating the $p = 0$ term from the rest we can use Eq.(4.3.10) to get it on the form

$$\frac{1}{2}V_\perp \int \frac{\mathrm{d}^2k}{(2\pi)^2}\sum_{M_N,k_x}\sqrt{k_x^2+k_\perp^2+M_N^2}. \tag{4.3.17}$$

This is the familiar expression for the (free) energy at $T = 0$ and is the only term that survives the limit $T \to 0$. Performing the integration and summation on the remaining parts lead to

$$\begin{aligned} F &= V_\perp \int \frac{\mathrm{d}^2k}{(2\pi)^2}\sum_{M_N,k_x}\left(\frac{1}{2}\sqrt{k_x^2+k_\perp^2+M_N^2}+\frac{1}{\beta}\ln\left(1-e^{-\beta\sqrt{k_x^2+k_\perp^2+M_N^2}}\right)\right) \\ &= \frac{V_\perp}{\beta}\int \frac{\mathrm{d}^2k}{(2\pi)^2}\sum_{M_N,k_x}\ln\left(2\sinh\left(\frac{\beta}{2}\sqrt{k_x^2+k_\perp^2+M_N^2}\right)\right). \end{aligned} \tag{4.3.18}$$

It is worth noting that for a boson with energy E_p contributes with

$$Z_p = \sum_{n=1}^{\infty} e^{-\beta E_p (n+1/2)} = \frac{1}{2\sinh(\beta E_p/2)}, \tag{4.3.19}$$

to the total partition function [36]. Summing over all energies yields the classical expression corresponding to the one above. We could in principle have started with with this expression, but since the next expression for the free energy occurs more naturally from the method in this chapter we chose otherwise.

4.3.2 A more usable expression for the free energy

In this section we will calculate the zeta function for the free energy and at the same time do the integration over the transverse modes. At the starting point the free energy reads

$$F = -\frac{V_\perp}{2\beta}\frac{\partial}{\partial s}\mu^{2s}\sum_{l=-\infty}^{\infty}\sum_{M_N,k_x}\int\frac{\mathrm{d}^2k}{(2\pi)^2}\left(\underbrace{M_N^2+\epsilon_l^2+k_x^2}_{A}+k_\perp^2\right)^{-s}. \tag{4.3.20}$$

We start by doing the integration over the transverse modes directly using a generalized polar coordinate transformation

$$\begin{aligned}
x_1 &= k_y = r\cos\theta_1 \\
x_2 &= k_z = r\sin\theta_1\cos\theta_2 \\
x_3 &= r\sin\theta_1\sin\theta_2\cos\theta_3 \\
&\vdots \\
x_{N_\perp-1} &= r\sin\theta_1 ... \sin\theta_{n-2}\cos\theta_{n-1} \\
x_{N_\perp} &= r\sin\theta_1 ... \sin\theta_{n-2}\sin\theta_{n-1}.
\end{aligned} \tag{4.3.21}$$

Here we introduce the variable $N_\perp$ as the number of variables we integrate over. In this case the $N_\perp$ is the number of transverse modes (equal to two). We also introduce

$$A = M_N^2 + \epsilon_l^2 + k_x^2, \tag{4.3.22}$$

since A does not depend on any of the variables we integrate over. This may seem like much trouble for nothing since an ordinary two dimensional coordinate transformation will do the trick. However this makes it easy to obtain the zero temperature limits. To find $E = F(T=0)$ we let

$$\sum_{l=-\infty}^{\infty} f(\epsilon_l) \to \beta\int_{-\infty}^{\infty}\frac{\mathrm{d}\epsilon}{2\pi}f(\epsilon). \tag{4.3.23}$$

By rewriting the free energy

$$F = -\frac{V_\perp}{2\beta}\frac{\partial}{\partial s}\mu^{2s}\sum_{l=-\infty}^{\infty}\sum_{M_N,k_x}\int\frac{\mathrm{d}^{N_\perp}k_\perp}{(2\pi)^{N_\perp}}\left(A+k_\perp^2\right)^{-s}, \tag{4.3.24}$$

we find the finite temperature expressions by setting $N_\perp = 2$. To get the zero temperature expressions:

1. change $N_\perp = 2$ to $N_\perp = 3$
2. remove the sum over l
3. set $\epsilon_l = 0$
4. let $V_\perp \to V_\perp\beta$.

After the coordinate transformation and introduction of $N_\perp$, we follow the same steps as in [40] and integrate out the angles

$$F = -\frac{V_\perp}{2\beta(2\pi)^{N_\perp}}\frac{\partial}{\partial s}\mu^{2s}\sum_{l=-\infty}^{\infty}\sum_{M_N,k_x}\frac{2\pi^{N_\perp/2}}{\Gamma(N_\perp/2)}\int_0^\infty \mathrm{d}r\ r^{N_\perp-1}(A+r^2)^{-s}. \tag{4.3.25}$$

The integral can be solved by performing the variable change $x = r^2/A$ and recognizing the integral representation of the Beta function (see Eq.(6.2.1) from [38])

$$B(q,v) = \int_0^\infty \frac{\mathrm{d}t\ t^{v-1}}{(1+t)^{v+q}}, \tag{4.3.26}$$

with $v = N_\perp/2$ and $q = s - N_\perp/2$. Using the following property of the Beta function (see Eq.(6.2.2) from [38])

$$B(q,v) = \frac{\Gamma(v)\Gamma(q)}{\Gamma(v+q)}, \tag{4.3.27}$$

we find

$$F = -\frac{V_\perp}{2\beta(2\pi)^{N_\perp}}\frac{\partial}{\partial s}\mu^{2s}\frac{\pi^{\frac{N_\perp}{2}}\Gamma\left(s-\frac{N_\perp}{2}\right)}{\Gamma(s)}\sum_{l=-\infty}^{\infty}\sum_{M_N,k_x}A^{\frac{N_\perp}{2}-s}. \tag{4.3.28}$$

In this approach we also need Eq.(4.3.16) to find the final expression for the free energy,

$$F = -\frac{V_\perp\pi^{\frac{N_\perp}{2}}}{2\beta(2\pi)^{N_\perp}}\Gamma\left(-\frac{N_\perp}{2}\right)\sum_{l=-\infty}^{\infty}\sum_{M_N,k_x}\left(M_N^2+\epsilon_l^2+k_x^2\right)^{\frac{N_\perp}{2}}. \tag{4.3.29}$$

The two approaches lead to different expressions for the free energy density. The choice of the former or latter expression depends on what kind of regularization procedure one prefer to use later. In [36] the former expression was used in connection with the argument principle. Since we want to work with zeta functions here we chose the latter. Eq.(4.3.29) will be frequently used in later chapters.

Zero temperature

By using the procedure to obtain the zero temperature limit on Eq.(4.3.29) we see that

$$E = -\frac{V_\perp \pi^{\frac{(N_\perp+1)}{2}}}{2(2\pi)^{N_\perp+1}}\Gamma\left(-\frac{N_\perp+1}{2}\right)\sum_{M_N,k_x}\left(M_N^2+k_x^2\right)^{\frac{N_\perp+1}{2}}. \qquad (4.3.30)$$

is an alternative expression for the zero point energy.

Chapter 5

Zero temperature

Before trying to handle finite temperature we calculate the Casimir energy and force at zero temperature. This has been done [19, 24, 20] for Dirichlet BC on the physical plates by applying the approximations of Section 4.2.3. By using the Abel-Plana formula [41, 42], instead of Epstein-Hurwitz zeta functions, there is no need to make these approximations, hence the results from this chapter are more accurate than previous results.

When $T = 0$ ($\beta = \infty$) Eq.(4.3.18) reduces to the familiar expression

$$E = \frac{V_\perp}{2} \int \frac{\mathrm{d}^2 k}{(2\pi)^2} \sum_{M_N, k_x} \sqrt{k_x^2 + k_\perp^2 + M_N^2}. \tag{5.0.1}$$

We can divide the energy into two separate parts $E = E(M_N = 0) + E(M_N > 0)$. With $E(M_N = 0)$ equal to the energy of the massless scalar in Minkowski spacetime ($E(M_N = 0) = E_{\mathrm{Mink}}$) treated in Section 3.2. For massive scalar fields there is no massless mode ($M_N = 0$) and the final expression (from the $M_N > 0$ modes) bears no resemblance to E_{Mink} at all. If the bulk scalar is massless we have a massless mode, and the total energy is equal to the energy in Minkowski spacetime plus corrections arising from the $M_N > 0$ modes.

Throughout this and the the following chapter we will assume no massless mode. In Section 4.2.2 we concluded that only when the field is even, minimally coupled and massless there exists a $M_N = 0$ mode. If we want to find the Casimir force and energy for such a field we simply to add the massless mode term. We will therefore start by finding the energy and force of Minkowski spacetime (or the $M_N = 0$ mode) first, both in this chapter and the finite temperature chapter. The physical implications of the massless mode will be dicussed thoroughly in Section 7.4.

5.1 The Abel-Plana formula

Considering that Eq.(5.0.1) is infinite as is stands we need to regularize it. There are several options and one of these is the generalized Abel-Plana formula [41, 42]

$$\sum_{n=1}^{\infty}\frac{\pi f(z_n)}{1+\sin(z_n)\cos(z_n+2\alpha)/z_n}=\underbrace{-\frac{\pi}{2}\frac{f(0)}{1-\beta_0/a-\beta_a/a}}_{1}$$
$$+\underbrace{\int_0^\infty \mathrm{d}z f(z)}_{2}+\underbrace{i\int_0^\infty \mathrm{d}z\frac{f\left(e^{i\pi/2}z\right)-f\left(e^{-i\pi/2}z\right)}{\frac{(\beta_0/a-1)(\beta_a/a-1)}{(\beta_0/a+1)(\beta_a/a+1)}e^{2z}-1}}_{3}. \tag{5.1.1}$$

Here, z_n denotes the n'th zero of the function $f(z)$ in the right half-plane of the complex plane. The zeros are arranged in ascending order $z_n < z_{n+1}$. The β's are those of Section 4.2.1 since this version of the Abel-Plana formula is especially designed to be used in Casimir effect problems with Robin BC.

5.1.1 Limitations of the Abel-Plana formula

Before we proceed the limitations of Eq.(5.1.1) must be addressed. Eq.(5.1.1) is not valid for all BC on the physical plates (i.e. all values of β_j). The Abel-Plana formula originates from the residue theorem. This version of the Abel-Plana formula is especially suitable for Casimir problems with Robin BC and a detailed derivation can be found in [41, 43]. The function $F_x(z = ak_x)$ given by Eq.(4.2.8) is central in the derivation since the sum over k_x in the energy is equal to the real zeros of $F(z)$. One of the conditions for Eq.(5.1.1) is that this function has no purely imaginary zeros ($z = 0$ is OK). To find the limitations on the β's we look at

$$F(iz)=i\left((1+\beta_0 a\beta_a a z^2)\sinh z-(\beta_0 a+\beta_a a)z\cosh z\right). \tag{5.1.2}$$

For us it is important that this function has no zeros (except $z = 0$) for Dirichlet-Dirichlet ($\beta_0 = \beta_a = 0$), Neumann-Neumann ($\beta_0 = \beta_a = \infty$) or Dirichlet-Neumann ($\beta_0 = 0, \beta_a = \infty$ or $\beta_0 = \infty, \beta_a = 0$) BC. Generally we have three different situations [43]

1. F(z) has no positive imaginary zeros for $\{\beta_0 a + \beta_a a \geq 1, \beta_0\beta_a \leq 0\} \cup \{b_{0,a} \leq 0\}$
2. F(z) has one single positive imaginary zero for $\{0 < \beta_0 a + \beta_a a < 1, \beta_0\beta_a \leq 0\} \cup \{\beta_0 a + \beta_a a \geq 1, b_{0,a} > 0\} \cup \{\beta_0 a + \beta_a a < 0, \beta_0\beta_a < 0\}$
3. F(z) has two positive imaginary zeros for $\{\beta_0 a + \beta_a a < 1, \beta_{0,1} > 0\}$

To each positive real zero is a corresponding negative purely imaginary zero. As long as we fulfill the condition of no imaginary zeros we need not to worry about the extra contributions the imaginary zeros would give.

5.1.2 Applying the Abel-Plana formula to the energy

We follow [42] closely in this section when using the Abel-Plana formula to perform the summation over k_x. From the equations of Section 4.2.1 we find the relation

$$1+\sin(z_n)\cos(z_n+2\alpha)/z_n = 1-\frac{\beta_0/a}{1+(\beta_0/az_n)^2}-\frac{\beta_a/a}{1+(\beta_a/az_n)^2}. \quad (5.1.3)$$

Hence we must choose

$$f(z)=\frac{1}{\pi}\sqrt{(z/a)^2+k_\perp^2+M_n^2}\left(1-\sum_{j=0,a}\frac{\beta_j/a}{1+(\beta_j/az)^2}\right) \quad (5.1.4)$$

to match the expression in Eq.(5.0.1) and Eq.(5.1.1). It is practical to evaluate the three integrals in Eq.(5.1.1) separately:

1.
$$\begin{aligned}&-\frac{V_\perp}{2}\int\frac{\mathrm{d}^2k_\perp}{(2\pi)^2}\sum_{M_N}\frac{\pi}{2}\frac{f(0)}{1-\beta_0/a-\beta_a/a}\\ =&-\frac{V_\perp}{4}\int\frac{\mathrm{d}^2k_\perp}{(2\pi)^2}\sum_{M_N}\sqrt{k_\perp^2+M_N^2}.\end{aligned} \quad (5.1.5)$$

   This term does not depend on a and will not give a contribution to the Casimir force between the plates in physical space.

2. We split the second integral into three parts

$$\begin{aligned}&\frac{V_\perp}{2}\int\frac{\mathrm{d}^2k_\perp}{(2\pi)^2}\sum_{M_N}\int_0^\infty\mathrm{d}z f(z)\\ =&\frac{V_\perp}{2}\int\frac{\mathrm{d}^2k_\perp}{(2\pi)^2}\sum_{M_N}\int_{-\infty}^\infty\frac{a}{2\pi}\mathrm{d}k_x\sqrt{k_\perp^2+k_x^2+M_N^2}\\ &-V_\perp\sum_{j=0,a}\frac{\beta_j}{\pi}\int\frac{\mathrm{d}^2k_\perp}{(2\pi)^2}\sum_{M_N}\int_0^\infty\mathrm{d}x\frac{\sqrt{k_\perp^2+x^2+M_N^2}}{1+\beta_j^2x^2}.\end{aligned} \quad (5.1.6)$$

   The notation $\sum_{j=0,a}$ refers to one term for β_0 and another for β_a. We recognize the first term as $-E(a\to\infty)$, the energy when the plates are sent to infinity or the energy with no plates present. The terms dependent on β_j vanish when we assume Neumann or Robin boundary conditions in any combination, and are in addition not dependent on a.

3. Since

$$f(e^{i\frac{\pi}{2}}z) = \begin{cases} \frac{1}{\pi}\sqrt{k_\perp^2 + M_N^2 - z^2/a^2}\left(1 - \sum_{j=0,a}\frac{\beta_j/a}{1-(\beta_j/az_n)^2}\right) \\ \text{for } (z/a)^2 \leq k^2 + M_N^2 \\ e^{i\frac{\pi}{2}}\frac{1}{\pi}\sqrt{z^2/a^2 - k_\perp^2 - M_N^2}\left(1 - \sum_{j=0,a}\frac{\beta_j/a}{1-(\beta_j/az_n)^2}\right) \\ \text{for } (z/a)^2 > k^2 + M_N^2 \end{cases} \tag{5.1.7}$$

and

$$f(e^{-i\frac{\pi}{2}}z) = \begin{cases} \frac{1}{\pi}\sqrt{k_\perp^2 + M_N^2 - z^2/a^2}\left(1 - \sum_{j=0,a}\frac{\beta_j/a}{1-(\beta_j/az_n)^2}\right) \\ \text{for } (z/a)^2 \leq k^2 + M_N^2 \\ e^{-i\frac{\pi}{2}}\frac{1}{\pi}\sqrt{z^2/a^2 - k_\perp^2 - M_N^2}\left(1 - \sum_{j=0,a}\frac{\beta_j/a}{1-(\beta_j/az_n)^2}\right) \\ \text{for } (z/a)^2 > k^2 + M_N^2 \end{cases} \tag{5.1.8}$$

the integrand of the third integral is zero for $(z/a)^2 < k^2 + M_N^2$. Changing the variable to $x = z/a$ we find

$$\begin{aligned} \Delta E =& i\frac{V_\perp}{2}\int\frac{\mathrm{d}^2k_\perp}{(2\pi)^2}\sum_{M_N}\int_0^\infty \mathrm{d}z \frac{f\left(e^{i\pi/2}z\right) - f\left(e^{-i\pi/2}z\right)}{\frac{(\beta_0/a-1)(\beta_a/a-1)}{(\beta_0/a+1)(\beta_a/a+1)}e^{2z} - 1} \\ =& -\frac{V_\perp}{\pi}\int\frac{\mathrm{d}^2k_\perp}{(2\pi)^2}\sum_{M_N}\int_{\sqrt{k_\perp^2+M_N^2}}^\infty \mathrm{d}x \frac{\sqrt{x^2 - k_\perp^2 - M_N^2}}{\frac{(\beta_0/a-1)(\beta_a/a-1)}{(\beta_0/a+1)(\beta_a/a+1)}e^{2ax} - 1} \\ & \times\left(a + \sum_{j=0,a}\frac{\beta_j}{(\beta_j x)^2 - 1}\right). \end{aligned} \tag{5.1.9}$$

We have introduced ΔE in the same way as in [42] and also copy the notation by collecting the rest of the energy into two parts

$$\begin{aligned} E_j =& -\frac{V_\perp}{8}\int\frac{\mathrm{d}^2k_\perp}{(2\pi)^2}\sum_{M_N}\sqrt{k_\perp^2 + M_N^2} \\ & -\frac{V_\perp\beta_j}{\pi}\int\frac{\mathrm{d}^2k_\perp}{(2\pi)^2}\sum_{M_N}\int_0^\infty \mathrm{d}x\frac{\sqrt{k_\perp^2 + x^2 + M_N^2}}{1+\beta_j^2x^2} \\ E_{\mathrm{NP}} =& \frac{V_\perp a}{2}\int\frac{\mathrm{d}^3k}{(2\pi)^3}\sqrt{k^2 + M_N^2}. \end{aligned} \tag{5.1.10}$$

E_{NP} is the energy when no plates are present, and E_j can be interpreted as the vacuum energy along the transverse directions induced by the plate at $x_0 = 0$ and $x_a = a$ respectively. The energy can be written as

$$E = E_{\mathrm{NP}} + \sum_{j=0,a}E_j + \Delta E. \tag{5.1.11}$$

Before discussing the energy further we need to introduce the piston model.

5.2 The piston model

In recent literature the piston model has attained a great deal of attention [44, 45, 46, 47, 48, 49, 50, 51]. We introduce the piston (Figure 5.1) with the same notation as in Chapter 4.3 of [32]. Instead of only using the energy E_{I}

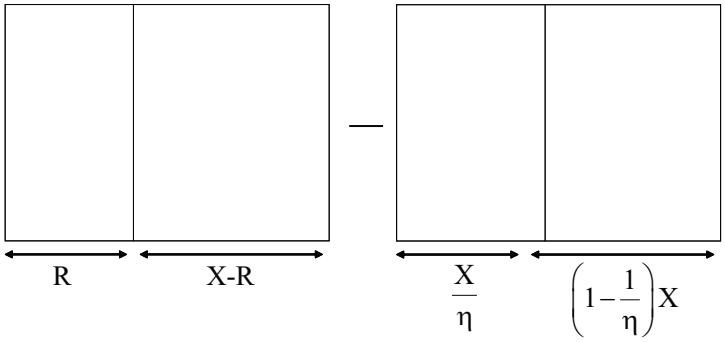

Figure 5.1: Illustration of the four cavities in the piston model.

of cavity I as the Casimir energy, we use

$$E_{\text{piston}} = E^I(a) + E^{II}(X-a) - E^{III}(X/\eta) - E^{IV}(X(1-1/\eta)). \quad (5.2.1)$$

Initially the system is in an unstressed situation where the cavities have size X/η and $X(1-1/\eta)$. Then we shift the middle plate so that the lengths of the two cavities are a and $X-a$; the system is now in a stressed situation. The Casimir energy is the sum the energies of two cavities in the stressed case (I and II) minus the energies of the cavities in the unstressed case (III and IV). The constant η is ~ 2, characterizing the unstressed situation. In the end we let $X \to \infty$ and effectively remove the rightmost plate from the setup.

For the three different parts of the energy in Eq.(5.1.11) the introduction of the piston model have different consequences. E_j does not depend on a, hence the sum of E_j over the four cavities is zero. E_{NP} is linear in a and will also drop out since $a + (X-a) - (X/\eta) - (X(1-1/\eta)) = 0$. Thus both E_j and E_{NP} vanish in the piston model. ΔE goes to zero when $a \to \infty$ and so $\Delta E^{\mathrm{II}}(X-a) - \Delta E^{\mathrm{III}}(X/\eta) - \Delta E^{\mathrm{IV}}(X(1-1/\eta)) = 0$. All in all we conclude that $E_{\text{piston}} = \Delta E$.

In the rest of this chapter we will work with the piston model. The notation $E^{\mathrm{BC}}_{\mathrm{RSI/RSII}}$ refer to the energy per surface area (i.e. $E_{\text{piston}}/V_\perp$) where the subscript refer to the specific model and the superscripts denotes the boundary conditions. The phrase 'energy density' may also be used for this quantity. Similarly $P^{\mathrm{BC}}_{\mathrm{RSI/RSII}}$ is the force per unit area.

5.3 Casimir energy and force in flat spacetime

As promised we find the Casimir energy and force in Minkowski spacetime of a massless scalar field, equal to the $M_N = 0$ mode of the bulk scalar field in RS. Hence we remove the sum over M_N in Eq.(5.1.9) and set $M_N = 0$. In the previous section we concluded that in the piston model only ΔE is interesting. Before presenting the final answer we have a couple of integrations left. A good start is to integrate out the angles of $\mathrm{d}^2k_\perp$, and we proceed by a series of variable changes

$$\begin{aligned}
E_{\text{Mink}} =& -\frac{1}{\pi}\int_0^\infty \frac{k_\perp \mathrm{d}k_\perp}{2\pi}\int_{\sqrt{k_\perp^2+M_N^2}}^\infty \mathrm{d}x\sqrt{x^2-k_\perp^2} \\
&\times \underbrace{\frac{a+\sum_{j=0,a}\frac{\beta_j}{(\beta_j x)^2-1}}{\frac{(\beta_0/a-1)(\beta_a/a-1)}{(\beta_0/a+1)(\beta_a/a+1)}e^{2ax}-1}}_{g(x)} \\
\overset{x=\sqrt{z^2-k_\perp^2}}{=}& -\frac{1}{2\pi^2}\int_0^\infty \mathrm{d}k_\perp \int_0^\infty \mathrm{d}y \frac{k_\perp y^2}{\sqrt{y^2+k_\perp^2}} g(\sqrt{y^2+k_\perp^2}) \qquad (5.3.1)\\
\overset{\substack{y=r\sin\theta\\ k_\perp=r\cos\theta}}{=}& -\frac{1}{2\pi^2}\underbrace{\int_0^{\frac{\pi}{2}}\mathrm{d}\theta\ \cos\theta\sin^2\theta}_{1/3}\int_0^\infty \mathrm{d}r\ r^3 g(r) \\
=& -\frac{1}{6\pi^2}\int_0^\infty \mathrm{d}r\ r^3 \frac{a+\sum_{j=0,a}\frac{\beta_j}{(\beta_j x)^2-1}}{\frac{(\beta_0/a-1)(\beta_a/a-1)}{(\beta_0/a+1)(\beta_a/a+1)}e^{2ax}-1}.
\end{aligned}$$

Let us tak a break to comment on the expression above. It is the energy of the cavity between two parallel plates in the piston model with arbitrary boundary conditions. It is valid for all values of β_0 and β_a that do not lead to imaginary zeros of $F_N(z)$. Since this expression holds for Dirichlet-Dirichlet (DD), Neumann-Neumann (NN) and Dirichlet-Neumann (DN) BC we will stick to these three specific examples in the following sections.

5.3.1 Dirichlet-Dirichlet or Neumann-Neumann boundary conditions

We assume either Dirichlet BC on both plates or Neumann BC on both plates. The energy is the same so we treat them as one case

$$E_{\text{Mink}}^{\text{DD,NN}} = -\frac{a}{6\pi^2}\int_0^\infty \mathrm{d}r \frac{r^3}{e^{2ar}-1}. \qquad (5.3.2)$$

To be able to solve the integral we expand the denominator in the exponential factor

$$\begin{aligned}\frac{1}{e^{2ar}-1} &= \frac{e^{-2ar}}{1-e^{-2ar}} \\ &= e^{-2ar}\left(1+e^{-2ar}+e^{-2(2ar)}+\ldots\right) = \sum_{n=1}^{\infty} e^{-2nar}\end{aligned} \tag{5.3.3}$$

giving

$$\begin{aligned}E_{\text{Mink}}^{\text{DD,NN}} &= -\frac{a}{6\pi^2}\sum_{n=1}^{\infty}\underbrace{\int_0^{\infty}\mathrm{d}r\; r^3 e^{-2anr}}_{\frac{6}{(2an)^4}} \\ &= -\frac{1}{16\pi^2 a^3}\underbrace{\sum_{n=1}\frac{1}{n^4}}_{\zeta_R(4)=\pi^4/90} = -\frac{\pi^2}{1440a^3}.\end{aligned} \tag{5.3.4}$$

This is the result already mentioned in Chapter 3. For the first time we have introduced the Riemann zeta function

$$\zeta_R(s) = \sum_{n=1}^{\infty}\frac{1}{n^s}. \tag{5.3.5}$$

The Casimir force of Minkowski spacetime is

$$P_{\text{Mink}}^{\text{DD,NN}} = -\frac{\pi^2}{480a^4}. \tag{5.3.6}$$

These two expressions will be used later to compare the Casimir effect in RSI and RSII with the Casimir effect in Minkowski spacetime.

5.3.2 Dirichlet-Neumann boundary conditions

Now we turn to Dirichlet boundary conditions on one plate and Neumann boundary conditions on the other. The resulting energy density is

$$E_{\text{Mink}}^{\text{DN}} = \frac{a}{6\pi^2}\int_0^{\infty}\mathrm{d}r\frac{r^3}{e^{2ar}+1}. \tag{5.3.7}$$

The expansion of the denominator is somewhat different

$$\begin{aligned}\frac{1}{e^{2ar}+1} &= \frac{e^{-2ar}}{1+e^{-2ar}} \\ &= e^{-2ar}\left(1-e^{-2ar}+e^{-2(2ar)}-\ldots\right) = -\sum_{n=1}^{\infty}(-1)^n e^{-2nar}.\end{aligned} \tag{5.3.8}$$

This leads to the energy

$$\begin{aligned} E^{\rm DN}_{\rm Mink} &= -\frac{a}{6\pi^2}\sum_{n=1}^{\infty}(-1)^n \underbrace{\int_0^\infty {\rm d}r\; r^3 e^{-2anr}}_{\frac{6}{(2an)^4}} \\ &= -\frac{1}{16\pi^2 a^3}\underbrace{\sum_{n=1}(-1)^n\frac{1}{n^4}}_{-\frac{7}{8}\zeta_R(4)=\pi^4/90} = \frac{7}{8}\frac{\pi^2}{1440a^3}. \end{aligned} \tag{5.3.9}$$

Here we have used that

$$\sum_{n=1}^{\infty}\frac{(-1)^n}{n^s} = -\sum_{n=1}^{\infty}\frac{1}{n^s} - 2\sum_{i=1}^{\infty}\frac{1}{(2n)^s} = -\left(1-\frac{1}{2^{s-1}}\right)\zeta_R(s) \tag{5.3.10}$$

is valid for all real $s > 1$. The corresponding Casimir force is

$$P^{\rm DN}_{\rm Mink} = \frac{7}{8}\frac{\pi^2}{480a^4} \tag{5.3.11}$$

and predicts a slightly smaller and repulsive Casimir force. The Casimir force for DD/NN BC is always attractive. The experimental verification of repulsive Casimir forces as a result of different boundary conditions is recent [52]. We are now armed with the Casimir energy and force in Minkowski spacetime for DD or NN and DN BC and ready to handle RSI and RSII.

5.4 Casimir energy and force in RSI

The well known expressions for the Casimir energy and force in Minkowski spacetime were derived more or less as an exersice before starting with RSI. We mention, once again, that only ΔE is important in the piston model. In this an the following chapter we pay no attention to the terms independent of a and linear in a as they cancel in the piston model. We start with Eq.(5.0.1) and perform variable changes similar to those in Eq.(5.3.1). Only

the last step is different

$$
\begin{aligned}
E_{\rm RSI} =& -\frac{1}{\pi}\int_0^\infty \frac{k_\perp {\rm d}k_\perp}{2\pi}\sum_{M_N}\int_{\sqrt{k_\perp^2+M_N^2}}^\infty {\rm d}x\sqrt{x^2-k_\perp^2-M_N^2} \\
&\times \underbrace{\frac{a+\sum_{j=0,a}\frac{\beta_j}{(\beta_j x)^2-1}}{\frac{(\beta_0/a-1)(\beta_a/a-1)}{(\beta_0/a+1)(\beta_a/a+1)}e^{2ax}-1}}_{g(x)} \\
\overset{y=\sqrt{x^2-k_\perp^2-M_N^2}}{=}& -\frac{1}{2\pi^2}\sum_{M_N}\int_0^\infty {\rm d}k_\perp\int_0^\infty {\rm d}y\frac{k_\perp y^2}{\sqrt{y^2+k_\perp^2+M_N^2}}g(\sqrt{y^2+k_\perp^2+M_N^2}) \\
\overset{\substack{y=r\sin\theta\\ k_\perp=r\cos\theta}}{=}& -\frac{1}{2\pi^2}\sum_{M_N}\underbrace{\int_0^{\frac{\pi}{2}}{\rm d}\theta\ \cos\theta\sin^2\theta}_{1/3}\int_0^\infty {\rm d}r\ \frac{r^4}{\sqrt{r^2+M_N^2}}g(\sqrt{r^2+M_N^2}) \\
\overset{x=\sqrt{r^2+M_N^2}}{=}& -\frac{1}{6\pi^2}\sum_{M_N}\int_{M_N}^\infty {\rm d}x\ (x^2-M_N^2)^{\frac{3}{2}}g(x) \\
=& -\frac{1}{6\pi^2}\sum_{M_N}\int_{M_N}^\infty {\rm d}x\ (x^2-M_N^2)^{\frac{3}{2}}\frac{a+\sum_{j=0,a}\frac{\beta_j}{(\beta_j x)^2-1}}{\frac{(\beta_0/a-1)(\beta_a/a-1)}{(\beta_0/a+1)(\beta_a/a+1)}e^{2ax}-1}.
\end{aligned}
\tag{5.4.1}
$$

Now we look at specific boundary conditions for simplicity.

5.4.1 Dirichlet-Dirichlet or Neumann-Neumann boundary conditions

The integral in Eq.(5.4.1) is simplified when assuming DD and NN boundary conditions

$$
E_{\rm RSI}^{\rm DD,NN} = -\frac{a}{6\pi^2}\sum_{M_N}\int_{M_N}^\infty {\rm d}x\ \frac{(x^2-M_N^2)^{\frac{3}{2}}}{e^{2ax}-1}. \tag{5.4.2}
$$

After expanding the denominator we find

$$
E_{\rm RSII}^{\rm DD,NN} = -\frac{a}{6\pi^2}\sum_{M_N}\sum_{n=1}^\infty\int_{M_N}^\infty (x^2-M_N^2)^{\frac{3}{2}}e^{-2anx}. \tag{5.4.3}
$$

The integral leads to modified Bessel functions of the second kind. We use 3.387(3) from [53],

$$
\int_1^\infty (x^2-1)^{\nu-1}e^{-\mu x}{\rm d}x = \frac{1}{\sqrt{\pi}}\left(\frac{2}{\mu}\right)^{\nu-\frac{1}{2}}\Gamma(\nu)K_{\nu-\frac{1}{2}}(\mu), \tag{5.4.4}
$$

to find

$$E_{\mathrm{RSI}}^{\mathrm{DD,NN}} = -\frac{1}{8\pi^2 a}\sum_{n=1}^{\infty}\sum_{M_N}\frac{M_N^2}{n^2}K_2(2aM_N n). \tag{5.4.5}$$

This is in accordance with [42] through that paper does not consider the Casimir effect rising from a bulk scalar in the RS model in particular. Still we have not specified M_N. The Casimir energy in RSI without approximations, and with $d = 10^{-12}$ is shown in Figure 5.2 for both DD, NN and DN boundary conditions.

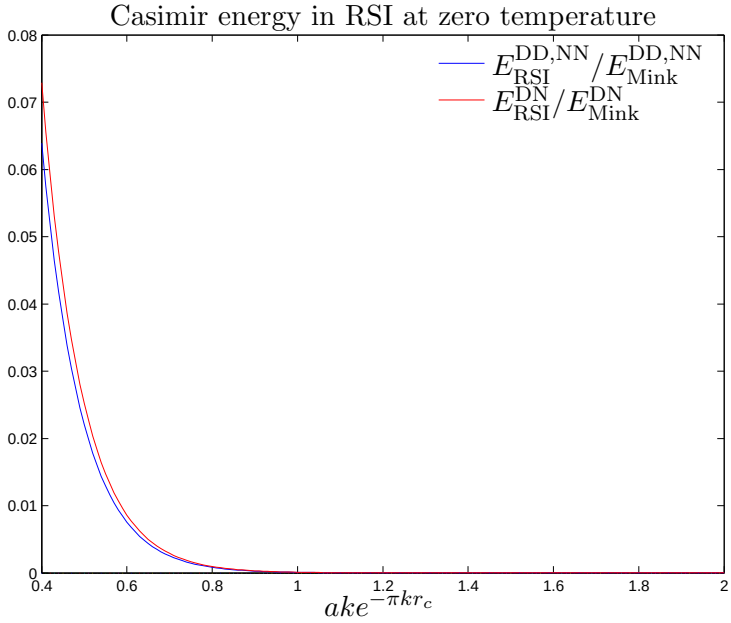

Figure 5.2: Plot of the Casimir energy in RSI with DD and NN and DN boundary conditions with $d = 10^{-12}$.

To find the Casimir force $P_{\mathrm{RSI}}^{\mathrm{DD,NN}}$ we differentiate the energy with respect to the plate separation

$$\begin{aligned} P_{\mathrm{RSI}}^{\mathrm{DD,NN}} &= -\frac{\partial E_{\mathrm{RSI}}^{\mathrm{DD,NN}}}{\partial a} \\ &= -\frac{3}{8\pi^2 a^2}\sum_{n=1}^{\infty}\sum_{M_N}\frac{M_N^2}{n^2}K_2\left(2aM_N n\right) \\ &\quad -\frac{1}{4\pi^2 a}\sum_{n=1}^{\infty}\sum_{M_N}\frac{M_N^3}{n}K_1\left(2aM_N n\right). \end{aligned} \tag{5.4.6}$$

We have used that the derivative of $K_\nu(z)$ is

$$\frac{\mathrm{d}}{\mathrm{d}z}K_\nu(z) = -\frac{\nu}{z}K_\nu - K_{\nu-1}. \tag{5.4.7}$$

Due to the nature of $K_\nu(z)$, the force is weak for large values of $ake^{-k\pi r_c}$

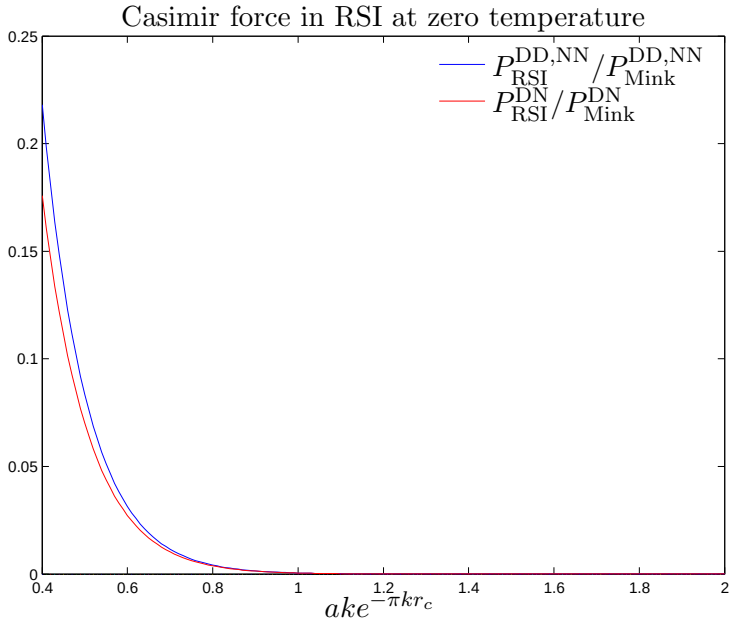

Figure 5.3: Plot of the Casimir force in RSI with DD and NN and DN boundary conditions with $d = 10^{-12}$.

and vanish as $a \to \infty$. From Chapter 2 we have $k \sim M_{\mathrm{Pl}}$ and $k\pi r_c \sim 12$ in order to solve the hierarchy problem. Because of this $k\pi e^{-k\pi r_c}$ given by the TeV scale. Inserting the $\hbar$'s and the c's we find $k\pi e^{-k\pi r_c}/(\hbar c) \sim 10^{18}\mathrm{m}^{-1}$. Thus the argument of the modified Bessel function is large at all values of a that are of interest. When a approaches the size of an atom ($\sim 10^{-10}$m) the model with two separate, parallel plates is not appropriate. In [38] we find the asymptotic expansion of $K_\nu(z)$ for large arguments

$$K_\nu(z) = \sqrt{\frac{\pi}{2z}}e^{-z}\left(1 + \frac{4\nu^2 - 1}{8z} + \frac{(4\nu^2 - 1)(4\nu^2 - 9)}{2!(8z)^2} + \dots\right). \tag{5.4.8}$$

The function approaches zero rapidly with increasing argument. As Figure 5.3 shows, the Casimir force in RSI is small compared to Minkowski spacetime even at relatively small values of $ake^{-k\pi r - c}$ (extremely small distances a).

5.4.2 Dirichlet-Neumann boundary conditions

Now we turn to Dirichlet BC on one plate and Neumann BC on the other. The resulting energy density is

$$E_{\text{RSI}}^{\text{DN}} = \frac{a}{6\pi^2}\sum_{M_N}\int_{M_N}^{\infty}\frac{(x^2-M_N^2)^{\frac{3}{2}}}{e^{2ax}+1}. \tag{5.4.9}$$

Using the same steps as with DD/NN we find that Casimir energy density with DN BC is

$$E_{\text{RSI}}^{\text{DN}} = -\frac{1}{8\pi^2 a}\sum_{n=1}^{\infty}\sum_{M_N}(-1)^n\frac{M_N^2}{n^2}K_2(2aM_Nn) \tag{5.4.10}$$

and accordingly the Casimir force is

$$\begin{aligned} P_{\text{RSI}}^{\text{DD,NN}} &= -\frac{\partial E_{\text{RSI}}^{\text{DD,NN}}}{\partial a} \\ &= -\frac{3}{8\pi^2 a^2}\sum_{n=1}^{\infty}\sum_{M_N}(-1)^n\frac{M_N^2}{n^2}K_2\left(2aM_Nn\right) \\ &\quad -\frac{1}{4\pi^2 a}\sum_{n=1}^{\infty}\sum_{M_N}(-1)^n\frac{M_N^3}{n}K_1\left(2aM_Nn\right). \end{aligned} \tag{5.4.11}$$

The behavior of the Casimir energy and force in RSI compared to the corresponding expression without RS is plotted in Figures 5.2 and 5.3. What characterizes the DN BC in comparison to DD/NN is the factor $(-1)^n$. As we will see this factor is present in every sum over n.

5.4.3 Approximations in RSI

Choosing the bulk scalar field to be even and minimally coupled with no boundary mass term (Neumann BC on the branes) and choosing the approximation $M_N/k \ll 1$, but $e^{k\pi r_c}M_N/k \not\ll 1$ as in Section 4.2.3 we get

$$E_{\text{piston}}^{\text{DD,NN}} = -\frac{k^2e^{-2k\pi r_c}}{8a}\sum_{n=1}\sum_{N=1}\frac{\left(N+\frac{1}{4}\right)^2}{n^2}K_2\left(2ak\pi e^{-k\pi r_c}\left(N+\nu-\frac{1}{4}\right)n\right), \tag{5.4.12}$$

and

$$\begin{aligned} P_{\text{RSI}}^{\text{DD,NN}} &= -\frac{\partial E_{\text{RSI}}^{\text{DD,NN}}}{\partial a} \\ &= -\frac{3k^2e^{-2k\pi r_c}}{8a^2}\sum_{n=1}\sum_{N=1}\frac{\left(N+\frac{1}{4}\right)^2}{n^2}K_2\left(2ak\pi e^{-k\pi r_c}\left(N+\nu-\frac{1}{4}\right)n\right) \\ &\quad -\frac{\pi k^3e^{-3k\pi r_c}}{4a}\sum_{n=1}\sum_{N=1}\frac{\left(N+\frac{1}{4}\right)^3}{n}K_1\left(2ak\pi e^{-k\pi r_c}\left(N+\nu-\frac{1}{4}\right)n\right). \end{aligned} \tag{5.4.13}$$

Here we observe that the energy is always negative and the plates always attract each other.

This expression is equal to the second half of Eq.(2.17) in [19] and we here comment on the differences. First let us summarize the assumptions made in [19]:

1. There is Dirichlet-Dirichlet BC on the physical plates
2. The field obey Neumann boundary conditions on the branes
3. $M_N/k \ll 1$
4. No boundary mass term and minimally coupled, massless scalar field in bulk. This leads to $\nu = 2$ (see Eq.(4.2.13)).

From Section 4.2.3 we find that the values of M_N with these assumptions are

$$M_N = k\pi e^{-k\pi r_c}\left(N + \frac{1}{4}\right),\ N = 1, 2, \ldots, \tag{5.4.14}$$

i.e. equal to the values in [19]. All in all the mathematics here and in [19] are the same. The physical setup is however different.

First of all [19] does not treat the piston model. The energy without plates ($a \to \infty$) is subtracted. This is equivalent to removing the first part of E_j from Section 5.1.2. But they do not remove terms independent of a. Since we only can measure energy differences in physics these are not noticeable. The terms independent a are lost due to differentiation when finding the Casimir force and can thus not be detected at all.

Secondly, the $M_N = 0$ mode is included because this is a massless field in bulk. As discussed in the beginning of this chapter the consequence of this is an additional term equal to the energy in ordinary 3+1 spacetime E_{Mink}. However the authors do not calculate the Casimir effect in the Randall-Sundrum model for a massless scalar field in bulk, but an electromagnetic field in bulk. This is sensible since it is the Casimir effect of the electromagnetic field that is measured by experiments. In Chapter 7 we call attention to the problems with using the results from scalar fields to draw conclusions on the electromagnetic field.

5.5 Casimir energy and force in RSII

In the RSII model $r_c \to \infty$ and the Kaluza-Klein modes are continuous. As pointed out in the beginning of this chapter we are dealing with a massive field so the $M_N = 0$ mode is excluded. We obtain RSII be replacing the sum over M_N with an integral

$$\sum_{M_N} \to \int_0^\infty \frac{\mathrm{d}M}{k}. \tag{5.5.1}$$

As in RSI the variable changes are similar to those in the Minkowski case

$$\begin{aligned}
E_{\rm RSII} =& -\frac{V_\perp}{\pi}\int_0^\infty \frac{{\rm d}M}{k}\int_0^\infty \frac{k_\perp {\rm d}k_\perp}{2\pi}\int_{\sqrt{k_\perp^2+M^2}}^\infty {\rm d}x\sqrt{x^2-k_\perp^2-M^2}\\
&\times \underbrace{\frac{a+\sum_{j=0,a}\frac{\beta_j}{(\beta_j x)^2-1}}{\frac{(\beta_0/a-1)(\beta_a/a-1)}{(\beta_0/a+1)(\beta_a/a+1)}e^{2ax}-1}}_{g(x)}\\
\overset{y=\sqrt{x^2-k_\perp^2-M^2}}{=}& -\frac{V_\perp}{2\pi^2}\int_0^\infty \frac{{\rm d}M}{k}\int_0^\infty {\rm d}k_\perp\int_0^\infty {\rm d}y\frac{k_\perp y^2}{\sqrt{y^k+k_\perp^2+M^2}}g(\sqrt{y^k+k_\perp^2+M^2})\\
\overset{\substack{M=r\sin\theta\sin\phi\\ y=r\sin\theta\cos\phi\\ k_\perp=r\cos\theta}}{=}& -\frac{V_\perp}{2\pi^2 k}\underbrace{\int_0^{\frac{\pi}{2}}{\rm d}\theta\ \cos\theta\sin^3\theta}_{1/4}\underbrace{\int_0^{\frac{\pi}{2}}{\rm d}\phi\ \cos^2\phi}_{\pi/4}\int_0^\infty {\rm d}r\ r^4 g(r)\\
=& -\frac{V_\perp}{32\pi k}\int_0^\infty {\rm d}r\ r^4\frac{a+\sum_{j=0,a}\frac{\beta_j}{(\beta_j r)^2-1}}{\frac{(\beta_0/a-1)(\beta_a/a-1)}{(\beta_0/a+1)(\beta_a/a+1)}e^{2ar}-1}.
\end{aligned} \tag{5.5.2}$$

As in previous sections we now study DD, NN and DN BC in particular.

5.5.1 Dirichlet-Dirichlet or Neumann-Neumann boundary conditions

If we assume Dirichlet (or Neumann) BC on both plates the energy density of RSII reduces to

$$\begin{aligned}
E_{\rm RSII}^{\rm DD,NN} =& -\frac{a}{32\pi k}\int_0^\infty {\rm d}r\frac{r^4}{e^{2ax}+1} = -\frac{a}{32\pi k}\sum_{n=1}^\infty\int_0^\infty {\rm d}r r^4 e^{-2anx}\\
=& -\frac{a}{32\pi k}\frac{24}{(2a)^5}\underbrace{\sum_{n=1}^\infty\frac{1}{n^5}}_{\zeta_R(5)} = -\frac{3\zeta_R(5)}{128\pi k a^4} = E_{\rm Mink}^{\rm DD,NN}\frac{135\zeta_R(5)}{4\pi^3 ka}.
\end{aligned} \tag{5.5.3}$$

Once again we have expanded the denominator in terms of e^{-2ax}. The Casimir energy is show in Figure 5.4. The Casimir force in Figure 5.5 is easily obtained by differentiating the energy

$$P_{\rm RSII}^{\rm DD,NN} = -\frac{3\zeta_R(5)}{32\pi k a^5} = P_{\rm Mink}^{\rm DD,NN}\frac{45\zeta_R(5)}{\pi^3 ak}. \tag{5.5.4}$$

We will discuss the differences between RSII and RSI in Chapter 7. We emphasize the overall factor $1/(ak)$ when comparing to Minkowski which, as we will se later, is typical for RSII.

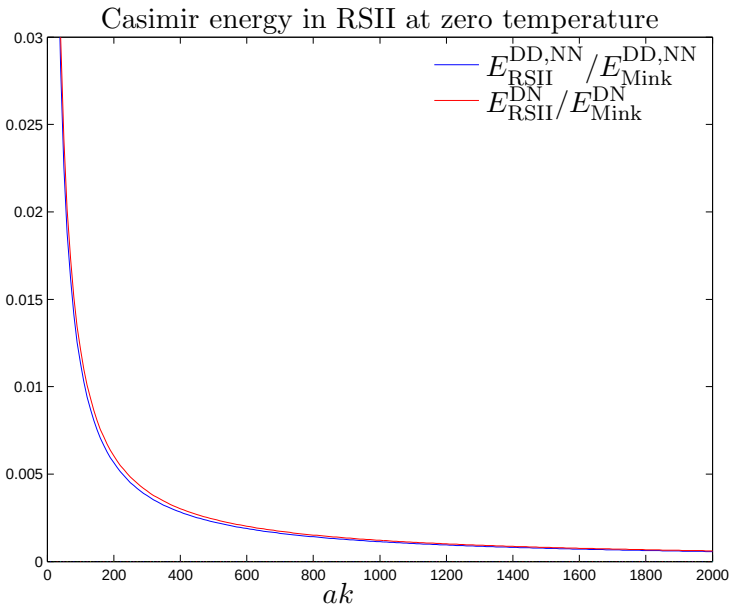

Figure 5.4: Plot of the energy in RSII with DD/NN and DN boundary conditions.

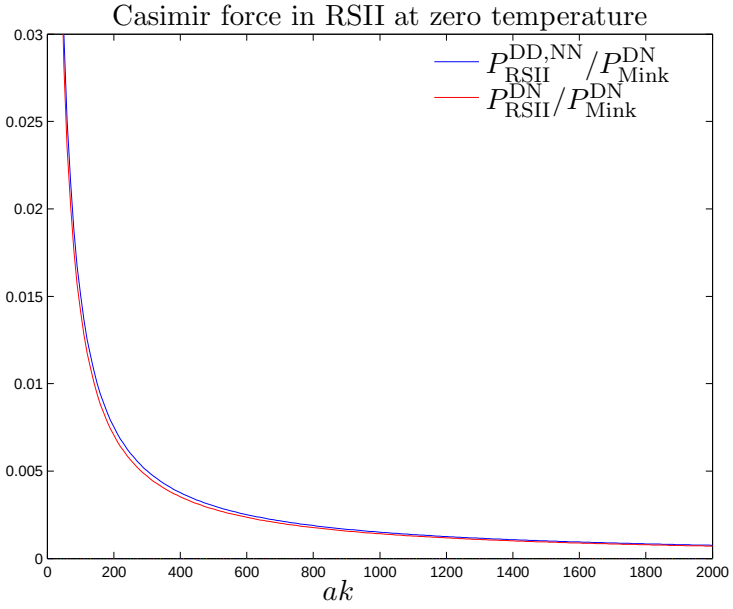

Figure 5.5: Plot of the force in RSII with DD/NN and DN boundary conditions.

5.5.2 Dirichlet-Neumann boundary conditions

By assuming Dirichlet BC on one plate and Neumann on the other we find

$$\begin{aligned} E^{\mathrm{DN}}_{\mathrm{RSII}} &= -\frac{a}{32\pi k}\sum_{n=1}^{\infty}(-1)^n\int_0^\infty \mathrm{d}r r^4 e^{-2anx} \\ &= -\frac{a}{32\pi k}\frac{24}{(2a)^5}\underbrace{\sum_{n=1}^{\infty}(-1)^n\frac{1}{n^5}}_{-\frac{15}{16}\zeta_R(5)} = \frac{15}{16}\frac{3V_\perp\zeta_R(5)}{128\pi k a^4} = E^{\mathrm{DN}}_{\mathrm{Mink}}\frac{2025\zeta_R(5)}{56\pi^3 ka}. \end{aligned} \tag{5.5.5}$$

and

$$P^{\mathrm{DN}}_{\mathrm{RSII}} = \frac{15}{16}\frac{3\zeta_R(5)}{32\pi k a^5} = P^{\mathrm{DN}}_{\mathrm{Mink}}\frac{675\zeta_R(5)}{16\pi^3 ka}. \tag{5.5.6}$$

The plots of the Casimir energy and force are shown in Figures 5.4 and 5.5 respectively. It is interesting to notice that by assuming Dirichlet BC on one brane and Neumann on the other we always seem to get repulsive forces.

This concludes our survey of the Casimir effect in RSI and RSII at zero temperature. We are now ready to proceed to finite temperatures.

Chapter 6

Finite temperature

In this section we want to find the Casimir free energy F and force P at finite temperature. We have an expression for the free energy but this expression is divergent and we will regularize it using zeta regularization. As in Chapter 5 we first deduce the free energy and force at high and low temperature in Minkowski spacetime, both to get familiar with the formalism and in order to have something to compare the RS results to.

6.1 Casimir free energy and force in flat spacetime

The starting point is Eq.(4.3.29) with $M_N = 0$

$$F = -\frac{V_\perp \pi^{N_\perp/2}}{2\beta(2\pi)^{N_\perp}}\Gamma\left(-\frac{N_\perp}{2}\right)\sum_{l=-\infty}^{\infty}\sum_{k_x}\left(k_x^2+\epsilon_l^2\right)^{\frac{N_\perp}{2}}, \tag{6.1.1}$$

with $\epsilon_l = 2\pi l/\beta$. We choose instead to look at

$$F(s) = -\frac{V_\perp}{8\pi\beta}\Gamma(s)\sum_{l=-\infty}^{\infty}\sum_{k_x}\left(k_x^2+\epsilon_l^2\right)^{-s}. \tag{6.1.2}$$

For $s = -N_\perp/2 = -1$ we regain the right expression for the free energy density. $F(s)$ is well-defined for large, positive $\mathrm{Re}(s)$ and we choose to analytically continue the function to the whole complex plane. Applying the Abel-Plana formula with

$$f(z) = \frac{1}{\pi}\left(\epsilon_l^2+(z/a)^2\right)^{-s}\left(1-\sum_{j=0,a}\frac{\beta_j/a}{1+(\beta_j z/a)^2}\right), \tag{6.1.3}$$

we first find the free energy and force with DD or NN BC and then with DN BC. In Appendix B we calculate the Casimir free energy for for a massless bulk scalar field in RSI. The calculations are similar to the zero temperature

case and for this reason we do not go though them again. In Minkowski spacetime the results for the free energy density can be retrieved by setting $M_N = 0$ and removing the sum over M_N. We give the result from the appendix and find the Casimir force. The method used later in this chapter for RSI gives, of course, the same result for Minkowski spacetime.

6.1.1 Dirichlet-Dirichlet or Neumann-Neumann boundary conditions

Eq.(B.10) gives us the Casimir free energy density with DD or NN BC

$$\begin{aligned} F_{\text{Mink}}^{\text{DD,NN}} =& -\frac{a\pi^{\frac{1}{2}}}{\beta(2\pi)^2}\sum_{l=-\infty}^{\infty}\sum_{n=1}\left(\frac{\epsilon_l^2}{n^2a^2}\right)^{\frac{3}{4}} K_{\frac{3}{2}}\left(2na|\epsilon_l|\right) \\ =& -\frac{\zeta_R(3)}{16\pi a^2\beta} - \frac{a}{2\beta}\left(\frac{2}{a\beta}\right)^{\frac{3}{2}}\sum_{l,n=1}^{\infty}\left(\frac{l}{n}\right)^{\frac{3}{2}} K_{\frac{3}{2}}\left(\frac{4\pi anl}{\beta}\right). \end{aligned} \tag{6.1.4}$$

Here we have inserted $\epsilon = 2\pi l/\beta$. The first term is the $l = 0$ term of the Matsubara frequencies and can be parted from the rest earlier in the calculation or by looking at the properties of $K_\nu(z)$ at small arguments.

High temperatures

By high temperature we mean $aT \gg 1$ since this is the only natural scale. The expression above is suitable in this limit

$$F_{\text{Mink}}^{\text{DD,NN}} = -T\frac{\zeta_R(3)}{16\pi a^2}\left(1 + \frac{8\pi}{\zeta_R(3)}\left(2aT\right)^{\frac{3}{2}}\sum_{l,n=1}^{\infty}\left(\frac{l}{n}\right)^{\frac{3}{2}} K_{\frac{3}{2}}\left(4\pi aTnl\right)\right). \tag{6.1.5}$$

The first term $-T\frac{\zeta_R(3)}{16\pi a^2}$ will dominate at high aT since $K_\nu(z)$ decreases with temperature. The Casimir force is

$$\begin{aligned} P_{\text{Mink}}^{\text{DD,NN}} =& -T\frac{\zeta_R(3)}{8\pi a^3} + \frac{T}{2}\left(\frac{2T}{a}\right)^{\frac{3}{2}}\sum_{l,n=1}^{\infty}\left(\frac{l}{n}\right)^{\frac{3}{2}} K_{\frac{3}{2}}\left(4\pi aTnl\right) \\ & - 2\pi aT^2\left(\frac{2T}{a}\right)^{\frac{3}{2}}\sum_{l,n=1}^{\infty}\frac{l^{\frac{5}{2}}}{n^{\frac{1}{2}}}K_{\frac{5}{2}}\left(4\pi aTnl\right). \end{aligned} \tag{6.1.6}$$

This is also dominated by the first term at large aT.

Low temperatures

The expression for high temperatures is not suitable for low temperatures. We go back to

$$\begin{aligned} F(s) =& -\frac{V_\perp}{\beta 8\pi}\Gamma(s)\sum_{l=-\infty}^{\infty}\sum_{k_x}\left(k_x^2+\epsilon_l^2\right)^{-s} \\ =& \underbrace{-\frac{V_\perp}{\beta 8\pi}\Gamma(s)\sum_{k_x}\left(k_x^2\right)^{-s}}_{F_{l=0}} \\ & -\frac{V_\perp}{\beta 8\pi}\Gamma(s)\sum_{l=1}^{\infty}\sum_{k_x}\left(k_x^2+\left(\frac{2\pi l}{\beta}\right)^2\right)^{-s}. \end{aligned} \tag{6.1.7}$$

Note our choice to keep k_x. The plan is to use the Abel-Plana formula later to find the DN BC expressions at the same time as DD/NN. Using the Mellin transform, Eq.(4.3.10), we write $F(s)$ as

$$\begin{aligned} F(s) =& F_{l=0} - \frac{V_\perp}{\beta 4\pi}\sum_{l=1}^{\infty}\sum_{k_x}\int_0^\infty \mathrm{d}t\; t^{s-1}e^{-t\left(k_x^2+\left(\frac{2\pi l}{\beta}\right)^2\right)} \\ =& F_{l=0} - \frac{V_\perp}{\beta 4\pi}\sum_{l=1}^{\infty}\sum_{k_x}\int_0^\infty \mathrm{d}t\; t^{s-1}S_2\left(t\left(\frac{2\pi}{\beta}\right)^2\right)e^{-tk_x^2}. \end{aligned} \tag{6.1.8}$$

Here we have introduced the function

$$S_\alpha(t) = \sum_{m=1}^{\infty} e^{-m^\alpha t}, \tag{6.1.9}$$

and in Appendix C we show that

$$S_2(t) = -\frac{1}{2} + \frac{1}{2}\sqrt{\frac{\pi}{t}} + \sqrt{\frac{\pi}{t}}S_2\left(\frac{\pi^2}{t}\right). \tag{6.1.10}$$

The first of the three terms coming from Eq.(6.1.10) cancels $F_{l=0}$ from Eq.(6.1.7) leaving

$$\begin{aligned} F(s) =& \underbrace{-\frac{V_\perp}{16\pi^{\frac{3}{2}}}\Gamma(s-1/2)\sum_{k_x}k_x^{-2(s-1/2)}}_{F(T=0)} \\ & -\frac{V_\perp}{8\pi^{\frac{5}{2}}}\sum_{k_x}\sum_{l=1}^{\infty}\int_0^\infty \mathrm{d}t\; t^{(s-1/2)-1}e^{-tk_x^2-\frac{\beta^2 l^2}{4t}}. \end{aligned} \tag{6.1.11}$$

The first term can be recognized as $E = F(T = 0)$. To realize this see Eq.(4.3.30) and remember to only include $M_N = 0$. The resulting integral is of the form

$$\int_0^\infty \mathrm{d}t\; t^{\nu-1}e^{-\beta/t-\gamma t} = 2\left(\frac{\beta}{\gamma}\right)^{\nu/2} K_\nu\left(2\sqrt{\beta\gamma}\right). \tag{6.1.12}$$

For $s = -1$ we find

$$F = E - \frac{1}{4\pi^{\frac{3}{2}}}\left(\frac{\beta}{2}\right)^{-\frac{3}{2}} \sum_{k_x}\sum_{l=1}^{\infty}\left(\frac{l}{k_x}\right)^{-\frac{3}{2}} K_{\frac{3}{2}}(k_x\beta l). \tag{6.1.13}$$

We can use the Abel-Plana formula if we choose

$$f(z) = \frac{1}{\pi}(z/a)^{\frac{3}{2}} K_{\frac{3}{2}}(\beta l z/a)\left(1 - \sum_{j=0,a}\frac{\beta_j/a}{1+(\beta_j z/a)^2}\right). \tag{6.1.14}$$

In Appendix B we show that the Abel-Plana formula with $f(z)$ of the form

$$f(z) = \frac{1}{\pi}(z/a)^{\nu} K_\nu(Az/a)\left(1 - \sum_{j=0,a}\frac{\beta_j/a}{1+(\beta_j z/a)^2}\right) \tag{6.1.15}$$

leads to

$$\Delta f^{\left\{{DD,NN \atop DN}\right\}} = \sum_{n=1}^{\infty}(-1)^{\{{2n \atop n}\}}\frac{a(2A)^\nu}{\sqrt{\pi}}\frac{\Gamma\left(\nu+\frac{1}{2}\right)}{\left((2an)^2+A^2\right)^{\nu+1/2}}. \tag{6.1.16}$$

Hence in the low temperature limit we have

$$\Delta F = \Delta E - \frac{2aV_\perp}{\pi^2}\sum_{n,l=1}^{\infty}\frac{1}{\left((2an)^2+(\beta l)^2\right)^2}. \tag{6.1.17}$$

The correction to the zero temperature energy should decay exponentially. By once more using the Mellin transform, but this time choosing $S_2(t(2a)^2)$ and Eq.(6.1.10) we can show that

$$\begin{aligned}\Delta F =& \Delta E + \frac{V_\perp}{\pi^{\frac{3}{2}}}\sum_{l=1}^{\infty}\frac{1}{(\beta l)^4} - \frac{V_\perp}{2\pi^{\frac{3}{2}}}\sum_{l=1}^{\infty}\frac{1}{(\beta l)^3} \\ &- \frac{2V_\perp}{(2a\beta)^{\frac{3}{2}}}\sum_{n,l=1}^{\infty}\left(\frac{n}{l}\right)^{\frac{3}{2}} K_{\frac{3}{2}}\left(\frac{\beta\pi l n}{a}\right).\end{aligned} \tag{6.1.18}$$

In the piston model we throw away all terms independent and linear in a. This way we are left with

$$F^{\mathrm{DD,NN}}_{\mathrm{Mink}} = E^{\mathrm{DD,NN}}_{\mathrm{Mink}} - \frac{2T^{\frac{3}{2}}}{(2a)^{\frac{3}{2}}}\sum_{n,l=1}^{\infty}\left(\frac{n}{l}\right)^{\frac{3}{2}} K_{\frac{3}{2}}\left(\frac{\pi l n}{aT}\right) \tag{6.1.19}$$

and find

$$\begin{aligned} P^{\mathrm{DD,NN}}_{\mathrm{Mink}} =& P^{\mathrm{DD,NN}}_{\mathrm{Mink}}(T=0) - \frac{3T^{\frac{3}{2}}}{\sqrt{2}a^{\frac{5}{2}}}\sum_{n,l=1}^{\infty}\left(\frac{n}{l}\right)^{\frac{3}{2}} K_{\frac{3}{2}}\left(\frac{\pi l n}{aT}\right) \\ & - \frac{\pi\sqrt{T/2}}{a^{\frac{7}{2}}}\sum_{n,l=1}^{\infty}\frac{n^{\frac{5}{2}}}{\sqrt{l}} K_{\frac{5}{2}}\left(\frac{\pi l n}{aT}\right). \end{aligned} \tag{6.1.20}$$

The Casimir energy and force is equal to the zero temperature expression plus correction terms. The correction terms decay exponentially as $T \to 0$.

6.1.2 Dirichlet-Neumann boundary conditions

Looking at Eq.(B.12) we find the Casimir free energy density with DN BC

$$\begin{aligned} F^{\mathrm{DN}}_{\mathrm{Mink}} =& -\frac{a\pi^{\frac{1}{2}}}{\beta(2\pi)^2}\sum_{l=-\infty}^{\infty}\sum_{n=1}(-1)^n\left(\frac{\epsilon_l^2}{n^2a^2}\right)^{\frac{3}{4}} K_{\frac{3}{2}}\left(2na|\epsilon_l|\right) \\ =& \frac{3\zeta_R(3)}{64\pi\beta a^2} - \frac{a}{2\beta}\left(\frac{2}{a\beta}\right)^{\frac{3}{2}}\sum_{n,l=1}^{\infty}(-1)^n\left(\frac{l}{n}\right)^{\frac{3}{2}} K_{\frac{3}{2}}\left(\frac{4\pi a n l}{\beta}\right). \end{aligned} \tag{6.1.21}$$

High temperature

The expression above is suitable for high temperatures

$$F^{\mathrm{DN}}_{\mathrm{Mink}} = T\frac{3\zeta_R(3)}{64\pi a^2} - T\frac{a}{2}\left(\frac{2T}{a}\right)^{\frac{3}{2}}\sum_{l=1}^{\infty}\sum_{n=1}(-1)^n\left(\frac{l}{n}\right)^{\frac{3}{2}} K_{\frac{3}{2}}\left(4\pi a T n l\right). \tag{6.1.22}$$

The first term $T\frac{3\zeta_R(3)}{64\pi a^2}$ is linear in T and will dominate at high temperatures. The Casimir force is

$$\begin{aligned} P^{\mathrm{DN}}_{\mathrm{Mink}} =& T\frac{3\zeta_R(3)}{32\pi a^3} + \frac{T}{2}\left(\frac{2T}{a}\right)^{\frac{3}{2}}\sum_{l,n=1}^{\infty}(-1)^n\left(\frac{l}{n}\right)^{\frac{3}{2}} K_{\frac{3}{2}}\left(4\pi a T n l\right) \\ & - 2\pi a T^2\left(\frac{2T}{a}\right)^{\frac{3}{2}}\sum_{l,n=1}^{\infty}(-1)^n\frac{l^{\frac{5}{2}}}{n^{\frac{1}{2}}} K_{\frac{5}{2}}\left(4\pi a T n l\right). \end{aligned} \tag{6.1.23}$$

As before this expression cannot be used in the low temperature limit.

Low temperature

Since we have already gone through the calculation at low temperatures for DD or NN BC we claim that

$$F^{\mathrm{DN}}_{\mathrm{Mink}} = E^{\mathrm{DN}}_{\mathrm{Mink}} - \frac{2T^{\frac{3}{2}}}{(2a)^{\frac{3}{2}}}\sum_{n,l=1}^{\infty}(-1)^n\left(\frac{n}{l}\right)^{\frac{3}{2}} K_{\frac{3}{2}}\left(\frac{\pi l n}{aT}\right) \tag{6.1.24}$$

and

$$\begin{aligned} P^{\mathrm{DN}}_{\mathrm{Mink}} =& P^{\mathrm{DN}}_{\mathrm{Mink}}(T=0) - \frac{3T^{\frac{3}{2}}}{\sqrt{2}a^{\frac{5}{2}}} \sum_{n,l=1}^{\infty} \left(\frac{n}{l}\right)^{\frac{3}{2}} K_{\frac{3}{2}}\left(\frac{\pi l n}{aT}\right) \\ & - \frac{\pi\sqrt{T/2}}{a^{\frac{7}{2}}} \sum_{n,l=1}^{\infty} (-1)^n \frac{n^{\frac{5}{2}}}{\sqrt{l}} K_{\frac{5}{2}}\left(\frac{\pi l n}{aT}\right). \end{aligned} \tag{6.1.25}$$

Now the reader might object that we cannot choose $S_2(t(2a)^2)$ because of the $(-1)^n$ in the sum over n. But for the sum over a real function $g(n)$ we have

$$\sum_{n=1}^{\infty}(-1)^n g(n) = -\left(\sum_{n=1}^{\infty} g(n) - 2\sum_{n=1}^{\infty} g(2n)\right). \tag{6.1.26}$$

Using this in the beginning we can treat the two sums separately using $S_2(t(2a)^2)$ and $S_2(t(4a)^2)$. In the end we can rewrite the free energy to Eq.(6.1.24) with the aid of Eq.(6.1.26).

The Casimir energy and force in Minkowski spacetime are known results. We derived them in order to get an easy transition to the RSI and RSII expressions as the formalism and techniques are very similar.

6.2 Casimir free energy and force in RSI

Instead of starting with Eq.(4.3.29)

$$F = -\frac{V_\perp \pi^{N_\perp/2}}{2\beta(2\pi)^{N_\perp}}\Gamma\left(-\frac{N_\perp}{2}\right) \sum_{l=-\infty}^{\infty} \sum_{M_N} \sum_{k_x} \left(k_x^2 + M_N^2 + \epsilon_l^2\right)^{\frac{N_\perp}{2}}. \tag{6.2.1}$$

we choose to look at

$$F(s) = -\frac{V_\perp \pi^{N_\perp/2}}{2\beta(2\pi)^{N_\perp}}\Gamma(s) \sum_{l=-\infty}^{\infty} \sum_{M_N} \sum_{k_x} \left(k_x^2 + M_N^2 + \epsilon_l^2\right)^{-s}, \tag{6.2.2}$$

which reduces to the correct expression for the free energy at $s = -N_\perp/2$. This function is also well-defined for large, positive $\mathrm{Re}(s)$ and we analytically continue the function to the whole complex plane as we always do with zeta functions. It is time to set out to find the regularized expression for the free energy density with DD or NN BC on the plates. In Appendix B we make use of the Abel-Plana formula to obtain the same answer and also find the free energy with DN BC. Different formulas yield the same result, as it should. In the section about DN BC we present the result from the appendix and motivate why it should be so.

6.2.1 Dirichlet-Dirichlet or Neumann-Neumann boundary conditions

We assume Dirichlet BC on both plates,

$$k_x = \frac{n\pi}{a},\ n = 1, 2, \dots \tag{6.2.3}$$

The only difference between the two types of conditions is that $n = 0, 1, 2, \dots$ for NN and $n = 1, 2, \dots$ for DD. The extra term originating from $n = 0$ is not dependent on a and will for this reason give no contribution in the piston model[1]. The procedure is the same as for low temperature Minkowski spacetime. Using the Mellin transform, Eq.(4.3.10), we write

$$\begin{aligned} F(s) =& -\frac{V_\perp \pi^{N_\perp/2}}{2\beta(2\pi)^{N_\perp}} \sum_{l=-\infty}^{\infty} \sum_{M_N} \sum_{n=1}^{\infty} \int_0^\infty \mathrm{d}t t^{s-1} \exp\left(-t\left(\frac{n^2\pi^2}{a^2} + M_N^2 + \epsilon_l^2\right)\right) \\ =& -\frac{V_\perp \pi^{N_\perp/2}}{2\beta(2\pi)^{N_\perp}} \sum_{l=-\infty}^{\infty} \sum_{M_N} \int_0^\infty \mathrm{d}t t^{s-1} S_2\left(t\frac{\pi^2}{a^2}\right) \exp\left(-t\left(M_N^2 + \epsilon_l^2\right)\right). \end{aligned} \tag{6.2.4}$$

We will again use the properties of the function $S_2(t)$ only this time we have chosen $S_2\left(t\left(\frac{\pi}{a}\right)^2\right)$ from the sum over n instead of $S_2\left(t\left(\frac{2\pi}{\beta}\right)^2\right)$ from the sum over l. Inserting from Eq.(6.1.10) gives

$$\begin{aligned} F(s) =& \frac{V_\perp \pi^{N_\perp/2}}{4\beta(2\pi)^{N_\perp}} \sum_{l=-\infty}^{\infty} \sum_{M_N} \Gamma(s)\left(M_N^2 + \epsilon_l^2\right)^{-s} \\ & - \frac{V_\perp a \pi^{(N_\perp-1)/2}}{4\beta(2\pi)^{N_\perp}} \sum_{l=-\infty}^{\infty} \sum_{M_N} \Gamma\left(s-\frac{1}{2}\right)\left(M_N^2 + \epsilon_l^2\right)^{-\left(s-\frac{1}{2}\right)} \\ & - \frac{V_\perp a \pi^{(N_\perp-1)/2}}{2\beta(2\pi)^{N_\perp}} \sum_{l=-\infty}^{\infty} \sum_{M_N} \sum_{n=1}^{\infty} \int_0^\infty \mathrm{d}t\ t^{\left(s-\frac{1}{2}\right)-1} \\ & \times \exp\left(-t(M_N^2 + \epsilon_l^2) - \frac{n^2a^2}{t}\right). \end{aligned} \tag{6.2.5}$$

Since the first term is independent of a and the second term is linear in a they both vanish in the piston model (Section 5.2). The last term is the only one left.

$$\begin{aligned} F_{\text{piston}}(s) =& -\frac{V_\perp a \pi^{(N_\perp-1)/2}}{\beta(2\pi)^{N_\perp}} \sum_{l=-\infty}^{\infty} \sum_{M_N} \sum_{n=1}^{\infty} \left(\frac{n^2a^2}{M_N^2 + \epsilon_l^2}\right)^{\frac{s-1/2}{2}} \\ & \times K_{s-\frac{1}{2}}\left(2na\sqrt{M_N^2 + \epsilon_l^2}\right). \end{aligned} \tag{6.2.6}$$

[1]For a massless bulk scalar we get an additional factor $\mathcal{N}/\beta \log \beta$, where $\mathcal{N}$ is the number of modes with $k_\perp + k_x + M_N^2 = 0$ [31].

This expression is finite for $s = -N_\perp/2 = -1$. We use the same notation as in Chapter 5 here. $F^{\rm BC}_{\rm RSI/RSII}$ is the free energy per surface area in the piston model in RSI or RSII with boundary conditions indicated by the superscript. Thus the energy reads

$$F^{\rm DD,NN}_{\rm RSI} = -\frac{a\pi^{1/2}}{\beta(2\pi)^2}\sum_{l=-\infty}^{\infty}\sum_{M_N}\sum_{n=1}^{\infty}\left(\frac{M_N^2+\epsilon_l^2}{n^2a^2}\right)^{\frac{3}{4}} K_{\frac{3}{2}}\left(2na\sqrt{M_N^2+\epsilon_l^2}\right). \tag{6.2.7}$$

This expression is valid both for DD and NN BC.

Note: The zero temperature energy can be obtained from Eq. (6.2.6) by following the procedure of Section 4.3.2 to remove the temperature dependence

$$E^{\rm DD,NN}_{\rm RSI} = -\frac{a\pi}{(2\pi)^3}\sum_{M_N}\sum_{n=1}^{\infty}\left(\frac{M_N^2}{n^2a^2}\right) K_2\left(2naM_N\right). \tag{6.2.8}$$

This is off course the same as in Chapter 5. The zero temperature limits can also be found by letting $\sum_{l=-\infty}^{\infty} \to \beta\int_{-\infty}^{\infty}\frac{{\rm d}\epsilon}{2\pi}$ in Eq.(6.2.7) and using Eq.(A.5) from Appendix A. The two alternatives for finding the $T \to 0$ can be used on all expression in this chapter and can be used as a check of the finite temperature expression.

High temperature limit

Remember that $\epsilon_l = 2\pi Tl$. The expressions above (Eq.(6.2.7) and Eq.(6.2.9)) are suitable at temperatures $2\pi T \gg k\pi e^{-k\pi r_c}$. This implies $2\pi Ta \gg 1$ since $ak\pi e^{-k\pi r_c} \gg 1$ for all relevant distances a. The critical point $2\pi T = k\pi e^{-k\pi r_c}$ corresponds to temperatures $T \sim 10^{15}$K which is immensely high. The free energy density is plotted for $d = 10^{-12}$ in Figure 6.1. The free energy decreases when aT increases, but increases with higher $2\pi Te^{-k\pi r_c}/k$. Due to the magnitude of $ke^{k\pi r_c}$ we will always have $2\pi Te^{-k\pi r_c}/k \ll 1$ at temperatures of interest. The finite temperature Casimir force in the RSI is

$$\begin{aligned} P^{\rm DD,NN}_{\rm RSI} = {} & \frac{\pi^{1/2}}{\beta(2\pi)^2}\sum_{l=-\infty}^{\infty}\sum_{M_N}\sum_{n=1}^{\infty}\left(\frac{M_N^2+(2\pi Tl)^2}{n^2a^2}\right)^{\frac{3}{4}} K_{\frac{3}{2}}\left(2na\sqrt{M_N^2+(2\pi Tl)^2}\right) \\ & -\frac{2\pi^{1/2}}{\beta(2\pi)^2}\sum_{l=-\infty}^{\infty}\sum_{M_N}\sum_{n=1}^{\infty}\frac{\left(M_N^2+(2\pi Tl)^2\right)^{\frac{5}{4}}}{\sqrt{na}} K_{\frac{5}{2}}\left(2na\sqrt{M_N^2+(2\pi Tl)^2}\right). \end{aligned} \tag{6.2.9}$$

This is plotted in Figure 6.2. The force behaves in the same way as the free energy. It decreases when aT increases, but increases with higher $2\pi Te^{-k\pi r_c}/k$. To get a contribution detectable with experiments we need aT not too high and $2\pi Te^{-k\pi r_c}/k$ not too low. Unfortunately the latter is somewhat difficult since the temperature is the only parameter that an

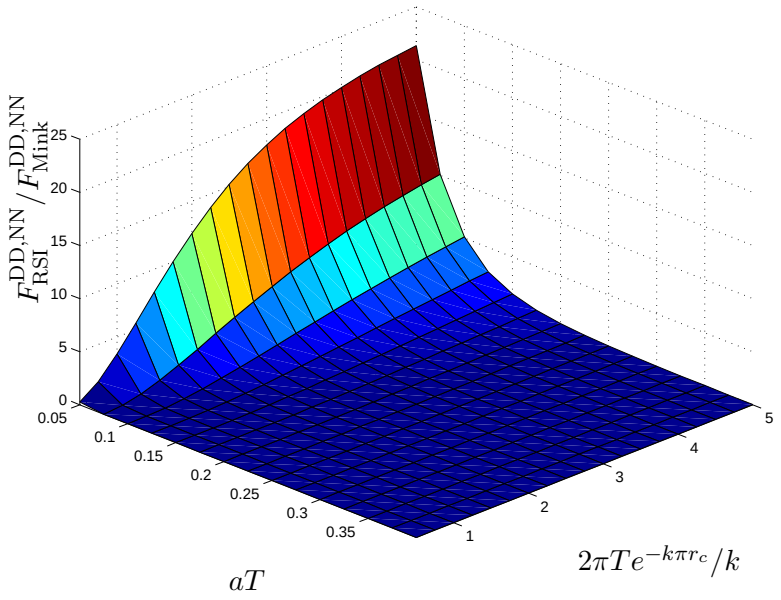

Figure 6.1: Plot of the ratio between Casimir free energy in Minkowski spacetime and RSI with DD or NN boundary conditions, $d = 10^{-12}$.

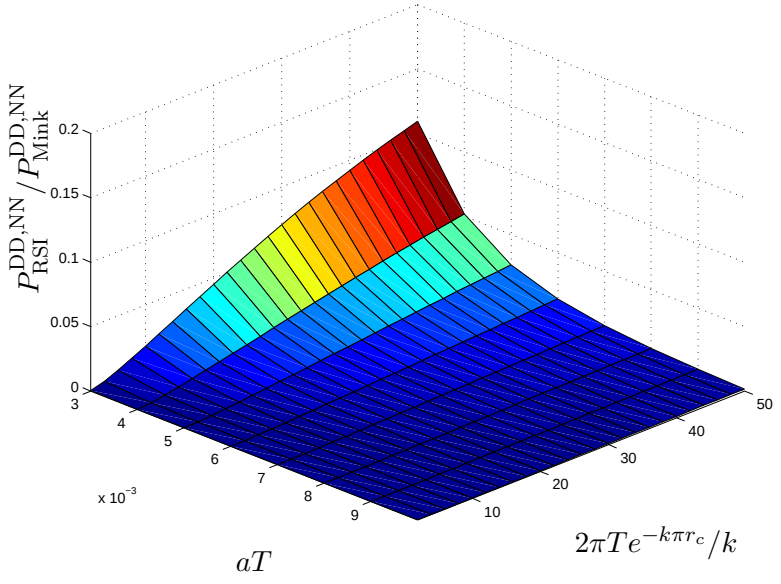

Figure 6.2: Plot of the ratio between Casimir free energy in Minkowski spacetime and RSI with DD or NN boundary conditions, $d = 10^{-12}$.

experimentalist can alter and temperatures as high as $T \sim 10^{15}$K are not reachable in a laboratory.

Since the high temperature limit is too high to be of physical importance we need to look at the low temperature limit.

Low temperature limit

It is interesting to see what happens when $2\pi T \ll k\pi e^{-k\pi r_c}$ but $2\pi Ta \gg 1$ or $2\pi Ta \ll 1$. Eq.(6.2.7) and Eq.(6.2.9) are not appropriate for this purpose. We once again go back to $F(s)$ from the beginning of the chapter.

$$\begin{aligned} F(s) =& -\frac{V_\perp \pi^{N_\perp/2}}{2\beta(2\pi)^{N_\perp}}\Gamma(s)\sum_{l=-\infty}^{\infty}\sum_{M_N}\sum_{k_x}\left(k_x^2+M_N^2+\left(\frac{2\pi}{\beta}\right)^2 l^2\right)^{-s} \\ =& \underbrace{-\frac{V_\perp \pi^{N_\perp/2}}{2\beta(2\pi)^{N_\perp}}\Gamma(s)\sum_{M_N}\sum_{k_x}\left(k_x^2+M_N^2\right)^{-s}}_{F_{l=0}} \\ & -\frac{V_\perp \pi^{N_\perp/2}}{\beta(2\pi)^{N_\perp}}\Gamma(s)\sum_{l=1}^{\infty}\sum_{M_N}\sum_{k_x}\left(k_x^2+M_N^2+\left(\frac{2\pi}{\beta}\right)^2 l^2\right)^{-s}. \end{aligned} \tag{6.2.10}$$

The $l=0$ term is separated from the rest and the second term is to account for both positive and negative values of l. Since the steps are completely analogous to the low temperature Minkowski calculations we jump right to the result

$$\begin{aligned} F =& E - \frac{1}{4\pi^{\frac{3}{2}}}\sum_{M_N}\sum_{k_x}\sum_{l=1}^{\infty}\left(\frac{2}{\beta l}\right)^{\frac{3}{2}}\left(k_x^2+M_N^2\right)^{\frac{3}{4}} \\ & \times K_{\frac{3}{2}}\left(\beta l\sqrt{k_x^2+M_N^2}\right) \\ =& E - \frac{T^3}{2\pi}\sum_{M_N}\sum_{k_x}\sum_{l=1}^{\infty}\frac{1}{l^3} \\ & \times\left(1+\frac{l}{T}\sqrt{k_x^2+M_N^2}\right)\exp\left(-\frac{l}{T}\sqrt{k_x^2+M_N^2}\right). \end{aligned} \tag{6.2.11}$$

Here we have used that $K_{\frac{3}{2}}(z) = \sqrt{\frac{\pi}{2z}}e^{-z}(1+1/z)$. It might be enlightening to see that this expression reduces to the free energy of the Minkowski space-time when setting $M_N = 0$. There are a lot of patterns in the expressions in this thesis and it is easier to not be overwhelmed by the large expressions if the reader is familiar with these patterns.

Until now we have not specified the boundary conditions on the plates in the low temperature limit. We can numerically find the first values of M_N. Due to the vast difference in magnitude of M_N and k_x, M_N is expected to

dominate. And since both β (at low temperature) and M_N are large, the smallest values of M_N will be enough to get a good approximation of the numerical value due to the exponential factor. Note that this expression approaches the zero point energy when $T \to 0$ as it should.

To get an expression applicable to all BC we turn to the Abel-Plana formula once more. As the function $f(z)$ we choose

$$\begin{aligned} f(z) =& \frac{1}{\pi}\left(1+\beta l\sqrt{(z/a)^2+M_N^2}\right)\exp\left(-\beta l\sqrt{(z/a)^2+M_N^2}\right) \\ & \times\left(1-\sum_{j=0,a}\frac{\beta_j/a}{1+(\beta_j z/a)^2}\right). \end{aligned} \tag{6.2.12}$$

Because of $\sqrt{k_x^2+M_N^2}$ in the argument of $K_{\frac{3}{2}}$ we are not able to choose $f(z)$ on the form Eq.(6.1.15) and accordingly we cannot use Eq.(6.1.16) derived in Appendix B. We go through the whole calculation rapidly and emphasize the differences. For Δf we find

$$\begin{aligned} \Delta f =& i\int_0^\infty \mathrm{d}z \frac{f\left(e^{i\pi/2}z\right)-f\left(e^{-i\pi/2}z\right)}{\frac{(\beta_0/a-1)(\beta_a/a-1)}{(\beta_0/a+1)(\beta_a/a+1)}e^{2z}-1} \\ =& \frac{2}{\pi}\int_{M_N a}^\infty \mathrm{d}z \frac{1-\sum_{j=0,a}\frac{\beta_j/a}{1-(\beta_j z/a)^2}}{\frac{(\beta_0/a-1)(\beta_a/a-1)}{(\beta_0/a+1)(\beta_a/a+1)}e^{2z}-1}\left[\sin\left(\beta l\sqrt{(z/a)^2-M_N^2}\right)\right. \\ & \left.+\beta l\sqrt{(z/a)^2-M_N^2}\cos\left(\beta l\sqrt{(z/a)^2-M_N^2}\right)\right]. \end{aligned} \tag{6.2.13}$$

We insert the values of β_j for DD or NN BC and Δf simplifies to

$$\begin{aligned} \Delta f =& \frac{2}{\pi}\int_{M_N a}^\infty \frac{\mathrm{d}z}{e^{2z}-1}\left[\sin\left(\beta l\sqrt{(z/a)^2-M_N^2}\right)\right. \\ & \left.-\beta l\sqrt{(z/a)^2-M_N^2}\cos\left(\beta l\sqrt{(z/a)^2-M_N^2}\right)\right]. \end{aligned} \tag{6.2.14}$$

After the variable change $x = z/a$ and expanding the denominator we find

$$\begin{aligned} \Delta f =& \frac{2a}{\pi}\sum_{n=1}^\infty\int_{M_N}^\infty \mathrm{d}x e^{-2nax}\left[\sin\left(\beta l\sqrt{x^2-M_N^2}\right)\right. \\ & \left.-\beta l\sqrt{x^2-M_N^2}\cos\left(\beta l\sqrt{x^2-M_N^2}\right)\right]. \end{aligned} \tag{6.2.15}$$

Because of the root this is a complicated integral. We solve it in in Appendix

A with the result

$$\int_C^\infty \mathrm{d}x \left(\sin\left(A\sqrt{x^2-C^2}\right) - A\sqrt{x^2-C^2}\cos\left(A\sqrt{x^2-C^2}\right)\right) e^{-Bx} = \frac{C^2A^3}{A^2+B^2} K_2\left(C\sqrt{A^2+B^2}\right). \tag{6.2.16}$$

In Δf we identify $A = \beta l$, $B = 2na$ and $C = M_N$. Finally the free energy density in the piston model with DD or NN BC can be presented,

$$\begin{aligned} F_{\mathrm{RSI}}^{\mathrm{DD,NN}} =& E_{\mathrm{RSI}}^{\mathrm{DD,NN}} - \frac{a}{\pi^2}\sum_{M_N}\sum_{l=1}^{\infty}\sum_{n=1}^{\infty} \frac{M_N^2}{(2na)^2+(\beta l)^2} \\ & \times K_2\left(M_N\sqrt{(2na)^2+(\beta l)^2}\right). \end{aligned} \tag{6.2.17}$$

The Casimir force is found by taking minus the derivative with respect to a

$$\begin{aligned} P_{\mathrm{RSI}}^{\mathrm{DD,NN}} &= P_{\mathrm{RSI}}^{\mathrm{DD,NN}}(T=0) \\ &- \frac{1}{\pi^2}\sum_{M_N}\sum_{l=1}^{\infty}\sum_{n=1}^{\infty} \frac{M_N^2 3(2na)^2-(\beta l)^2}{\left((2na)^2+(\beta l)^2\right)^2} K_2\left(M_N\sqrt{(2na)^2+(\beta l)^2}\right) \\ &- \frac{1}{\pi^2}\sum_{M_N}\sum_{l=1}^{\infty}\sum_{n=1}^{\infty} \frac{M_N(2na)^2}{\left((2na)^2+(\beta l)^2\right)^{\frac{3}{2}}} K_1\left(M_N\sqrt{(2na)^2+(\beta l)^2}\right). \end{aligned} \tag{6.2.18}$$

From this expression we can find the limits $at \ll 1$ and $aT \gg 1$. However there is not much point since both $M_N a \gg 1$ and $M_N/T \gg 1$. The corrections will in both cases be negligible.

6.2.2 Dirichlet-Neumann boundary conditions

We now look at DN BC in the high and low temperature limit. The difference from DD or NN BC is minimal. We will not plot the free energy and force since the behaviour is very similar to DD or NN BC.

High temperature limit

An educated guess on the free energy of DN BC at high temperatures would be

$$F_{\mathrm{RSI}}^{\mathrm{DN}} = -\frac{a\pi^{\frac{1}{2}}}{\beta(2\pi)^2}\sum_{l=-\infty}^{\infty}\sum_{M_N}\sum_{n=1}(-1)^n \left(\frac{M_N^2+\epsilon_l^2}{n^2a^2}\right)^{\frac{3}{4}} K_{\frac{3}{2}}\left(2na\sqrt{M_N^2+\epsilon_l^2}\right). \tag{6.2.19}$$

The argument for such a guess is that the difference between the expression for DD or NN and DN at zero temperature is a factor of $(-1)^n$ in the sum

over n. Hence this expression gives the correct zero temperature limit. The guess turns out to be correct and the derivation is given in Appendix B. From the free energy we find the Casimir force at finite temperature

$$P_{\rm RSI}^{\rm DN} = \frac{\pi^{1/2}}{\beta(2\pi)^2}\sum_{l=-\infty}^{\infty}\sum_{M_N}\sum_{n=1}^{\infty}(-1)^n\left(\frac{M_N^2+\epsilon_l^2}{n^2a^2}\right)^{\frac{3}{4}}K_{\frac{3}{2}}\left(2na\sqrt{M_N^2+\epsilon_l^2}\right)$$
$$-\frac{2\pi^{1/2}}{\beta(2\pi)^2}\sum_{l=-\infty}^{\infty}\sum_{M_N}\sum_{n=1}^{\infty}(-1)^n\frac{\left(M_N^2+\epsilon_l^2\right)^{\frac{5}{4}}}{\sqrt{na}}K_{\frac{5}{2}}\left(2na\sqrt{M_N^2+\epsilon_l^2}\right). \tag{6.2.20}$$

Low temperature

To find the Casimir free energy and force at low temperatures with DD or NN BC we used the Abel-Plana formula. As in Chapter 5 the only difference between DD or NN and DN is the factor $(-1)^n$. With ease we find the free energy in the low temperature limit to be

$$\begin{aligned}F_{\rm RSI}^{\rm DN} =& E_{\rm RSI}^{\rm DN} - \frac{a}{\pi^2}\sum_{M_N}\sum_{l=1}^{\infty}\sum_{n=1}^{\infty}(-1)^n\frac{M_N^2}{(2na)^2+(\beta l)^2}\\ &\times K_2\left(M_N\sqrt{(2na)^2+(\beta l)^2}\right),\end{aligned} \tag{6.2.21}$$

and the Casimir force

$$\begin{aligned}P_{\rm RSI}^{\rm DN} &= P_{\rm RSI}^{\rm DD,NN}(T=0)\\ &-\frac{1}{\pi^2}\sum_{M_N}\sum_{l=1}^{\infty}\sum_{n=1}^{\infty}(-1)^n\frac{M_N^2 3(2na)^2-(\beta l)^2}{\left((2na)^2+(\beta l)^2\right)^2}K_2\left(M_N\sqrt{(2na)^2+(\beta l)^2}\right)\\ &-\frac{1}{\pi^2}\sum_{M_N}\sum_{l=1}^{\infty}\sum_{n=1}^{\infty}(-1)^n\frac{M_N(2na)^2}{\left((2na)^2+(\beta l)^2\right)^{\frac{3}{2}}}K_1\left(M_N\sqrt{(2na)^2+(\beta l)^2}\right).\end{aligned} \tag{6.2.22}$$

6.3 Casimir free energy and force in RSII

In RSII the Kaluza-Klein modes are continuous and we must replace

$$\sum_{M_N} \to \int_0^\infty \frac{{\rm d}M}{k} \tag{6.3.1}$$

as in Section 5.5.

6.3.1 Dirichlet-Dirichlet or Neumann-Neumann boundary conditions

Going from RSI to RSII we let M be continuous (Eq.(6.3.1)) in Eq.(6.2.7). The integral over $K_{\frac{3}{2}}(z)$ is solved in Appendix A (Eq.(A.5)) and the result is

$$\int_0^\infty \mathrm{d}z \left(z^2+x^2\right)^{\frac{3}{4}} K_{\frac{3}{2}}\left(a\sqrt{z^2+x^2}\right) = \sqrt{\frac{\pi}{2a}}x^2 K_2(ax). \tag{6.3.2}$$

The integral makes it rather trivial to find the free energy in RSII

$$\begin{aligned} F_{\mathrm{RSII}}^{\mathrm{DD,NN}} =& -\frac{1}{8\pi ak\beta}\sum_{l=-\infty}^{\infty}\sum_{n=1}^{\infty}\frac{\epsilon_l^2}{n^2}K_2\left(2|\epsilon_l|an\right) \\ =& -\frac{\pi^3}{1440\beta k a^3} - \frac{\pi}{ak\beta^3}\sum_{l=1}^{\infty}\sum_{n=1}^{\infty}\frac{l^2}{n^2}K_2\left(\frac{4\pi aln}{\beta}\right). \end{aligned} \tag{6.3.3}$$

The first term is the $l=0$ contribution. This can be found either by using the limiting form of $K_\nu(z)$ for small arguments or extracting $l=0$ from the sum all the way back in Eq.(4.3.29). The second term gets an additional factor of 2 to account for both the positive and negative values of l.

High temperature limit

Eq.(6.3.3) is suitable to find the high temperature limit in RSII since the argument of $K_\nu(z)$ increases with temperature. The dominating term at high temperatures correspond to Matsubara frequency $l=0$ and is linear in T. With high temperatures it is understood that $aT \gg 1$. This is a different scale than we used in Section 6.2. Since the Kaluza-Klein modes are continuous in RSII we do not get a scale from the light mode masses (M_N) as we did in RSI. Hence the only scale left is to use the magnitude of a. The free energy in RSII with DD or NN boundary conditions is shown in Figure 6.3 as a function of aT and ak. We observe that the ratio between the Minkowski and RSII does not change noticeably in the figure. This is because $aT > 100$ and we can disregard the Bessel functions. In both Minkowski spactime and RSII the free energy is dominated by a term linear in T, thus their ratio is constant in T. In the ak-direction we observe the $1/(ak)$ behaviour. The Casimir force in the high temperature limit is

$$\begin{aligned} P_{\mathrm{RSII}}^{\mathrm{DD,NN}} =& -\frac{3\pi^3}{1440\beta k a^4} - \frac{3\pi T^3}{a^2 k}\sum_{n,l=1}^{\infty}\frac{l^2}{n^2}K_2\left(4\pi aTln\right) \\ & -\frac{4\pi^2 T^4}{ak}\sum_{n,l=1}^{\infty}\frac{l^3}{n}K_1\left(4\pi aTln\right). \end{aligned} \tag{6.3.4}$$

and is plotted in Figure 6.4. The force ratio is also approximately constant in aT and exhibit the $1/(ak)$ behaviour.

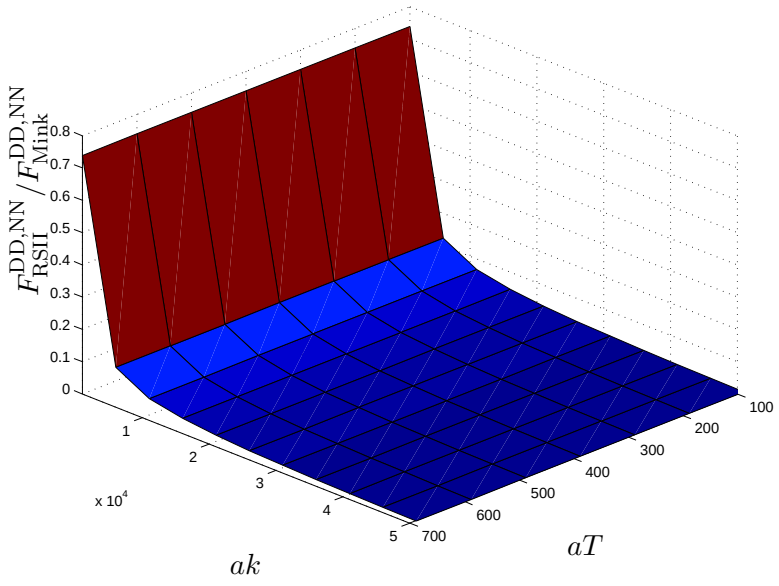

Figure 6.3: Plot of the ratio between Casimir free energy in Minkowski spacetime and RSII with DD or NN boundary conditions.

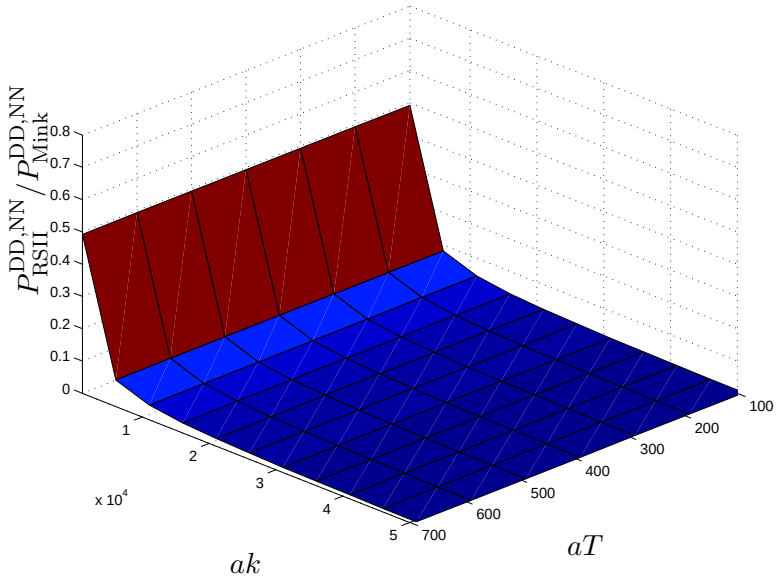

Figure 6.4: Plot of the ratio between Casimir force in Minkowski spacetime and RSII with DD or NN boundary conditions.

Low temperature limit

The lowest corrections to the zero temperature case can not be extracted form Eq.(6.3.3) so we devote a new section to this. We start with Eq.(4.3.20)

from Section 4.3.2

$$F = -\frac{V_\perp}{2\beta}\frac{\partial}{\partial s}\mu^{2s}\sum_{l=-\infty}^{\infty}\sum_{k_x}\int_0^\infty \frac{\mathrm{d}M}{k}\int\frac{\mathrm{d}^2k_\perp}{(2\pi)^2}\left(M^2+\left(\frac{2\pi l}{\beta}\right)^2+k_x^2+k_\perp^2\right)^{-s}. \tag{6.3.5}$$

The integral over M runs from 0 to ∞ while the integrals over the $k_\perp$'s run from $-\infty$ to ∞. By rewriting the integral over M we can use the same steps as in Section 4.3.2 only using $N_\perp = 3$ since we integrate over the two transverse directions plus M. To stress what we are doing we introduce new variables $k_1' = k_y$, $k_2' = k_z$ and $k_3' = M$

$$\begin{aligned} F =& -\frac{V_\perp}{2\beta}\frac{2\pi}{2k}\frac{\partial}{\partial s}\mu^{2s}\sum_{l=-\infty}^{\infty}\sum_{k_x}\int\frac{\mathrm{d}^3k'}{(2\pi)^3}\left(\underbrace{\left(\frac{2\pi l}{\beta}\right)^2+k_x^2}_{A}+k'^2\right)^{-s} \\ =& -\frac{V_\perp\pi}{2\beta k}\frac{\pi^{N_\perp/2}}{(2\pi)^{N_\perp}}\Gamma\left(-\frac{N_\perp}{2}\right)\sum_{l=-\infty}^{\infty}\sum_{k_x}\left(\left(\frac{2\pi l}{\beta}\right)^2+k_x^2\right)^{\frac{N_\perp}{2}}. \end{aligned} \tag{6.3.6}$$

There is no need to go though the low temperature calculation one more time. We start with the Mellin transform, Eq.(4.3.10), and use the property in Eq.(6.1.10) of the function $S_2(t)$ with argument $t\left(\frac{2\pi}{\beta}\right)^2$. On the way we identify the zero point energy, and without assuming anything about the boundary conditions we find

$$F = -\frac{3\zeta_R(5)}{128\pi k a^4} - \frac{1}{2\pi k\beta^2}\sum_{l=1}^{\infty}\sum_{k_x}\frac{k_x^2}{l^2}K_2\left(k_x\beta l\right). \tag{6.3.7}$$

Since the sum over k_x is on the form of Eq.(6.1.15) we can use Eq.(6.1.16) to find

$$\Delta F = -\frac{3\zeta_R(5)}{128\pi k a^4} - \frac{3a}{2\pi k}\sum_{n,l=1}^{\infty}\frac{1}{\left((2an)^2+(\beta l)^2\right)^{\frac{5}{2}}}. \tag{6.3.8}$$

This can also be realized by using the formula

$$\int_0^\infty \mathrm{d}z\ z^2K_2(az) = \frac{3\pi}{2a^3} \tag{6.3.9}$$

from Appendix A on Eq.(6.2.17). We will use the same trick as in the low temperature Minkowski spacetime. Using the Mellin transformation and $S_2((2a)^2t)$. Disregarding all terms independent and linear in a we are left with

$$F = -\frac{3\zeta_R(5)}{128\pi k a^4} - \frac{\pi T^2}{2ka^2}\sum_{n,l=1}^{\infty}\left(\frac{n}{l}\right)^2K_2\left(\frac{\pi nl}{aT}\right). \tag{6.3.10}$$

This is the same that we would get by inserting $k_x = \pi n/a$ $(n = 1, 2, \ldots)$ in Eq.(6.3.7). The Casimir force in the low temperature limit is

$$P_{\mathrm{RSII}}^{\mathrm{DD,NN}} = -\frac{3\zeta_R(5)}{32\pi k a^5} + \frac{\pi^2 T}{2ka^4}\sum_{n,l=1}^{\infty}\frac{n^3}{l}K_1\left(\frac{\pi n l}{aT}\right). \tag{6.3.11}$$

6.3.2 Dirichlet-Neumann boundary conditions

In this last section on finite temperature Casimir effect not much additional calculation is needed. We will not plot the free energy and force since the behaviour is very similar to DD or NN BC in RSII as well.

High temperature limit

We find the free energy of RSII with DN boundary conditions from Eq.(6.2.19). After changing the sum over M_N to an integral we make use of Eq. (A.5).

$$F_{\mathrm{RSII}}^{\mathrm{DN}} = \frac{7}{64\pi\beta k a^3} - \frac{\pi}{ak\beta^3}\sum_{l=1}^{\infty}\sum_{n=1}^{\infty}(-1)^n\frac{l^2}{n^2}K_2\left(\frac{4\pi a l n}{\beta}\right). \tag{6.3.12}$$

The Casimir force in this case is

$$\begin{aligned} P_{\mathrm{RSII}}^{\mathrm{DN}} = &-\frac{21}{64\pi\beta k a^4} - \frac{3\pi T^3}{a^2 k}\sum_{n,l=1}^{\infty}(-1)^n\frac{l^2}{n^2}K_2\left(4\pi a T l n\right) \\ &-\frac{4\pi^2 T^4}{ak}\sum_{nl=1}^{\infty}(-1)^n\frac{l^3}{n}K_1\left(4\pi a T l n\right). \end{aligned} \tag{6.3.13}$$

Low temperature limit

From the low temperature section of DD/NN BC in RSII we find

$$F_{\mathrm{RSII}}^{\mathrm{DN}} = \frac{15}{16}\frac{3V_\perp\zeta_R(5)}{128\pi k a^4} - \frac{\pi T^2}{2ka^2}\sum_{n,l=1}^{\infty}(-1)^n\left(\frac{n}{l}\right)^2 K_2\left(\frac{\pi n l}{aT}\right). \tag{6.3.14}$$

The only difference form the DD/NN expression is the factor of $(-1)^n$. The factor can be accounted for by using Eq.(6.1.26). The Casimir force in RSII in the low temperature limit is

$$P_{\mathrm{RSII}}^{\mathrm{DN}} = \frac{15}{16}\frac{3\zeta_R(5)}{32\pi k a^5} + \frac{\pi^2 T}{2ka^4}\sum_{n,l=1}^{\infty}(-1)^n\frac{n^3}{l}K_1\left(\frac{\pi n l}{aT}\right). \tag{6.3.15}$$

This concludes our calculations.

Chapter 7

Discussion

Up until now (June 09) only a handful of articles have been published on the Casimir effect in Randall-Sundrum models, and all of them in Physical Review D in 2007, 2008 and 2009. In addition, three articles have been posted on the ArXiv in 2009, but have yet to be published in a journal[23, 24, 25]. In other words; this topic gained interest recently.

The first article published was written by Frank, Turan and Ziegler [19] and the third by Frank, Saad and Turan [20]. From now on this group will be referred to as Frank et. al. Their two articles cover the Casimir force in both RSI/RSII and RSI-q/RSII-q. RSI-q and RSII-q being the generalization of the Randall-Sundrum models to q extra compactified dimensions on the branes, the 3-branes in RSI/RSII are replaced by (3+q)-branes. In this thesis we have not considered the RSI-q/RSII-q models at all. However the generalization to (3+q)-branes is not complicated once we have agreed on how find to the Casimir force in RSI/RSII. The second and fourth articles to be published were written by Linares, Morales-Técotl and Pedraza. This group will be referred to as Linares et. al. Their focus was on the RSII/RSII-q. While Frank et. al. used zeta functions to find the Casimir force, Linares et. al. used the Green's function formalism. Surprisingly the two methods gave incompatible answers. In ordinary Minkowski spacetime, all regularization techniques produce the same result.

In this thesis we choose to work with zeta functions, following Frank et. al. The proofs of the Abel-Plana formula and the property of $S_2(t)$ (Eq.(6.1.10)) are both based on the residue theorem from complex analysis [54], so they have the same origin. The reason for choosing this approach is that the author is more familiar with zeta than Green's functions.

We will return to the differences between zeta and Green's function after a brief account and discussion of the the results obtained in the previous chapters for RSI and RSII. A review of the localization of the modes are in order, with special attention to the massless mode. We round off with a section on comparison with experimental data.

7.1 The RSI results

There are a few articles on the Casimir force on physical plates induced by a bulk scalar in RSI. Most important is the 2007 article by Frank et. al.[19]. There also exist a couple of articles on the ArXiv[1] written by Hongbo Cheng [23, 24, 25]. We will only comment on Ref.[24] and Ref.[25] because all the information of Ref.[23] is contained in Ref.[24]. All articles except Ref.[25] assume zero temperature.

In Section 5.4.3 we made some comments on the differences and similarities between the results given here and the article by Frank et. al. Let us repeat them and discuss the results some more.

In the article the Casimir energy and force of a massless bulk scalar field were investigated at zero temperature with Dirichlet BC. Since the field was massless the $M_N = 0$ mode was included. In order to make the results comparable to experiments some changes were done. Most terms were multiplied with a factor p to account for the polarizations of the photon, and the modes polarized in the direction of the plates were subtracted. The modes polarized in the direction of the plates are not dependent on the distance between the physical plates a, and will give no contribution to the Casimir force. They will also be removed in the piston model. How to go from a scalar field to an electromagnetic field is not yet resolved and we will return to this later on. The last difference was an overall factor of 2, but since we cannot see how this factor occurs we have not included it.

In contrast to this thesis, where we have worked with the piston model, Frank et. al. have confined themselves to subtracting the energy density when no plates are present. Because of this, their energy density contains some terms that, since they are independent of a, will give no contribution to the Casimir force.

All these differences aside, the expressions are the same if we make the approximations from Section 4.2.3 ($M_N/k \ll 1$ and $e^{k\pi r_c} M_N/k \not\ll 1$). Frank et. al. have a different procedure for finding the energy density. From Section 4.2.3 the masses of the Kaluza-Klein can be expressed as $M_N = k\pi e^{-\pi k r_c}(N + 1/4)$, with $N = 1, 2, \ldots$. This enables them to use zeta functions of the Epstein-Hurwitz type [33]. As discussed in Section 4.2.3 the error in M_N is substantial for the first mode masses and then becomes negligible. In the energy density (Eq.(5.4.5)) we sum over all values of M_N of a function proportional to $K_\nu(2aM_N n)$. For large values of z we have $K_\nu(z) = \sqrt{\pi/(2z)}e^{-z}$. We can conclude that the first couple of values of M_N are the most important to the energy density, since the energy density is exponentially decreasing in M_N. In this thesis we have shown that the approximation $M_N = k\pi e^{-\pi k r_c}(N + 1/4)$ is not necessary to find the Casimir energy and force. We obtained the same result without using

[1] http://arxiv.org/

this explicit expression for M_N and Epstein-Hurwitz zeta functions. We use merely the Abel-Plana formula. Hence, our answers are more accurate.

In the article by Hongbo Cheng [24] the same Casimir energy and force is found. Although considering a massless scalar the $M_N = 0$ mode is not included. Cheng has not made an attempt to go from the scalar field to the electromagnetic field and also uses the piston model. In that respect his work is similar to ours. The approximation $M_N = k\pi e^{-\pi k r_c}(N + 1/4)$ is used throughout the article together with Epstein-Hurwitz zeta functions, following Frank et. al. Due to a small error in the calculation some of the modified Bessel functions in Casimir force have an argument with an extra factor $\sqrt{\pi}$. This again leads Cheng to the conclusion that the Casimir force in RSI is repulsive at small distances. The results are in conflict with both the results here and the results by Frank et. al. While Frank et. al. find

$$\begin{aligned} P_{\text{RSI}} =& P_{\text{Mink}} - \frac{p\kappa^2}{4\pi^2 a^2}\left(\sum_{n=1}^{\infty}\sum_{N=0}^{\infty}\frac{(N+1/4)^2}{n^2}K_2(2a\kappa n(N+1/4))\right. \\ &\left. + a\kappa\sum_{n=1}^{\infty}\sum_{N=0}^{\infty}\frac{(N+1/4)^3}{n}K_3(2a\kappa n(N+1/4))\right) \\ &- \frac{p\kappa^2}{64\pi^2 a^2}\left(\sum_{n=1}^{\infty}\frac{1}{n^2}K_2(a\kappa n/2) + a\kappa\sum_{n=1}^{\infty}\frac{1}{n}K_3(a\kappa n/2)\right), \end{aligned}$$

with $\kappa = \pi k e^{-k\pi r_c}$, Cheng find

$$\begin{aligned} P_{\text{RSI}} =& -\frac{\kappa^2}{2a^2}\left(\sum_{n=1}^{\infty}\sum_{N=0}^{\infty}\frac{(N+1/4)^2}{n^2}K_2(2a\kappa n(N+1/4))\right. \\ &\left. + a\kappa\sum_{n=1}^{\infty}\sum_{N=0}^{\infty}\frac{(N+1/4)^3}{n}K_3(2a\kappa n(N+1/4))\right) \\ &+ \frac{\pi\kappa^2}{32a^2}\left(\sum_{n=1}^{\infty}\frac{1}{n^2}K_2(a\kappa n/(2\sqrt{\pi})) + a\kappa\sum_{n=1}^{\infty}\frac{1}{n}K_3(a\kappa n/(2\sqrt{\pi}))\right). \end{aligned}$$

Note that for Frank et. al. the $N = 0$ term exactly cancels the positive part of the force, but for Cheng this is not so. This leads to repulsive Casimir forces at small a. Why do we claim that Frank et. al. is right and Cheng is wrong? In both articles they started with rewriting the sum over N from 1 to ∞, to 0 to ∞, in order to use the Epstein-Hurwitz zeta functions. To do this they both added and subtracted a $N = 0$ term[2]. The two last Bessel functions are the subtracted $N = 0$ term in both articles, and should cancel the two $N = 0$ terms from the sum. This happens for Frank et. al., but not for Cheng. The Casimir force of RSI at zero temperature is always attractive when we are assuming Dirichlet boundary conditions on both plates.

[2] $\sum_{N=0}^{\infty} f(N) = \sum_{N=1}^{\infty} f(N) - f(N=0)$, for any function $f(N)$.

At finite temperature there are two interesting limits; the high and low temperature limit. With high temperature we mean high in comparison to the non-zero Kaluza-Klein masses. This leads to $2\pi T \gg k\pi e^{-k\pi r_c}$ or $T \gg 10^{15}K$. As in Minkowski spacetime, the high temperature Casimir force is linear in T. The values of M_N are large in comparison to T and a at any reasonable temperature and distance, and accordingly the Casimir force due to a massive field in RSI is very small.

The low temperature limit is of more physical interest. For all practical purposes T is much less than 10^{15}K. As expected the Casimir force is that of zero temperature plus corrections that vanish when $T \to 0$. As usual the corrections contains modified Bessel functions of the second kind, this time with argument $M_N/T\sqrt{(2naT)^2 + l^2}$. We wanted to study the low temperature limit to see if it was possible to see some interesting temperature dependence for $aT \ll 1$ or $aT \gg 1$. Since the low temperature limit is based on $M_N \ll T$, it is clear that if $aT \ll 1$ the argument of K_ν would be large ($\sim M_M|l|/T$). When $aT \gg 1$ the argument would still be large since $M_N a \gg 1$ for values of a greater than $10^{-18}m$ (if we choose $k\pi r_c \sim 12$ and $k \sim M_{\rm Pl}$).

Remark: Ref. [25] was about the Casimir force in RSI at finite temperature. But the author of this article found the internal energy[3] and used $-\partial U/\partial a$ instead of $-\partial F/\partial a$ to find the Casimir force. This is not the correct way to find the finite temperature Casimir force [16], and accordingly the results obtained are not in agreement with ours.

7.2 The RSII results

As already mentioned there are two groups that have published articles about the Casimir effect in RSII and with contradictory results. We will devote a separate section to this subject and will only comment on the articles using zeta functions here. From the article by Frank et. al. [19] we have

$$P_{\rm RSII}^{\rm DD,NN} = P_{\rm Mink,EM}\left(1 + \frac{45p}{2\pi^3}\frac{\zeta_R(5)}{ak}\right)$$

at zero temperature. The factor of 2 is because they use the force of an electromagnetic field in Minkowski spacetime[4]. Here, p is the number of polarizations of the photon. To get scalar field results we set $p = 1$ and find an expression in exact agreement ours[5]. The second term in RSII Casimir force is proportional to $1/a^5$, in contrast to the ordinary Casimir force which

[3] The internal energy U are related to the free energy (or Helmholtz free energy) by $U = \partial(\beta F)/\partial\beta$.

[4] In RSII they have dropped the factor of 2 that is supposed to account for the 'volume of the orbifold' in RSI

[5] In our results we do not have the first term from the $M_N = 0$ mode since we study a massive scalar field in bulk.

goes as $1/a^4$. I is natural to ask how large the second term is compared to the ordinary Casimir force at distances typically used in experiments. For $k \sim M_{\rm Pl}$ we find that the $\frac{45}{\pi^3}\frac{\zeta_R(5)}{ak}$ is $\sim 10^{-27}$ for $a = 1\mu$m and $\sim 10^{-24}$ for $a = 1$nm. For a massless scalar field the correction term is too small to be observable.

In RSII there is only one natural high temperature limit, the same as for Minkowski spacetime, namely $aT \gg 1$. We observe an interesting result. The Minkowski case the free energy times a^3 is a function of aT, $F_{\rm Mink}a^3 = f(aT)$ and the same applies for the force with a^4, $F_{\rm Mink}a^4 = f(aT)$. For RSII we have $F_{\rm RSII}a^3 = \frac{1}{ak}f(aT)$ and $P_{\rm RSII}a^4 = \frac{1}{ak}f(aT)$. The overall factor $1/ak$ is typical for comparison between Minkowski and RSII. This factor too small to be detectable with today's experiments when $k \sim M_{\rm Pl}$.

7.3 Zeta regularization versus Green's functions

In this thesis we will not conclude about what is the right or wrong approach to this problem; zeta regularization versus Green's functions. We merely call attention to the curtail differences and interpret the models. Only experiments can give the answer if it turns out that we are really living in a Randall-Sundrum like brane-world. In this section we choose to focus on the first article from Frank et. al.[19] because this only considers RSI/RSII, not RSI-q/RSII-q, and the second article from from Linares et. al.[22] because RSII can be obtained from RSII-q by setting $q = 0$.

Zeta regularization

Let us start with Frank et. al. since it is this method that is used in this thesis. We are calculating the free energy density of the system, but what does the system consist of? In Minkowski spacetime we are looking at the free energy of a scalar field from the four cavities in the piston model. The four cavities are all four-dimensional (in terms of spacetime dimensions), but when looking at the RS model the four cavities are five-dimensional. A four-dimensional observer observes the scalar bulk field as a tower of scalar fields with mass M_N, but we are not finding the Casimir force of a tower of scalar fields in Minkowski spacetime. We are finding the Casimir effect from a bulk scalar field, and accordingly the area of which we are calculating the free energy also includes a slice of the bulk. The idea is illustrated in Figure 7.1. We can see this from the Kaluza-Klein decompositions of the bulk scalar fields (Section 2.4)

$$\Psi(x,\phi) = \sum_N X_N(x)\psi_N(\phi),$$

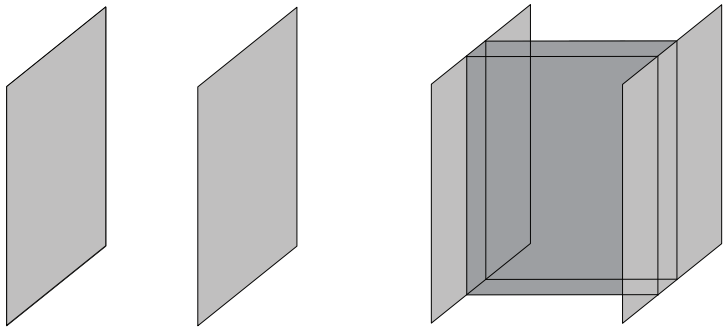

Figure 7.1: Illustration of the Randall-Sundrum model with one compactified dimension. To the left the two branes of RSI and to the right the area that we find the free energy of.

or (Section 4.1)

$$\Phi(\tilde{x}, z) = \sum_{N,p} c_N(p)\chi_p(\tilde{x})\psi_N(z).$$

The x (or $\tilde{x}$) dependent part of the field (x being the directions parallel to the branes) does not only apply for a brane, it spreads over the whole space. By compactifying one of the directions we found the free energy of a slice of the whole space as in Figure 7.1. Thus we must conclude that a four-dimensional experimentalist, living on the visible brane, influences the scalar field in the whole bulk by compactifying one of the dimensions on his/her brane. Forcing the field to be zero (with DD BC) at $x = 0$ and $x = a$ at one brane causes to field to be zero at $x = 0$ and $x = a$ both in the bulk and on the other brane.

The Kaluza-Klein decomposition is an ansatz, but this ansatz gives a solution to the equations of motion for the bulk scalar that satisfy the boundary conditions. Hence it is a valid solution to the problem.

Green's functions

We now turn to the Green's function method. Let us first look at the criticism raised by Linares et. al. in [22] of what they call the 'dimensional regularization' procedure used by the other groups (though Frank et. al. used zeta functions). Their claim was that it was blind to the curvature of the background. The argument was that that the Casimir force in an Euclidean space with d spatial dimensions is

$$P_d = -\frac{d}{a^{d+1}}\Gamma\left(\frac{d+1}{2}\right)(4\pi)^{-(d+1)/2}\zeta_R(d+1)$$

and if you add one four- and one five-dimensional massless scalar field you find

$$P_4 + P_5 = P_4 \left(1 + \frac{45\zeta_R(5)}{\pi^4 a}\right).$$

Comparison to the RSII force reveals that these two differ only by a factor of $\frac{\pi}{k}$ in the last term[6]. The prefactor is due to[7]

$$\int_0^\infty \frac{\mathrm{d}M}{k} = \frac{\pi}{k}\int_{-\infty}^\infty \frac{\mathrm{d}M}{2\pi}.$$

With this in mind they made their claim that dimensional regularization is blind to the curvature of the background. On the other hand, by using Green's functions you would automatically get the different modes weighed by a factor of $\psi(0)^2$, the mode wave function at the brane squared. For a massless bulk scalar field the group found

$$P_{\mathrm{RSII}}^{\mathrm{Linares}} = \frac{2}{3}\left(P_{\mathrm{Mink}}(M_0 = 0) + \int_0^\infty \frac{\mathrm{d}M}{k}\psi_N(0)^2 P_{\mathrm{Mink}}(M_N)\right),$$

where $P_{\mathrm{Mink}}(m)$ is the Casimir force of a scalar field with mass m in Minkowski spacetime. In contrast to the other group

$$P_{\mathrm{RSII}}^{\mathrm{Frank}} = \left(P_{\mathrm{Mink}}(M_0 = 0) + \int_0^\infty \frac{\mathrm{d}M}{k} P_{\mathrm{Mink}}(M_N)\right).$$

Where do the weighing-factor of $\psi_N(0)^2$ and the factor $\frac{2}{3}$ come from? The Green's function for the bulk scalar field is

$$G_{RSII} = \psi_0(y)\psi_0(y')G_{\mathrm{Mink}}(x,x';0) + \int_0^\infty \mathrm{d}M\psi_M(y)\psi_M(y')G_{\mathrm{Mink}}(x,x';M),$$

where $G_{\mathrm{Mink}}(x,x';m)$ is the Green's function for a scalar field in Minkowski spacetime with mass m. The corresponding Casimir force per unit area is

$$P_{\mathrm{RSII}}^{\mathrm{Linares}} = \frac{1}{V_\perp}\int_0^{V_\perp}\mathrm{d}x_\perp \int_{-\infty}^\infty \mathrm{d}y e^{-3k|y|}\left[\langle T_{zz}^{\mathrm{in}}\rangle_{\mathrm{RSII}}\big|_{x=a,y=0} - \langle T_{zz}^{\mathrm{out}}\rangle_{\mathrm{RSII}}\big|_{x=a,y=0}\right]$$

with

$$\left\langle T_{zz}^{\mathrm{in/out}}\right\rangle_{\mathrm{RSII}}\Big|_{x=a,y=0} = \frac{1}{2i}\partial_x\partial_{x'}G_{\mathrm{RSII}}^{\mathrm{in/out}}(x,y;x',y')\Big|_{x_\perp\to x'_\perp, x\to x'=a, y\to y'=0}.$$

[6]Going through the details in [22] you will find some some missing factors of 2 here and there. The argumentation in the article is however right.

[7]Note that we used this trick when calculating the low temperature limit in RSII.

It is important to notice is that the Green's function is evaluated on the brane at $y = 0$. Combining the equations above we find

$$P_{\text{RSII}}^{\text{Linares}} =$$
$$\underbrace{\int_{-\infty}^{\infty} \mathrm{d}y e^{-3k|y|}}_{2/(3k)} \Bigg[\underbrace{\psi_0(0)^2}_{k} \underbrace{\frac{1}{V_\perp} \int_0^{V_\perp} \mathrm{d}x_\perp \, \frac{1}{2i} \partial_x \partial_{x'} G_{\text{Mink}}^{\text{in/out}}(x, x'; 0) \Big|_{x_\perp \to x'_\perp, x \to x' = a}}_{P_{\text{Mink}}(0)}$$
$$+ \int_0^\infty \mathrm{d}M \psi_M(0)^2 \underbrace{\int_0^{V_\perp} \mathrm{d}x_\perp \, \frac{1}{2i} \partial_x \partial_{x'} G_{\text{Mink}}^{\text{in/out}}(x, x'; M) \Big|_{x_\perp \to x'_\perp, x \to x' = a}}_{P_{\text{Mink}}(M)} \Bigg]$$
$$= \frac{2}{3} \left(P_{\text{Mink}}(M_0 = 0) + \int_0^\infty \frac{\mathrm{d}M}{k} \psi_N(0)^2 P_{\text{Mink}}(M_N) \right).$$

Note that this includes partly removing the y-dependence of the integrand before integrating over y. The two groups use not only different regularization techniques, but also a different system over which the Casimir force is calculated. While Linares et. al. try to limit their system to the brane by setting $y = 0$ in the Green's function, Frank et. al. find the Casimir energy and later force with the system containing a slice of the bulk, not only the brane.

As far as we can see, this is the only difference in the physical pictures of the two groups. You might think that Linares et. al. would get the same as Frank et. al. by keeping the y-dependence in the Green's function, but they do not. If the factor $e^{-3k|y|}$ in the integrand had been $e^{-2k|y|}$ we could have used the normalization condition

$$\int_{-\infty}^{\infty} \mathrm{d}y e^{-2k|y|} \psi_N(y)^2 = 1$$

to get the same Casimir force. The factor 3 is not only responsible for the factor 2/3 in their energy, but for giving a different Casimir force than Frank et. al. even when keeping $y \neq 0$ in the Green's function.

7.4 The massless mode and its localization

As mentioned at the end of Section 4.2.2 the contribution from the massless mode to the Casimir force is under debate. In RSI the massless mode is localized near the hidden brane and in RSII near the visible brane. We choose to work with massive scalar. When using zeta regularization the only difference between the massive and the massless scalar is a term equal to the free energy or force of a massless scalar in ordinary flat spacetime (E_{Mink}). Both Linares et. al. and Antonino Flachi and Takahiro Tanaka[37] have other theories on how the modes contribute with respect to their localization.

In the previous section we explained how Linares et. al. let $y = 0$ in the Green's function to get the modes weighted by $\psi_N(0)^2$ in RSII. Since the massless mode in RSII is localized near the (only) brane at $y = 0$, the influence from this mode was pretty large (2/3 of that of a massless scalar confined to the brane). They also identified a quasilocalized mode for a massive bulk field in RSII, also contributing to the Casimir force by $\sim$2/3 of that of a massless field confined to the brane.

Flachi and Tanaka also believe that the modes located near the physical plates should contribute the most. They argue that setting $X_N(x)$ (or $\chi_p(\tilde{x})$) from the Kaluza-Klein expansion equal to 0 at the physical plates (for Dirichlet BC) is the same as artificially expanding the physical plates into the bulk. This will, in their opinion, overestimate of the actual Casimir force. If they are right all the expressions in this thesis can be seen as an upper limit to the Casimir force. Their solution to the overestimation is to impose slightly different boundary conditions on the modes. Instead of setting $X_N(0) = X_N(a) = X_N(X)$ for each mode they want to set the total field to be zero. To achieve this they set $X_N(0) = X_N(X)$ $(N = 0, 1)$ and $X_1(a) + \epsilon X_0(a) = 0$, to be the boundary conditions. Remember, in the piston model there are two cavities with length a and $X - a$ in the stressed situation and two cavities with length X/η and $(1-1/\eta)X$ in the unstressed situation. In their work [37] only the massless and the first massive mode were included, but it is possible to generalize to all the massive modes. The constant ϵ is determined by the overlap of the wave functions of the massless and the massive modes. It is small since the massless mode is localized differently from the other modes. Their way of finding the Casimir force is to expand the energy in ϵ and find the results order by order. Their result contains only terms small in comparison to ordinary Casimir effect.

We are now finished with presenting and commenting on some of the unsolved issues in connection to Casimir effect of a scalar field in the Randall-Sundrum models. For closure we return to actual experiments.

7.5 Comparison with experimental data

Can the results from this thesis and other work on Casimir effect in the Randall-Sundrum model be used to experimentally verify, disprove or limit some constants of the Randall-Sundrum model? In several of the mentioned articles on bulk scalar fields the results are compared to experiments. Is this justified?

The experiments on Casimir effect are from the electromagnetic field. Using ideal metals the electromagnetic field must obey electromagnetic BC. A scalar field with Dirichlet BC is often used because of its simplicity. In nature a scalar field describes spin 0 particles. The only known spin 0 particles in nature is the Higgs boson and the mesons. The mesons are so

called pseudo scalars with parity -1 and the Higgs is scalar with parity +1. How we in practice can confine the scalar fields to a cavity is not known, so experimentalists have to work with the electromagnetic fields. Working theoretically with a scalar field does not include struggling with polarizations, and the final answer differs, at most times, from the electromagnetic case by a factor of 2 (due to the polarizations). Hence the behavior of the scalar field mimics the behavior of an electromagnetic field in most cases.

How to transform from a scalar field to an electromagnetic field in extra dimensional models is not trivial when the extra dimensional space is not Euclidean [55]. A good example of this is the contradictory results of Poppenhaeger, Hossenfelder, Hofmann and Bleicher [26] and Edery and Marachevsky [27]. Both studied the Casimir effect from an electromagnetic field in the presence of an extra compactified dimension with the extra dimension being a circle ($M^4 \times S^1$) with radius R. Poppenhaeger et. al used polarization factors in the same way as both Frank et. al. and Linares et. al.: The energy of a scalar field is multiplied with a factor p accounting for the possible polarizations of the photon ($p = 3$ both for $M^4 \times S^1$ and RS) and subtracting a term due to the modes polarized in the direction of the plates. The energy of the scalar field in the circle model is the sum over an infinite tower of four dimensional massive scalar fields, with mass $\pi n/R$ ($n = 0, 1, \ldots$). On the other hand Edery and Marachevsky start with the (4+1)-dimensional Maxwell action and reduces it to a (3+1)-dimensional action to extract physics from a four-dimensional view[8]. This yields a (3+1)-dimensional Maxwell field, a scalar field (which gives no contribution to the Casimir force) plus an infinite set of four-dimensional massive gauge fields (Proca fields) with mass n/R ($n = 0, 1, \ldots$).

This conflict is not yet resolved even though this problem includes a far simpler metric than the Randall-Sundrum metric. It would not be a wild guess to believe that following Edery and Marachevsky's in reducing the (4+1)-dimensional Maxwell action would lead to other answers than the ones obtained by both Frank et. al. or Linares et. al.

A lot of key questions are still unanswered: What is the correct way to go about when finding the Casimir effect for a scalar field in the Randall-Sundrum model; Green's functions or zeta regularization? Should the Kaluza-Klein modes be weighted, to account for their localization in the extra dimension with respect to the physical plates on the visible brane? How do we go from a scalar field to an electromagnetic field in a higher dimensional spacetime? If these questions are sorted out we still have to wait for Casimir experiments to become more accurate. The theoretical results so far suggest that the extra dimensional effect is extremely small. Chances are that LHC have provided evidence for the existence or exclusion of extra dimension

[8] Reducing the higher dimensional theory to a four-dimensional theory is the same as we did in Section 4.1.

theories long before that time [12, 11].

Bibliography

[1] Lisa Randall and Raman Sundrum. Large mass hierarchy from a small extra dimension. *Phys. Rev. Lett. D*, 83(17):3370–3373, 1999.

[2] Walter D. Goldberger and Mark B. Wise. Bulk fields in the Randall-Sundrum compactification scenario. *Physical Review D*, 60:107505, 1999.

[3] Walter D. Goldberger and Mark B. Wise. Modulus Stabilization with Bulk Fields. *Physical Review Letters*, 83:4922–4925, 1999.

[4] Walter D. Goldberger and Mark B. Wise. Phenomenology of a stabilized modulus. *Phys.Lett.B*, 475:275–279, 2000.

[5] A. Flachi and D. J. Toms. Quantized bulk scalar fields in the Randall-Sundrum brane model. *Nuclear Physics B*, 610:144–168, 2001.

[6] Yuval Grossman and Matthias Neubert. Neutrino masses and mixings in non-factorizable geometry. *Physics Letters B*, 474:361–371, 2000.

[7] Tony Gherghetta and Alex Pomarol. Bulk fields and supersymmetry in a slicee of AdS. *Nuc. Phys. B*, 586:141–162, 2000.

[8] Alex Pomarol. Gauge bosons in a five-dimensional theory with localized gravity. *Physics Letters*, 486:153–157, 2000.

[9] H. Davoudiasl, J.L. Hewett, and T.G.Rizzo. Bulk Gauge Fields in the Randall-Sundrum Model. *Physics Letters B*, 473:43–49, 2000.

[10] H. Davoudiasl, J.L. Hewett, and T.G.Rizzo. Experimental Probes of Localized Gravity: On and Off the Wall. *Physical Review D*, 63:075004, 2001.

[11] Ben Lillie, Lisa Randall, and Lian-Tao Wang. The Bulk RS KK-gluon at the LHC. *ArXiv:0701166v1 [hep-ph]*, 2007.

[12] Stephan J. Huber, Chin-Aik Lee, and Qaisar Shafi. Kaluza-Klein excitations of W and Z at the LHC? *Physics Letters B*, 531:112–118, 2002.

[13] Masato ITO. Newton's law in braneworlds with an infinite extra dimension. *Physics Letters B*, 528:269–273, 2002.

[14] Petter Callin and Finn Ravndal. Lagrangian formalism of gravity in the Randall-Sundrum model. *Phys. Rev. D*, 72:064026, 2005.

[15] Peter Callin and Finn Ravndal. Higher order corrections to the Newtonian potential in the Randall-Sundrum model. *Physical Review D*, 70:104009, 2004.

[16] K.A. Milton. *Physical Manifestations of Zero-Point Energy, The Casimir Effect*. World Scientific, Singapore, 2001.

[17] Iver Brevik, Simen A. Ellingsen, and Kimball A. Milton. Thermal corrections to the Casimir Effect. *New Journal of Physics*, 8:236, 2006.

[18] L.P. Teo. Finite temperature Casimir effect in spacetime with extra compactified dimensions. *Physics Letters B*, 672:190–195, 2009.

[19] Ismail Turan Maria Frank and Lorric Ziegler. Casimir force in Randall-Sundrum models. *Physical Review D*, 76:015008, 2007.

[20] Nasser Saad Mariana Frank and Ismail Turan. The Casimir Force in Randall Sundrum Models with $q + 1$ dimensions. *Physical Review D*, 78:055014, 2008.

[21] Hugo A. Morales-Técotl Román Linares and Omar Pedraza. Casimir force for a scalar field in warped brane worlds. *Physical Review D*, 77:066012, 2008.

[22] Hugo A. Morales-Técotl Román Linares and Omar Pedraza. Brane world corrections to the scalar vacuum force in the Randall-Sundrum ii-p scenario. *Physical Review D*, 78:066013, 2008.

[23] Hongbo Cheng. The nature of Casimir force between parallel plates in Randall-Sundrum models. *ArXiv:0902.1610v2 [hep-th]*, 2009.

[24] Hongbo Cheng. The Casimir force on a piston in Randall-Sundrum models. *ArXiv:0904.4183v1 [hep-th]*, 2009.

[25] Hongbo Cheng. The Casimir force on a piston at finite temperature in Randall-Sundrum models. *ArXiv:0906.4022v1 [hep-th]*, 2009.

[26] Stefan Hofmann Katja Poppenhaeger, Sabine Hossenfelder and Marcus Bleicher. The Casimir effect in the presence of compactified universal extra dimensions. *Physical Review D*, 78:066013, 2008.

[27] Ariel Edery and Valery N. Marachevsky. Compact dimensions and the Casimir effect: the Proca connection. *Journal of High Energy Physics*, 12(35), 2008.

[28] Lisa Randall and Raman Sundrum. An Alternative to Compactification. *Physical Review Letters*, 83:4690–4693, 1999.

[29] F. Mandl and G. Shaw. *Quantum field theory*. John Wiley & Sons, Chichester, England, 1984.

[30] P. C. Hemmer. *Kvantemekanikk*. Tapir Akademiske Forlag, Trondhem, 2005.

[31] S.C. Lim and L. P. Teo. Finite temperature Casimir energy in closed rectangular cavities: a rigorous derivation based on zeta function technique. *ArXiv:0804.3916v1 [hep-th]*, 2008.

[32] E. Elizalde, S.D. Odintsov, A. Romeo, A.A. Bytsenko, and S. Zerbini. *Zeta Regularization Techniques with Applications*. World Scientific, Singapore, 1994.

[33] Emilio Elizalde. *Ten Physical Applications of Spectral Zeta Functions*. Springer-Verlag, Berlin, 1996.

[34] M.Reuter and W. Dittrich. Regularisation schemes for the Casimir effect. *Eur. J. Phys.*, 6:33–40, 1985.

[35] S. Ichinose. Casimir Energy for ads5 Electromagnetism and Cosmological Constant Problem. *arXiv:0903.4971v2 [hep-th]*, 2009.

[36] Shin'ichi Nojiri Iver Brevik, Kimball A. Milton and Sergei D. Odintsov. Quantum (in)stability of a brane-world AdS_5 universe at nonzero temperature. *Nuclear Physics B*, 599:305–318, 2001.

[37] Antonio Flachi and Takahiro Tanaka. Casimir Effect on the brane. *ArXiv:0906.2898v1 [hep-th]*, 2009.

[38] Milton Abramowitz and Irene A. Stegun. *Handbook of Mathematical functions with Formulas, Graphs and Mathematical Tables*. Dover Publications, Inc., New York, 1972.

[39] G. L. Klimchitskaya B. Geyer and V. M. Mostepanenko. Thermal Casimir effect in ideal metal rectangular boxes. *Eur. Phys. J. C*, 57:823–834, 2008.

[40] Xin zhou Li, Hong bo Cheng, and Xiang hua Zhai. Attractive or repulsive nature of the casimir force for rectangular cavity. *Physical Review B*, 56(4):2155–2162, 1997.

[41] Aram A. Saharian. The generalized Abel-Plana formula with applications to Bessel functions and Casimir effect. *ArXiv:0708.1187v1 [hep-th]*, 2007.

[42] S. D. Odintsov E. Elizalde and A. A. Saharian. Repulsive Casimir effect from extra dimensions and Robin boundary conditions: from branes to pistons. *Physical Review D*, 79:065023, 2009.

[43] August Romea and Aram A Saharian. Casimir effect for scalar fields under Robin boundary conditions on plates. *J. Phys. A: Math. Gen. A*, 35:1297–1320, 2002.

[44] Hongbo Cheng. The casimir force on a piston in the spacetime with extra compacitifed dimensions. *Phys.Lett.B*, 668:72–77, 2008.

[45] R. M. Cavalcanti. Casimir force on a piston. *Physical Review D*, 69:065015, 2004.

[46] Klaus Kristen and S. A. Fulling. Kaluza-Klein models as pistons. *Arxiv:0901.1902v1*, 2009.

[47] M. Kardar M. P. Hertzberg, R. L. Jaffe and A. Scardicchio. Casimir forces in a piston geometry at zero and finite temperature. *Physical Review D*, 76:045016, 2007.

[48] S. A. Fulling and Klaus Kirsten. Comment on: "The Casimir force on a piston in the spcetime with extra compactified dimensions" [Phys. Lett. B 668 (2008) 72]. *ArXiv:0811.0779v1 [hep-th]*, 2008.

[49] S. C. Lim and L. P. Teo. Repulsive Casimir force at zero and finite temperature. *New Journal of Physics*, 11:013055, 2009.

[50] L. P. Teo. Finite temperature Casimir effect in Kaluza-Klein spacetime. *ArXiv:0901.2195v1 [hep-th]*, 2009.

[51] L. P. Teo. Finite temperature Casimir effect for massive scalar field in spacetime with extra dimensions. *ArXiv:0903.3765v2 [hep-th]*, 2009.

[52] Johanna Miller. Casimir forces between solids can be repulsive. *Physics today*, 19, 2009.

[53] I.S. Gradshteyn and I.M. Ryzhik. *Table of integrals, series and products*. Academic Press Inc., Calefornia, USA, 1980.

[54] Erwin Kreyszig. *Advanced Engineering Mathematics, 8th edition*. John Wiley & Sons, Inc., Singapore, 1999.

[55] Jan Ambjørn and Stephen Wolfram. Properties of the Vacuum. I. Mechanical and Thermodynamic. *Annals of Physics*, 147:1–32, 1983.

Appendix A

Properties of $K_\nu(z)$

In this thesis we encounter the modified Bessel function of second kind $K_\nu(z)$ a lot. This appendix includes the proof for some of the key tricks to essential problems.

When taking the limit $r_c \to \infty$ of $T \to 0$ needed to solve the integral

$$\int_0^\infty \mathrm{d}z \left(z^2 + x^2\right)^{\frac{3}{4}} K_{\frac{3}{2}}\left(a\sqrt{z^2+x^2}\right) \tag{A.1}$$

we will show that I_1 is equal to $K_2(ax)$ times some constant and start by the variable change $u = \sqrt{(z/x)^2 + 1}$

$$\begin{aligned} & x^{\frac{5}{2}} \int_1^\infty \frac{\mathrm{d}u\ u^{\frac{5}{2}}}{\sqrt{u^2-1}} K_{\frac{3}{2}}(axu) \\ =& \sqrt{\frac{\pi}{2a}} x^2 \int_1^\infty \frac{\mathrm{d}u\ u^2}{\sqrt{u^2-1}} \left(1 + \frac{1}{axu}\right) e^{-axu}. \end{aligned} \tag{A.2}$$

Here we have used $K_{\frac{3}{2}}(z) = \sqrt{\frac{\pi}{2z}} e^{-z}(1 + 1/z)$ (10.2.17 from [38]). The integral representation of $K_2(ax)$ is (9.6.22 from [38])

$$K_2(ax) = \frac{\pi^{\frac{1}{2}} \left(\frac{1}{2}ax\right)^2}{\Gamma\left(\frac{5}{2}\right)} \int_1^\infty \mathrm{d}u\ e^{-axu}(u^2-1)^{\frac{3}{2}}. \tag{A.3}$$

It is not easy to recognize the integral above, but after several partial integrations we find

$$K_2(ax) = \frac{\pi^{\frac{1}{2}} \left(\frac{1}{2}ax\right)^2}{\Gamma\left(\frac{5}{2}\right)} \frac{3}{(ax)^2} \int_1^\infty \frac{\mathrm{d}u\ u^2}{\sqrt{u^2-1}} \left(1 + \frac{1}{axu}\right) e^{-axu}. \tag{A.4}$$

Thus the integral yields

$$\int_0^\infty \mathrm{d}z \left(z^2 + x^2\right)^{\frac{3}{4}} K_{\frac{3}{2}}\left(a\sqrt{z^2+x^2}\right) = \sqrt{\frac{\pi}{2a}} x^2 K_2(ax). \tag{A.5}$$

The next integral is much simpler. We need

$$\int_0^\infty \mathrm{d}z\ z^2 K_2(az). \tag{A.6}$$

Using the substitution $u = az$ we find

$$\frac{1}{a^3}\int_0^\infty \mathrm{d}u\ u^2 K_2(u) = \frac{3\pi}{2a^3} u\left(K_2(u)L_1(u) + K_1(u)L_2(u)\right)\Big|_0^\infty. \tag{A.7}$$

$L_\nu(z)$ is the modified Struve function. The properties of $L_\nu(z)$ and $K_\nu(z)$ can be found in [38]. For small argument $K_\nu(z) \approx \frac{1}{2}\Gamma(\nu)(z/2)^{-\nu}$ and $L_\nu(z) \approx (z/2)^{\nu+1}1/(\Gamma(3/2)\Gamma(3/2+\nu)$, thus $u(K_2(u)L_1(u)+K_1(u)L_2(u)) \to 0$ when $u \to 0$. At large argument $L_n(z) \approx I_n(z)$ (n integer), where $I_\nu(z)$ is the modified Bessel function of the first kind. Using that $I_\nu(z)K_{\nu+1}(z) + I_{\nu+1}(z)K_\nu(z) = 1/z$ we end at the result

$$\int_0^\infty \mathrm{d}z\ z^2 K_2(az) = \frac{3\pi}{2a^3}. \tag{A.8}$$

Now we need to solve the integral

$$\int_C \mathrm{d}x \left(A\sqrt{x^2-C^2}\cos\left(A\sqrt{x^2-C^2}\right) - \sin\left(A\sqrt{x^2-C^2}\right)\right) e^{-Bx}. \tag{A.9}$$

Since the integral is included in this appendix it is off cource related to $K_\nu(z)$. First we use the substitution $u = \sqrt{x^2-C^2}$ and end up with

$$\begin{aligned}
&\int_0^\infty \frac{\mathrm{d}u}{\sqrt{u^2+C^2}}(Au^2\cos(Au) - u\sin(Au))e^{-B\sqrt{u^2+C^2}} \\
=&\int_0^\infty \mathrm{d}u\ A\sqrt{u^2+C^2}\cos(Au)e^{-B\sqrt{u^2+C^2}} \\
-&\int_0^\infty \mathrm{d}u\ A\frac{1}{\sqrt{u^2+C^2}}\cos(Au)e^{-B\sqrt{u^2+C^2}} \\
-&\int_0^\infty \frac{\mathrm{d}u}{\sqrt{u^2+C^2}}u\sin(Au))e^{-B\sqrt{u^2+C^2}} \\
=&A\frac{\partial^2}{\partial B^2}\int_0^\infty \mathrm{d}u\ \frac{1}{\sqrt{u^2+C^2}}\cos(Au)e^{-B\sqrt{u^2+C^2}} \\
-&A\int_0^\infty \mathrm{d}u\ \frac{1}{\sqrt{u^2+C^2}}\cos(Au)e^{-B\sqrt{u^2+C^2}} \\
-&\int_0^\infty \frac{\mathrm{d}u}{\sqrt{u^2+C^2}}u\sin(Au))e^{-B\sqrt{u^2+C^2}}.
\end{aligned} \tag{A.10}$$

We have done some rewriting in order to use 3.961 (1)

$$\int_0^\infty \frac{x\mathrm{d}x}{\sqrt{\gamma^2+x^2}}e^{-\beta\sqrt{\gamma^2+x^2}}\sin(ax) = \frac{a\gamma}{\sqrt{a^2+\beta^2}}K_1\left(\gamma\sqrt{a^2+\beta^2}\right) \tag{A.11}$$

and (2) from [53]

$$\int_0^\infty \frac{\mathrm{d}x}{\sqrt{\gamma^2+x^2}} e^{-\beta\sqrt{\gamma^2+x^2}} \cos(ax) = K_0\left(\gamma\sqrt{a^2+\beta^2}\right). \tag{A.12}$$

This yields

$$\begin{aligned}
&\int_C^\infty \mathrm{d}x \left(A\sqrt{x^2-C^2}\cos\left(A\sqrt{x^2-C^2}\right) - \sin\left(A\sqrt{x^2-C^2}\right)\right) e^{-Bx} \\
=&A\frac{\partial^2}{\partial B^2} K_0\left(C\sqrt{A^2+B^2}\right) - \frac{AM}{\sqrt{A^2+B^2}} K_1\left(C\sqrt{A^2+B^2}\right) \\
&- AM^2 K_0\left(C\sqrt{A^2+B^2}\right).
\end{aligned} \tag{A.13}$$

Now we could waste time differentiating and simplifying by hand using the connections between K_0, K_1 and K_2 or we can let Maple do it for us. Either way we find

$$\begin{aligned}
&\int_C^\infty \mathrm{d}x \left(A\sqrt{x^2-C^2}\cos\left(A\sqrt{x^2-C^2}\right) - \sin\left(A\sqrt{x^2-C^2}\right)\right) e^{-Bx} \\
=&-\frac{M^2A^3}{A^2+B^2} K_2\left(C\sqrt{A^2+B^2}\right).
\end{aligned} \tag{A.14}$$

Appendix B

Applications of the Abel-Plana formula

With the intention not to not overwhelm the reader with mathematics we have gathered some of the calculations using the Abel-Plana formula in this appendix. The calculations are not essential to the physical problem and similar calculations are already included in the main part of the thesis. There are however some small difficulties that is essential if you want to get the full picture.

Free energy density in RSI using the Abel-Plana formula

We wish to regularize the free energy density for a massless bulk scalar field

$$F = -\frac{V_\perp}{2\beta(2\pi)^2}\Gamma(s)\sum_{-\infty}^{\infty}\sum_{M_N}\sum_{k_x}\left(M_N^2+\epsilon_l^2+k_x^2\right)^{-s} \tag{B.1}$$

for $s=-1$ using the Abel-Plana formula

$$\begin{aligned}\sum_{n=1}^{\infty}\frac{\pi f(z_n)}{1+\sin(z_n)\cos(z_n+2\alpha)/z_n} = -\frac{\pi}{2}\frac{f(0)}{1-\beta_0/a-\beta_a/a}+\int_0^\infty \mathrm{d}z f(z) \\ + i\int_0^\infty \mathrm{d}z \frac{f\left(e^{i\pi/2}z\right)-f\left(e^{-i\pi/2}z\right)}{\frac{(\beta_0/a-1)(\beta_a/a-1)}{(\beta_0/a+1)(\beta_a/a+1)}e^{2z}-1}.\end{aligned} \tag{B.2}$$

We have already concluded in Section 5.1.2 that only the last integral is relevant in the piston model. The expression for the free energy density is slightly different from the zero temperature energy. The integration over

the transverse directions are already completed and we have $(\ldots)^{-s}$ instead of $(\ldots)^{\frac{1}{2}}$. By inspecting the formulas we see that

$$f(z) = \frac{1}{\pi}\left(M_N^2 + \epsilon_l^2 + (z/a)^2\right)^{-s}\left(1 - \sum_{j=0,a}\frac{\beta_j/a}{1+(\beta_j z/a)^2}\right). \tag{B.3}$$

For $(z/a)^2 \leq M_N^2 + \epsilon_l^2$

$$f\left(e^{i\pi/2}z\right) - f\left(e^{-i\pi/2}z\right) = 0, \tag{B.4}$$

i.e. the integrand is zero, in contrast to for $(z/a)^2 > M_N^2 + \epsilon_l^2$, where

$$\begin{aligned} &f\left(e^{i\pi/2}z\right) - f\left(e^{-i\pi/2}z\right) = \\ &\frac{1}{\pi}\underbrace{\left(e^{-i\pi s} - e^{i\pi s}\right)}_{-2i\sin(s\pi)}\left((z/a)^2 - (M_N^2+\epsilon_l^2)\right)^{-s}\left(1 - \sum_{j=0,a}\frac{\beta_j/a}{1-(\beta_j z/a)^2}\right). \end{aligned} \tag{B.5}$$

Hence the free energy for the piston model is

$$\begin{aligned} F = &-\frac{V_\perp}{\beta(2\pi)^2}\Gamma(s)\sin(\pi s)\sum_{l=-\infty}^{\infty}\sum_{M_N} \\ &\times\int_{a\sqrt{M_N^2+\epsilon_l^2}}^{\infty}\mathrm{d}z\frac{\left((z/a)^2-(M_N^2+\epsilon_l^2)\right)^{-s}}{\frac{(\beta_0/a-1)(\beta_a/a-1)}{(\beta_0/a+1)(\beta_a/a+1)}e^{2z}-1}\left(1-\sum_{j=0,a}\frac{\beta_j/a}{1-(\beta_j z/a)^2}\right). \end{aligned} \tag{B.6}$$

This expression is not valid for all values of β_0 and β_j. We consider the two situations. Dirichlet-Dirichlet (DD) or Neumann-Neumann (NN) and Dirichlet-Neumann (DN) boundary conditions.

DD or NN boundary conditions

We assume DD or NN boundary conditions and perform the substitution $x = a\sqrt{M_N^2+\epsilon_l^2}$

$$\begin{aligned} F_{\mathrm{RSI}}^{\mathrm{DD,NN}} = &-\frac{a}{\beta(2\pi)^2}\Gamma(s)\sin(\pi s)\sum_{l=-\infty}^{\infty}\sum_{M_N} \\ &\times(M_N^2+\epsilon_l^2)^{-s+1}\int_1^\infty \mathrm{d}x\frac{\left(x^2-1\right)^{-s}}{e^{2a\sqrt{M_N^2+\epsilon_l^2}}-1}. \end{aligned} \tag{B.7}$$

We expand the denominator in terms of $e^{-2a\sqrt{M_N^2+\epsilon_l^2}}$ and use Eq.(5.4.4)

$$\begin{aligned} F_{\text{RSI}}^{\text{DD,NN}} = &- \frac{a}{\beta(2\pi)^2\pi^{\frac{1}{2}}}\Gamma(s)\sin(\pi s)\sum_{l=-\infty}^{\infty}\sum_{M_N}\sum_{n=1} \\ &\times\left(\frac{M_N^2+\epsilon_l^2}{n^2a^2})^{-s+1}\right)^{\frac{-s+1/2}{2}} K_{-s+1/2}\left(2na\sqrt{M_N^2+\epsilon_l^2}\right). \end{aligned} \tag{B.8}$$

In the limit $s \to -1$ the $\sin(\pi s)$ is zero and $\Gamma(s)$ is infinite. However the product is finite due to a property of the Gamma function

$$\Gamma(x)\Gamma(1-x) = \frac{\pi}{\sin(x\pi)} \Rightarrow \Gamma(x)\sin(x\pi) = \frac{\pi}{\Gamma(1-x)}. \tag{B.9}$$

The free energy is

$$F_{\text{RSI}}^{\text{DD,NN}} = -\frac{a\pi^{\frac{1}{2}}}{\beta(2\pi)^2}\sum_{l=-\infty}^{\infty}\sum_{M_N}\sum_{n=1}\left(\frac{M_N^2+\epsilon_l^2}{n^2a^2}\right)^{\frac{3}{4}} K_{\frac{3}{2}}\left(2na\sqrt{M_N^2+\epsilon_l^2}\right). \tag{B.10}$$

This is off course the same that we found in Chapter 5 using zeta regularization. Only the Abel-Plana formula allows us to find the free energy density with other boundary conditions as well, such as Dirichlet-Neumann.

DN boundary conditions

Assuming Dirichlet boundary conditions on one plate and Neumann on the other we find

$$\begin{aligned} F_{\text{RSI}}^{\text{DN}} = &\frac{a}{\beta(2\pi)^2}\Gamma(s)\sin(\pi s)\sum_{l=-\infty}^{\infty}\sum_{M_N} \\ &\times (M_N^2+\epsilon_l^2)^{-s+1}\int_1^{\infty}\mathrm{d}x\frac{\left(x^2-1\right)^{-s}}{e^{2a\sqrt{M_N^2+\epsilon_l^2}}+1}. \end{aligned} \tag{B.11}$$

The steps is identical to the calculation with DD or NN, only we get a factor of $(-1)^n$ due to the positive sign in the denominator. The free energy density with DN boundary conditions is

$$F_{\text{RSI}}^{\text{DN}} = \frac{a\pi^{\frac{1}{2}}}{\beta(2\pi)^2}\sum_{l=-\infty}^{\infty}\sum_{M_N}\sum_{n=1}(-1)^n\left(\frac{M_N^2+\epsilon_l^2}{n^2a^2}\right)^{\frac{3}{4}} K_{\frac{3}{2}}\left(2na\sqrt{M_N^2+\epsilon_l^2}\right). \tag{B.12}$$

The Abel-Plana formula when $f(z)$ contains $K_\nu(z)$

A few times in this thesis we run into expressions like

$$\sum_{k_x} k_x^{\nu} K_{\nu}(Ak_x) \tag{B.13}$$

where the sum over k_x runs over the zeros of $F_x(k_x)$ given by Eq.(4.2.8). We want to apply the Abel-Plana formula, Eq.(5.1.1), to find an easier expression for k_x. For this reason we choose to find Δf with

$$f(z) = \frac{1}{\pi}(z/a)^\nu K_\nu(Az/a)\left(1 - \sum_{j=0,a}\frac{\beta_j/a}{1+(\beta_j z/a)^2}\right), \tag{B.14}$$

since only Δf is important in the piston model. Using the properties of the Bessel functions (see e.g. [38]) we can show that

$$f\left(e^{i\frac{\pi}{2}}z\right) - f\left(e^{-i\frac{\pi}{2}}z\right) = -i(z/a)^\nu J_\nu(Az/a)\left(1 - \sum_{j=0,a}\frac{\beta_j/a}{1-(\beta_j z/a)^2}\right), \tag{B.15}$$

where $J_\nu(z)$ is the Bessel function of the first kind. Inserting this into Eq.(5.1.1) we find

$$\Delta f = \int_0^\infty \mathrm{d}z \frac{(z/a)^\nu J_\nu(Az/a)}{\frac{(\beta_0/a-1)(\beta_a/a-1)}{(\beta_0/a+1)(\beta_a/a+1)}e^{2z}-1}\left(1 - \sum_{j=0,a}\frac{\beta_j/a}{1-(\beta_j z/a)^2}\right). \tag{B.16}$$

Assuming DD/NN or DN boundary conditions and expanding the denominator in terms of e^{-2z} we can write

$$\Delta f^{\left\{{DD,NN \atop DN}\right\}} = \sum_{n=1}^\infty (-1)^{\left\{{2n \atop n}\right\}} \int_0^\infty \mathrm{d}z (z/a)^\nu J_\nu(Az/a) e^{-2zn}. \tag{B.17}$$

After the variable change $t = Az/a$ and asking Maple to solve the integral

$$\int_0^\infty \mathrm{d}x\ x^\nu J_\nu(x) e^{-Kx} = \frac{\Gamma\left(\nu+\frac{1}{2}\right)2^\nu}{\sqrt{\pi}(K^2+1)^{\nu+1/2}} \tag{B.18}$$

we find

$$\Delta f^{\left\{{DD,NN \atop DN}\right\}} = \sum_{n=1}^\infty (-1)^{\left\{{2n \atop n}\right\}} \frac{a(2A)^\nu}{\sqrt{\pi}} \frac{\Gamma\left(\nu+\frac{1}{2}\right)}{((2an)^2+A^2)^{\nu+1/2}}. \tag{B.19}$$

Appendix C

Proof of formula for $S_2(t)$

We start by defining

$$S_\alpha^s(t) = \sum_{m=1}^{\infty} \frac{1}{m^{s+1}} \sum_{a=0}^{\infty} (-1)^a \frac{m^{\alpha a}}{\Gamma(a+1)} t^a, \tag{C.1}$$

which reduces to

$$S_\alpha(t) \equiv S_\alpha^{-1}(t) = \sum_{m=1}^{\infty} e^{-m^\alpha t}, \tag{C.2}$$

when $s = -1$. The Gamma function has single poles for $z = -n$, $n = 1, 2, ...$, with residues $\underset{z=-n}{\text{Res}} = \frac{(-1)^n}{n!}$. With the aid of the properties of the Gamma function (C.1) and the residue theorem [54] can be written as

$$S_\alpha^s(t) = \sum_{m=1}^{\infty} \oint_C \frac{\mathrm{d}a}{2\pi i} t^{-a} m^{-\alpha a} \Gamma(a), \tag{C.3}$$

where the closed loop C consists of the straight line $\text{Re}(a) = a_0$ (C_{a_0}) with $0 \leq a_0 \leq 1$ and the semicircle to the left (C_{sc}) with infinite radius as in figure C.1. The contribution of the semicircle is zero and by interchanging the summation and the integration we obtain

$$\begin{aligned} S_\alpha^s(t) &= \int_{C_{a_0}} \frac{\mathrm{d}a}{2\pi i} t^{-a} \Gamma(a) \sum_{m=1}^{\infty} \frac{1}{m^{s+1}} \\ &= \int_{C_{a_0}} \frac{\mathrm{d}a}{2\pi i} t^{-a} \Gamma(a) \zeta(s+1+\alpha a). \end{aligned} \tag{C.4}$$

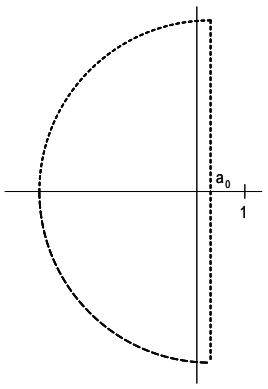

Figure C.1: The closed loop C consisting of the straight line $\mathrm{Re}(a) = a_0$ with $0 \leq a_0 \leq 1$ and the semicircle to the left with infinite radius.

To close the loop again one has to take into account the contribution from the semicircle.

$$\begin{aligned} S_\alpha^s(t) &= \oint_C \frac{\mathrm{d}a}{2\pi i} t^{-a}\Gamma(a)\zeta(s+1+\alpha a) - \int_{C_{sc}} \frac{\mathrm{d}a}{2\pi i} t^{-a}\Gamma(a)\zeta(s+1+\alpha a) \\ &= \oint_C \frac{\mathrm{d}a}{2\pi i} t^{-a}\Gamma(a)\zeta(s+1+\alpha a) - \Delta_\alpha^s(t) \\ &= \sum_{a=0}^{\infty} t^a \frac{(-1)^a}{a!}\zeta(s+1-\alpha a) + \frac{1}{\alpha}\Gamma\left(-\frac{s}{\alpha}\right) t^{-1/\alpha} - \Delta_\alpha^s(t). \end{aligned} \tag{C.5}$$

To calculate the Epstein zeta function we only need $S_2(t)$

$$\begin{aligned} S_2(t) &= \sum_{a=0}^{\infty} t^a \frac{(-1)^a}{a!}\zeta(-2a) + \frac{1}{2}\sqrt{\frac{\pi}{t}} - \Delta_2^{-1} \\ &= -\frac{1}{2} + \frac{1}{2}\sqrt{\frac{\pi}{t}} - \Delta_2^{-1}. \end{aligned} \tag{C.6}$$

Here we have used that $\zeta(-2n) = 0$, $n = 1, 2, ..$, and $\zeta(0) = -1/2$. The only thing left is to calculate

$$\Delta_2^{-1} = \int_{C_{a_0}} \frac{\mathrm{d}a}{2\pi i} t^{-a}\Gamma(a)\zeta(2a). \tag{C.7}$$

Using the reflection formula for the zeta function

$$\Gamma\left(\frac{z}{2}\right)\zeta(z) = \pi^{z-1/2}\Gamma\left(\frac{1-z}{2}\right)\zeta(1-z) \tag{C.8}$$

with $z = 2a$ and the relation

$$\Gamma\left(\frac{z}{2}\right)\zeta(z) = \int_0^\infty \mathrm{d}x\; x^{z/2-1} S_2(t) \tag{C.9}$$

with $\zeta = 1 - 2a$ we get

$$\Delta_2^{-1} = \int_{C_{a_0}} \frac{\mathrm{d}a}{2\pi i} t^{-a} \pi^{2a-1/2} \Gamma\left(\frac{1-2a}{2}\right) \zeta(1-2a). \tag{C.10}$$

The expression can be integrated directly by first using the substitution $u = \frac{xt}{\pi^2}$ and later $v = R \ln u$.

$$\begin{aligned}
\Delta_2^{-1} &= \int_{C_{a_0}} \frac{\mathrm{d}a}{2\pi i} t^{-1/2} \pi^{1/2} \int_0^\infty \mathrm{d}u \; u^{-(a+1/2)} S_2\left(\frac{u\pi^2}{t}\right) \\
&= \sqrt{\frac{\pi}{t}} \lim_{R\to\infty} \int_0^\infty \mathrm{d}u S_2\left(\frac{u\pi^2}{t}\right) \int_{-R}^{R} \frac{\mathrm{d}y}{2\pi i} u^{-(a_0+1/2)} e^{-(iy)\ln(u)} \\
&= -\sqrt{\frac{\pi}{t}} \lim_{R\to\infty} \int_0^\infty \mathrm{d}u S_2\left(\frac{u\pi^2}{t}\right) \frac{1}{2\pi i} u^{-(a_0+1/2)} \frac{e^{-iR\ln u} - e^{iR\ln u}}{\ln u} \\
&= -\sqrt{\frac{\pi}{t}} \lim_{R\to\infty} \int_0^\infty \mathrm{d}u S_2\left(\frac{u\pi^2}{t}\right) u^{-(a_0+1/2)} \frac{\sin R\ln t}{\ln t} \\
&= \sqrt{\frac{\pi}{t}} \Im \lim_{R\to\infty} \int_0^\infty \mathrm{d}v S_2\left(\frac{\pi^2}{t} e^{v/R}\right) e^{-(a_0-1/2)v/R} \frac{e^{iv}}{v} \\
&= -\sqrt{\frac{\pi}{t}} S_2\left(\frac{\pi^2}{t}\right)
\end{aligned} \tag{C.11}$$

The final expression for $S_2(t)$ is

$$S_2(t) = -\frac{1}{2} + \frac{1}{2}\sqrt{\frac{\pi}{t}} + \sqrt{\frac{\pi}{t}} S_2\left(\frac{\pi^2}{t}\right), \tag{C.12}$$

which was what we set out to prove.